Report on the Quality of Land Surface Observations in Region II (Asia)

January – June 2023

No. 65

December 2023

RSMC Tokyo
Lead Center for Monitoring Quality of Land Surface Observations

Japan Meteorological Agency
3-6-9 Tranomon, Minato City, Tokyo 105-8431
Japan

Report on the Quality of Land Surface Observations in Region II
(No. 65)
January – June 2023

Summary

In its role as a Lead Center, RSMC Tokyo has issued the 65th report on the land surface observation quality monitoring for the period from January to June 2023. The report includes a consolidated list of stations suspected of producing low-quality observation data.

（1）SLP

As a result of monitoring, three stations (41396, 44424, 48963) were newly added to the lists.

（2）MSLP

As a result of monitoring, one station (40877) was excluded from the consolidated lists of the previous report (July – December 2022), and six stations (31445, 38318, 47020, 48065, 48961, 48963) were newly added to the lists.

（3）GZ

As a result of monitoring, one station (41249) was newly added to the lists.

1. Introduction

Pursuant to Paragraph 22 of Attachment II.7 of the Manual on the Global Data Processing and Forecasting System (WMO No. 485), the Regional Specialized Meteorological Center (RSMC) Tokyo was designated by the President of the Commission for Basic Systems (CBS) as a Lead Center for monitoring the quality of land surface observations (i.e., SYNOP) in Region II in March 1991. The Center is responsible for monitoring the quality of land surface observations and maintaining consolidated lists of stations suspected of reporting low-quality observation data together with adequate evidence. The lists are to be passed on to the WMO Secretariat and monitoring centers participating in this activity as well as to Members of Regional Association (RA) II for their reference.

2. Monitored Data

Monitored surface observation data are obtained at 00, 06, 12 and 18 UTC and collected at RSMC Tokyo before the data cut-off time, defined as the end of the period in which observation data are gathered for operational analysis. The cut-off times for Japan Meteorological Agency (JMA) global analysis are shown in Table 1.

Table 1 Data cut-off times for JMA global analysis.

Analysis time	Data cut-off time
00 UTC	11:50 UTC
06 UTC	13:50 UTC
12 UTC	23:50 UTC
18 UTC	01:50 UTC

The observation elements monitored are (1) station level pressure, (2) mean sea level pressure and (3) geopotential height, hereafter referred to as SLP, MSLP and GZ, respectively. In accordance with the Manual on Codes (WMO No. 306) Volume II, GZ data on an agreed standard pressure level are reported at the stations whose elevation is higher than 800 m. Standard pressure levels defined in line with station elevation are shown in Table 2.

Table 2 Elevation of stations reporting GZ data and corresponding standard pressure levels.

Station elevation (m)	Pressure level (hPa)
800 - 2,300	850
2,300 - 3,700	700
Higher than 3,700	500

The numbers of stations reporting SLP, MSLP and/or GZ data in Region II are shown in Table 3, and the locations of these land surface stations are shown in Figure 1.

Table 3 Numbers of stations reporting SLP, MSLP and/or GZ data in Region II

Element	Number of stations
SLP	1949
MSLP	2045
GZ	92

3. Monitoring Methods

The three items described below are examined for each element.

(i) Monthly statistics on observation deviations from the most recent forecast of JMA ' s global model (referred to as first-guess values) (observation minus guess, hereafter referred to as O-G) and on related trends over the monitoring period

(ii) Monthly statistics on deviations from values observed at surrounding stations

(iii) Reference information from other monitoring centers

Information on the latitude, longitude and altitude of each station is necessary for calculation of first-guess values. Such data for land surface station locations is retrieved from the surface-based observing

system component of the Observing Systems Capability Analysis and Review Tool (OSCAR/Surface)* , replacing WMO No. 9, Volume A.

The monitoring procedure has two steps as outlined below.

(1) Exclusion of data with gross errors from the statistical calculation sample

The following thresholds are applied for the gross error check in the first step:

|O-G| >= 15 hPa for SLP and MSLP
|O-G| >= 100 gpm for GZ

Gross error data are excluded from the calculation of BIAS (the mean of O-G) and SD (the standard deviation of O-G).

(2) Identification of suspect stations

When the total number of observations (NOBS) is 181 or more, the next criteria are applied:

- BIAS	|BIAS| >= 3 hPa for SLP and MSLP
	|BIAS| >= 30 gpm for GZ
- SD	SD >= 5 hPa for SLP and MSLP
	SD >= 40 gpm for GZ
- Percentage of gross errors (PGE)	PGE >= 25%

Stations with even one statistic exceeding the threshold are considered suspect.

Note:

(i) The quality of observation data from stations is not checked when the NOBS value is less than 181 or the difference between the station elevation and the model elevation is greater than 1,000 m. MSLP reports are also not checked for stations located at altitudes higher than 1,000 m above sea level.

(ii) In case of low quality of the first-guess field, those statistics can exceed the threshold and the stations are listed in the consolidated list. To avoid such situations, statistics of surrounding stations and information from other monitoring centers are also used to judge whether the quality of the station's first-guess field value is appropriate.

*https://oscar.wmo.int/surface/index.html#/

4. Monitoring Results

4.1 Consolidated list of suspect stations throughout the period

Table 4 List of suspect land surface stations during the period from January to June 2023

WMO IDENT	LAT (N)	LON (E)	H (m)	HM (m)	ELEM	NOBS	PGE (%)	SD	BIAS	RMS
30673	53.8	119.7	625	747	SLP	723	0	0.9	-8.6	8.6
					MSLP	724	0	1.4	-0.2	1.4
35284	50.6	70.0	384	330	SLP	724	0	0.7	6.6	6.6
					MSLP	724	0	0.8	0.7	1.1
35615	47.6	53.3	-21	-16	SLP	660	0	0.6	0.2	0.6
					MSLP	660	0	0.7	5.2	5.2
35701	47.2	51.0	-27	-24	SLP	703	0	0.5	0.0	0.5
					MSLP	703	0	0.7	6.4	6.4
38262	43.0	59.8	93	64	SLP	724	0	0.8	3.6	3.7
					MSLP	724	0	0.7	0.4	0.8
38313	43.7	69.0	405	737	SLP	696	73	1.1	13.6	13.6
					MSLP	696	0	2.9	-1.5	3.3
38318	42.1	68.1	183	214	SLP	674	0	0.7	-8.4	8.4
					MSLP	674	0	0.9	-4.2	4.3
38836	38.6	68.7	800	1034	SLP	700	1	1.3	-2.9	3.2
					MSLP	700	0	1.9	-4.0	4.4
38875	39.0	73.6	3930	4259	SLP	345	100	0.0	-14.1	14.1
					-	-	-	-	-	-
38880	38.0	58.4	312	199	SLP	724	2	1.0	11.8	11.8
					MSLP	723	0	1.0	0.0	1.0
38944	37.5	69.4	447	622	SLP	697	0	1.2	-5.7	5.8
					MSLP	699	1	1.4	-5.8	6.0
41252	23.2	56.4	327	344	SLP	506	100	*****	*****	*****
					MSLP	508	0	1.2	0.0	1.2
41265	22.8	58.5	469	585	SLP	655	0	0.5	-5.1	5.1
					MSLP	602	0	0.7	-2.0	2.1
41315	17.3	54.1	881	641	SLP	683	97	0.3	14.7	14.7
					GZ850	676	89	57.0	-10.3	57.9
41573	33.9	73.4	2127	1411	SLP	710	0	1.4	9.0	9.1
					GZ850	711	0	13.6	-0.6	13.6
42056	32.7	74.8	323	295	SLP	716	0	0.9	-6.8	6.9
					MSLP	137	84	5.9	-6.1	8.5
42083	31.1	77.2	2202	1552	SLP	349	87	0.3	14.8	14.8
					GZ850	4	100	*****	*****	*****
42111	30.3	78.1	683	851	SLP	702	0	1.1	5.6	5.7
					MSLP	702	0	1.5	-2.0	2.5
42114	30.4	78.4	770	1482	SLP	353	100	0.0	-13.9	13.9
					-	-	-	-	-	-

WMO IDENT	LAT (N)	LON (E)	H (m)	HM (m)	ELEM	NOBS	PGE (%)	SD	BIAS	RMS
42147	29.5	79.7	2311	1687	SLP	353	1	0.4	4.7	4.7
					-	-	-	-	-	-
42299	27.3	88.6	1756	1964	SLP	361	0	0.8	0.3	0.9
					GZ850	361	0	9.5	55.5	56.3
43113	17.5	74.1	661	707	SLP	181	0	0.8	-3.9	4.0
					MSLP	181	0	1.1	-0.1	1.1
43418	8.6	81.2	79	12	SLP	718	0	0.4	4.6	4.6
					MSLP	719	0	0.6	-0.2	0.6
43479	7.0	81.1	670	911	SLP	490	0	0.5	-9.8	9.8
					-	-	-	-	-	-
44406	29.3	80.9	617	1459	SLP	442	0	1.9	4.1	4.5
					MSLP	442	0	3.4	-3.0	4.5
44429	28.0	82.5	634	809	SLP	440	0	0.6	-3.7	3.7
					MSLP	439	0	1.7	0.1	1.7
47037	40.0	125.3	99	217	SLP	720	0	1.3	-4.2	4.4
					MSLP	720	0	1.4	-4.2	4.4
47102	38.0	124.7	146	4	SLP	724	0	0.6	12.3	12.3
					MSLP	724	0	0.6	-1.1	1.3
47145	36.8	127.3	26	126	SLP	724	0	0.6	-7.2	7.2
					MSLP	724	0	0.6	0.0	0.6
47152	35.6	129.3	36	115	SLP	724	0	0.7	-6.1	6.1
					MSLP	724	0	0.7	-0.7	1.0
48018	24.2	96.3	95	204	SLP	531	0	1.2	3.8	4.0
					MSLP	531	0	1.2	-0.3	1.2
48062	20.1	92.9	5	0	SLP	509	0	0.9	6.3	6.4
					MSLP	509	0	0.8	-0.5	0.9
48085	17.6	94.6	3	54	SLP	528	0	0.9	6.8	6.9
					MSLP	528	0	0.8	-0.4	0.9
48107	15.3	97.9	7	60	SLP	531	0	1.0	-3.5	3.6
					MSLP	532	0	1.0	0.2	1.0
48921	21.6	101.9	1360	1049	SLP	514	3	1.4	-4.2	4.4
					GZ850	510	100	*****	*****	*****
48925	20.7	102.0	636	960	SLP	487	0	1.0	-3.8	3.9
					MSLP	487	0	1.7	-1.9	2.5
48935	19.5	103.1	1094	1204	SLP	517	2	0.8	0.3	0.9
					GZ850	515	10	7.1	-86.7	87.0
48952	15.7	106.4	180	288	SLP	516	0	1.2	3.5	3.7
					MSLP	516	0	1.2	2.3	2.6
54945	35.5	119.6	37	14	SLP	724	0	0.5	-3.5	3.5
					MSLP	724	0	0.5	0.0	0.5
56946	23.6	99.4	1104	1355	SLP	724	0	0.8	-4.3	4.4
					MSLP	723	0	2.8	0.0	2.8
56951	24.0	100.2	1503	1981	SLP	724	0	0.8	-12.9	12.9
					MSLP	724	0	3.2	0.8	3.3
57731	28.0	108.3	418	697	SLP	723	100	0.3	-14.7	14.7

WMO IDENT	LAT (N)	LON (E)	H (m)	HM (m)	ELEM	NOBS	PGE (%)	SD	BIAS	RMS
					MSLP	723	0	1.2	0.7	1.4
58921	26.0	117.4	204	516	SLP	724	0	0.8	-6.6	6.6
					MSLP	724	0	0.9	-0.1	0.9
59632	22.0	108.6	6	23	SLP	724	0	0.5	-5.3	5.3
					MSLP	724	0	0.5	-0.1	0.5

WMO IDENT:	WMO station identification number
LAT:	station latitude
LON:	station longitude
H:	barometer elevation
HM:	model elevation
ELEM:	observed element
NOBS:	total number of observations during the period
PGE:	percentage of gross errors
SD:	standard deviation of (observation - guess)
BIAS:	bias of (observation - guess)
RMS:	root mean square of (observation - guess)

RUSSIAN FEDERATION IN ASIA

30673 - Negative bias of O-G at the station level (Figures 2 and 3)

KAZAKHSTAN

35284 - Positive bias of O-G at the station level (Figures 4 and 5)

35615 - Positive bias of O-G at the mean sea level (Figures 6 and 7)

35701 - Positive bias of O-G at the mean sea level (Figures 6 and 8)

38313 - Positive bias of O-G at the station level (Figures 11 and 12)

38318 - Negative bias of O-G at the station level (Figures 11 and 13)

UZBEKISTAN

38262 - Positive bias of O-G at the station level (Figures 9 and 10)

TAJIKISTAN

38836 - Negative bias of O-G at the mean sea level (Figures 14 and 15)

38875 - Mostly positive bias of O-G at the station level (Figures 16 and 17)

38944 - Negative bias of O-G at the station level and the mean sea level (Figures 11, 14 and 19)

TURKMENISTAN

38880 - Positive bias of O-G at the station level (Figures 9 and 18)

OMAN

41252 - Positive bias of O-G at the station level (Figures 20 and 21)

41265 - Negative bias of O-G at the station level (Figures 20 and 22)

41315 - Positive bias of O-G at the station level and large deviation of O-G at 850 hPa or 700 hPa (Figures 23, 24 and 25)

PAKISTAN

41573 - Positive bias of O-G at the station level (Figures 26 and 27)

INDIA

42056 - Negative bias of O-G at the station level (Figures 26 and 28)

42083 - Positive bias of O-G at the station level (Figures 26 and 29)

42111 - Positive bias of O-G at the station level (Figures 26 and 30)

42114 - Negative bias of O-G at the station level (Figures 26 and 31)

42147 - Positive bias of O-G at the station level (Figures 26 and 32)

42299 - Positive bias of O-G at 850 hPa (Figures 33 and 34)

43113 - Negative bias of O-G at the station level (Figures 35 and 36)

SRI LANKA

43418 - Positive bias of O-G at the station level (Figures 37 and 38)

43479 - Negative bias of O-G at the station level (Figures 37 and 39)

NEPAL

44406 - Positive bias of O-G at the station level (Figures 26 and 40)

44429 - Negative bias of O-G at the station level (Figures 26 and 41)

KOREA, DEMOCRATIC PEOPLE'S REPUBLIC OF

47037 - Negative bias of O-G at the station level and the mean sea level (Figures 42, 43 and 44)

KOREA, REPUBLIC OF

47102 - Positive bias of O-G at the station level (Figures 42 and 45)

47145 - Negative bias of O-G at the station level (Figures 42 and 46)

47152 - Negative bias of O-G at the station level (Figures 42 and 47)

MYANMAR

48018 - Positive bias of O-G at the station level (Figures 48 and 49)

48062 - Positive bias of O-G at the station level (Figures 48 and 50)

48085 - Positive bias of O-G at the station level (Figures 48 and 51)

48107 - Negative bias of O-G at the station level (Figures 48 and 52)

LAO PEOPLE'S DEMOCRATIC REPUBLIC

48921 - Negative bias of O-G at the station level and 850 hPa (Figures 53, 54 and 55)

48925 - Negative bias of O-G at the station level (Figures 53 and 56)

48935 - Negative bias of O-G at 850 hPa (Figures 57 and 58)

48952 - Positive bias of O-G at the station level (Figures 53 and 59)

CHINA

54945 - Negative bias of O-G at the station level (Figures 42 and 60)

56946 - Negative bias of O-G at the station level (Figures 53 and 61)

56951 - Negative bias of O-G at the station level (Figures 53 and 62)

57731 - Negative bias of O-G at the station level (Figures 63 and 64)

58921 - Negative bias of O-G at the station level (Figures 65 and 66)

59632 - Negative bias of O-G at the station level (Figures 67 and 68)

4.2 Stations where quality deteriorated during the period

Table 5 List of suspect land surface stations where quality deteriorated during the period

WMO IDENT	LAT (N)	LON (E)	H (m)	HM (m)	ELEM	NOBS	PGE (%)	SD	BIAS	RMS
31445	51.5	128.1	200	195	SLP	645	0	0.6	0.4	0.7
					MSLP	645	0	1.1	10.9	11.0
38318	42.1	68.1	183	214	SLP	674	0	0.7	-8.4	8.4
					MSLP	674	0	0.9	-4.2	4.3
41249	23.9	56.2	633	784	SLP	676	0	0.5	-0.7	0.9
					GZ850	602	92	63.8	7.1	64.2
41396	16.0	49.0	700	801	SLP	401	0	0.6	6.5	6.5
					MSLP	401	0	0.8	0.5	0.9
44424	29.3	82.2	2300	3290	SLP	438	0	1.3	-6.2	6.3
					GZ700	436	0	14.0	-48.8	50.8
47020	41.0	126.6	306	677	SLP	719	0	1.1	0.1	1.1
					MSLP	719	0	2.2	9.1	9.4
48065	20.1	94.9	75	98	SLP	4	0	0.5	2.2	2.3
					MSLP	477	0	1.0	-5.9	6.0
48961	14.2	103.5	23	42	SLP	718	0	1.6	1.3	2.1
					MSLP	718	0	1.6	4.1	4.4
48963	12.8	102.6	170	353	SLP	636	65	4.4	-0.8	4.5
					MSLP	636	68	1.0	1.1	1.5

RUSSIAN FEDERATION IN ASIA

31445 - Positive bias of O-G at the mean sea level (Figures 69 and 70)

KAZAKHSTAN

38318 - Negative bias of O-G at the mean sea level (Figures 71 and 72)

OMAN

41249 - Large deviation of O-G at 850 hPa or 700 hPa (Figures 73 and 74)

YEMEN

41396 - Positive bias of O-G at the station level (Figures 75 and 76)

The positive bias of O-G at the station level appears to have been observed since March 2023.

NEPAL

44424 - Negative bias of O-G at the station level (Figures 26 and 77)

KOREA, DEMOCRATIC PEOPLE'S REPUBLIC OF

47020 - Positive bias of O-G at the mean sea level (Figures 43 and 78)

MYANMAR

48065 - Negative bias of O-G at the mean sea level (Figures 79 and 80)

CAMBODIA

48961 - Positive bias of O-G at the mean sea level (Figures 81 and 82)

48963 - Mostly positive bias of O-G at the station level and the mean sea level (Figure 83)

4.3 Stations improved and excluded from the previous consolidated list

IRAN, ISLAMIC REPUBLIC OF

40877 - The negative bias of O-G at the mean sea level has improved since January 2023. (Figure 84)

5. Possible Causes of Remarkable and Sustained Biases

The following are possible causes of remarkable and sustained biases

(i) The barometer used for observation is not correctly calibrated.

(ii) The latitude, longitude or altitude of the station in OSCAR/Surface has not been updated in a timely and appropriate manner. This could result in remarkable biases because it may cause incorrect calculated first-guess field values.

(iii) Biases are specific to the NWP model used in quality monitoring.
Note: Model biases are likely to appear in relatively large areas.

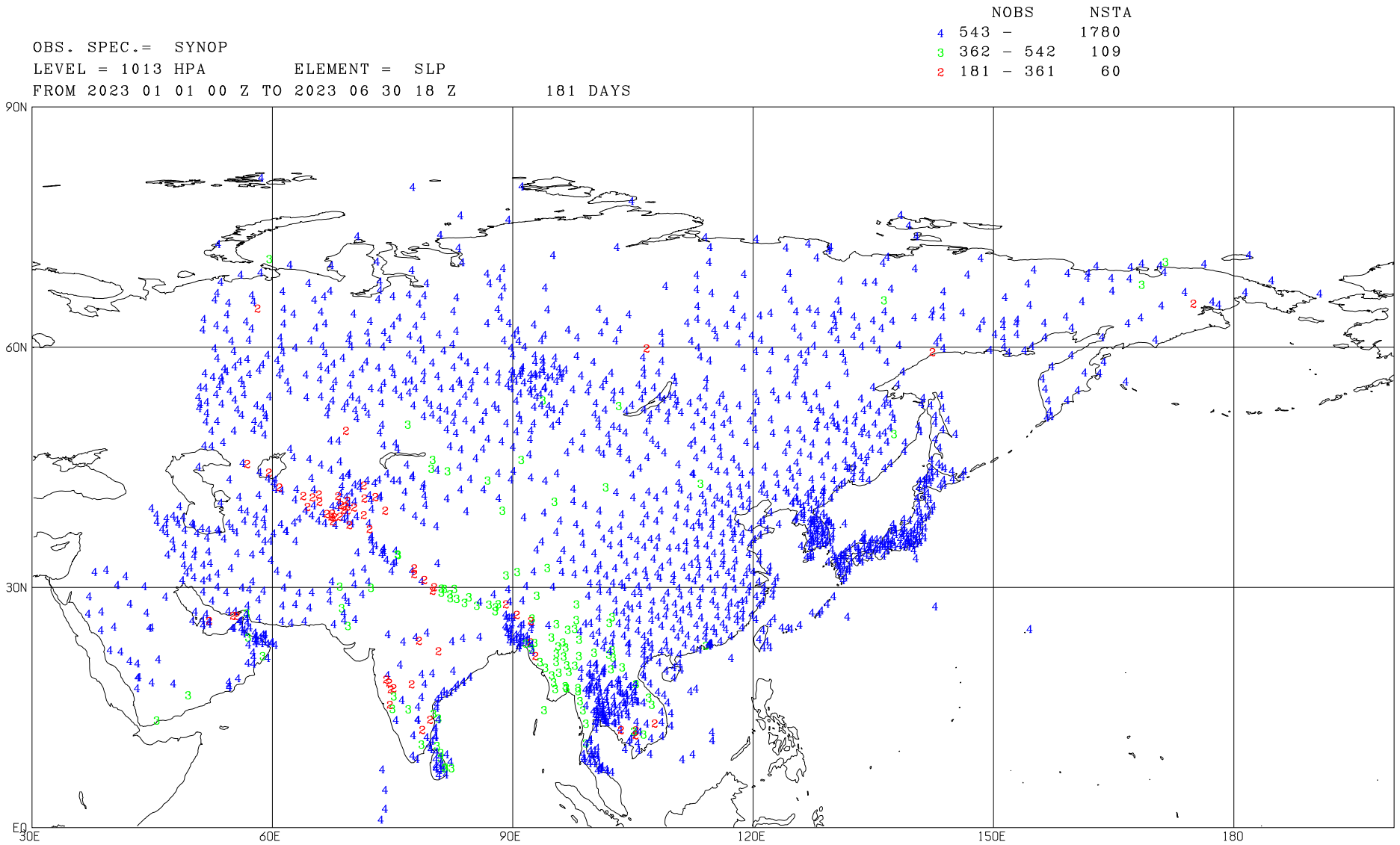

Figure 1(a) Location of all land surface stations reporting station level pressure (SLP) observations in Region II over the six-month period from January to June 2023. Numbers (2, 3, 4) show the total number of observations (NOBS) received at RSMC Tokyo. The total numbers of stations (NSTA) reporting SLP are shown at the top of the figure.

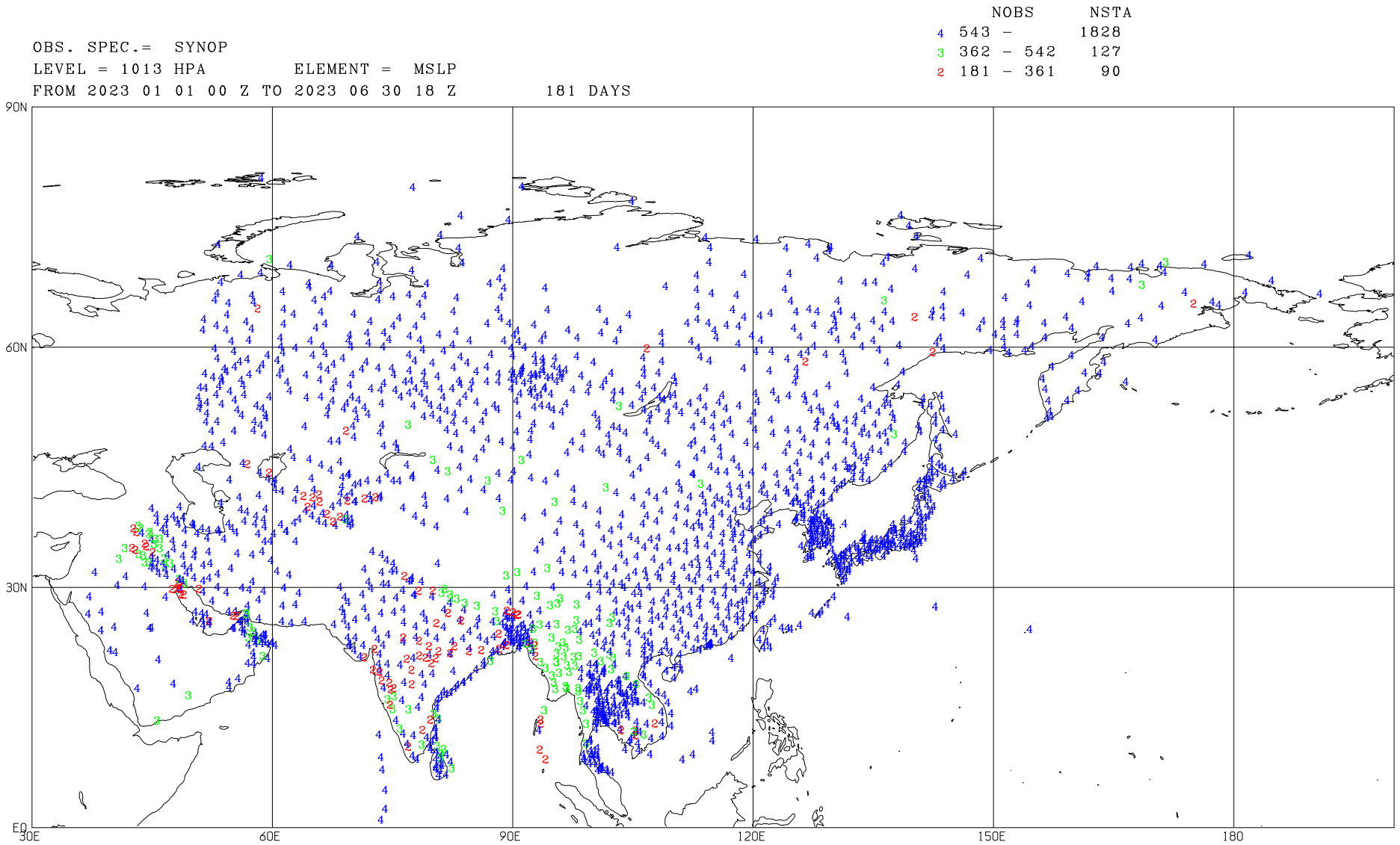

Figure 1(b) Location of all land surface stations reporting mean sea level pressure (MSLP) observations in Region II over the six-month period from January to June 2023. Numbers (2, 3, 4) show the total number of observations (NOBS) received at RSMC Tokyo. The total numbers of stations (NSTA) reporting MSLP are shown at the top of the figure.

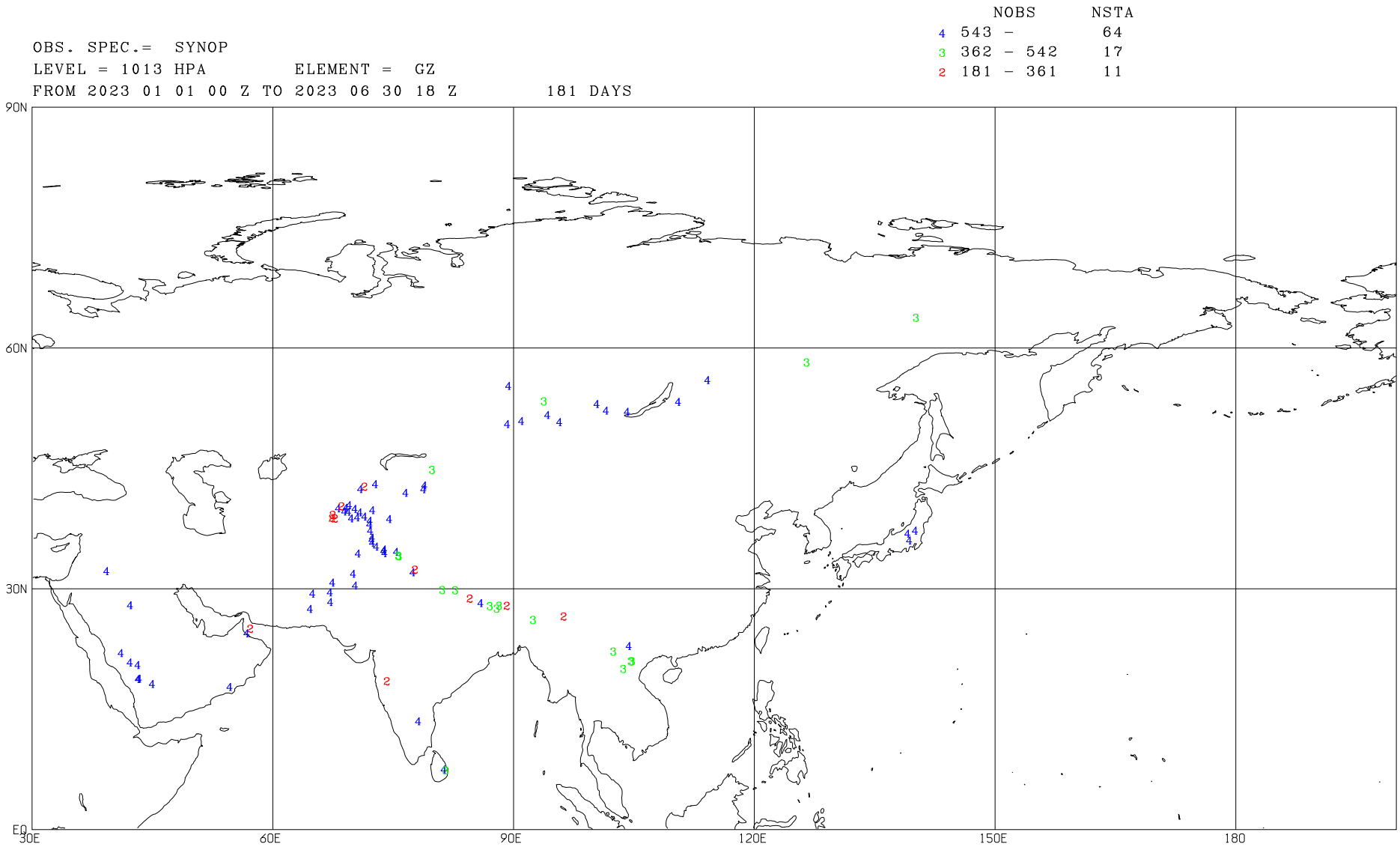

Figure 1(c) Location of all land surface stations reporting geopotential height (GZ) observations in Region II over the six-month period from January to June 2023. Numbers (2, 3, 4) show the total number of observations (NOBS) received at RSMC Tokyo. The total numbers of stations (NSTA) reporting GZ are shown at the top of the figure.

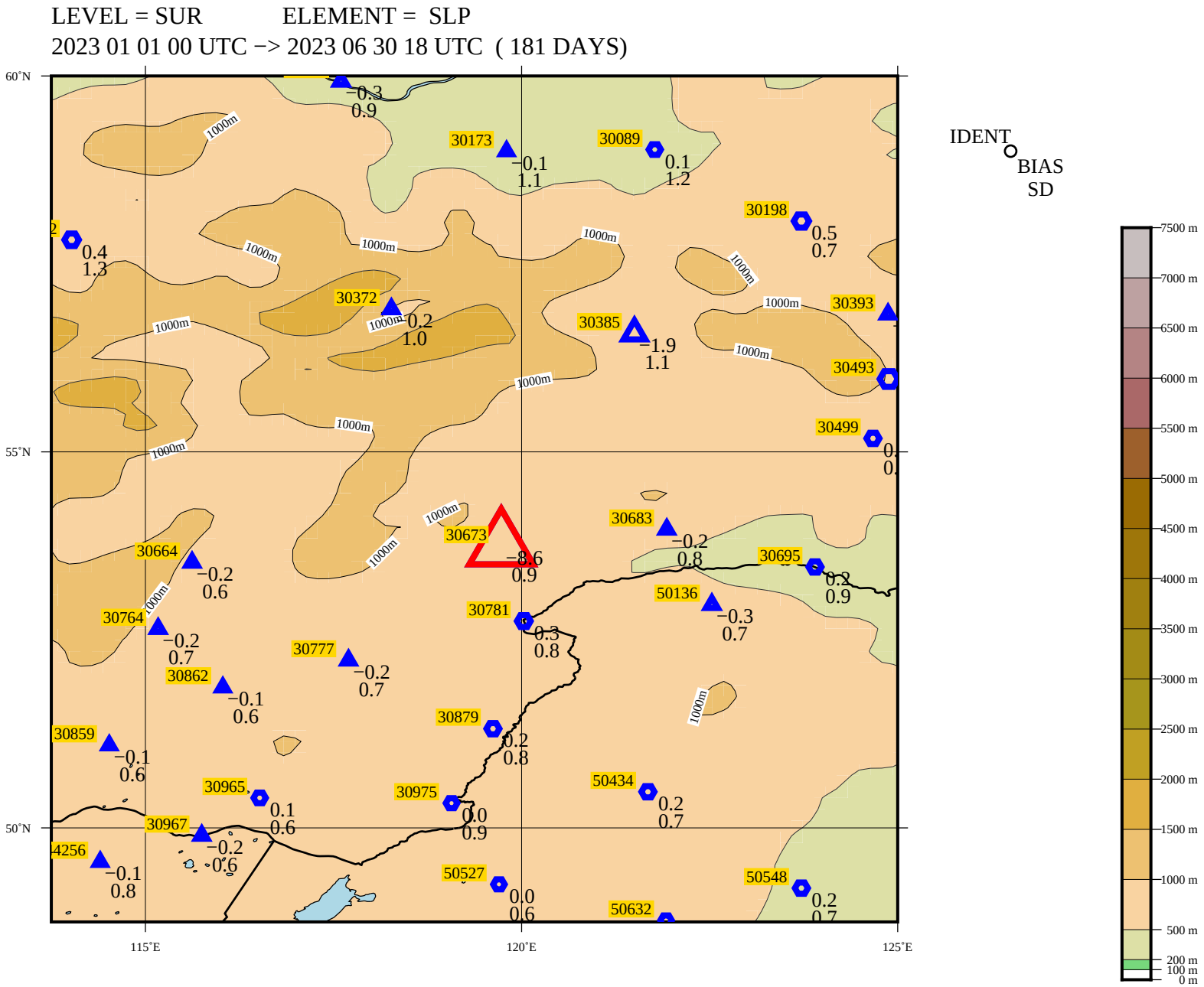

Figure 2 BIAS and SD of SLP for station 30673 (red) and surrounding stations (blue).
The number to the upper left of each symbol is the WMO IDENT, and those to the lower right are the values of BIAS and SD.
The size of each symbol is proportional to the value of BIAS, with hexagonal forms representing positive bias and triangular forms representing negative bias.

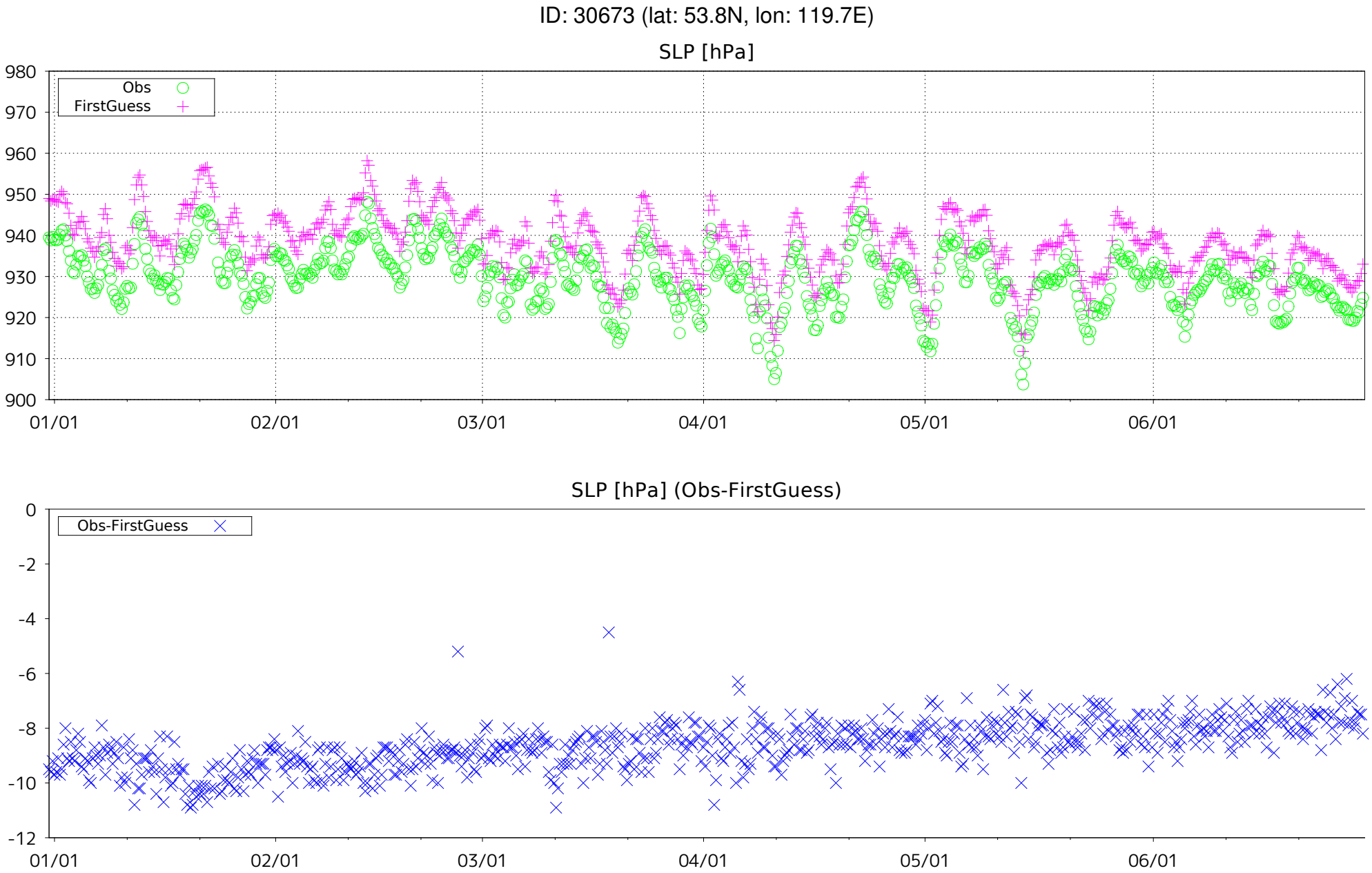

Figure 3 Time-series representation of SLP Obs minus FirstGuess for station 30673

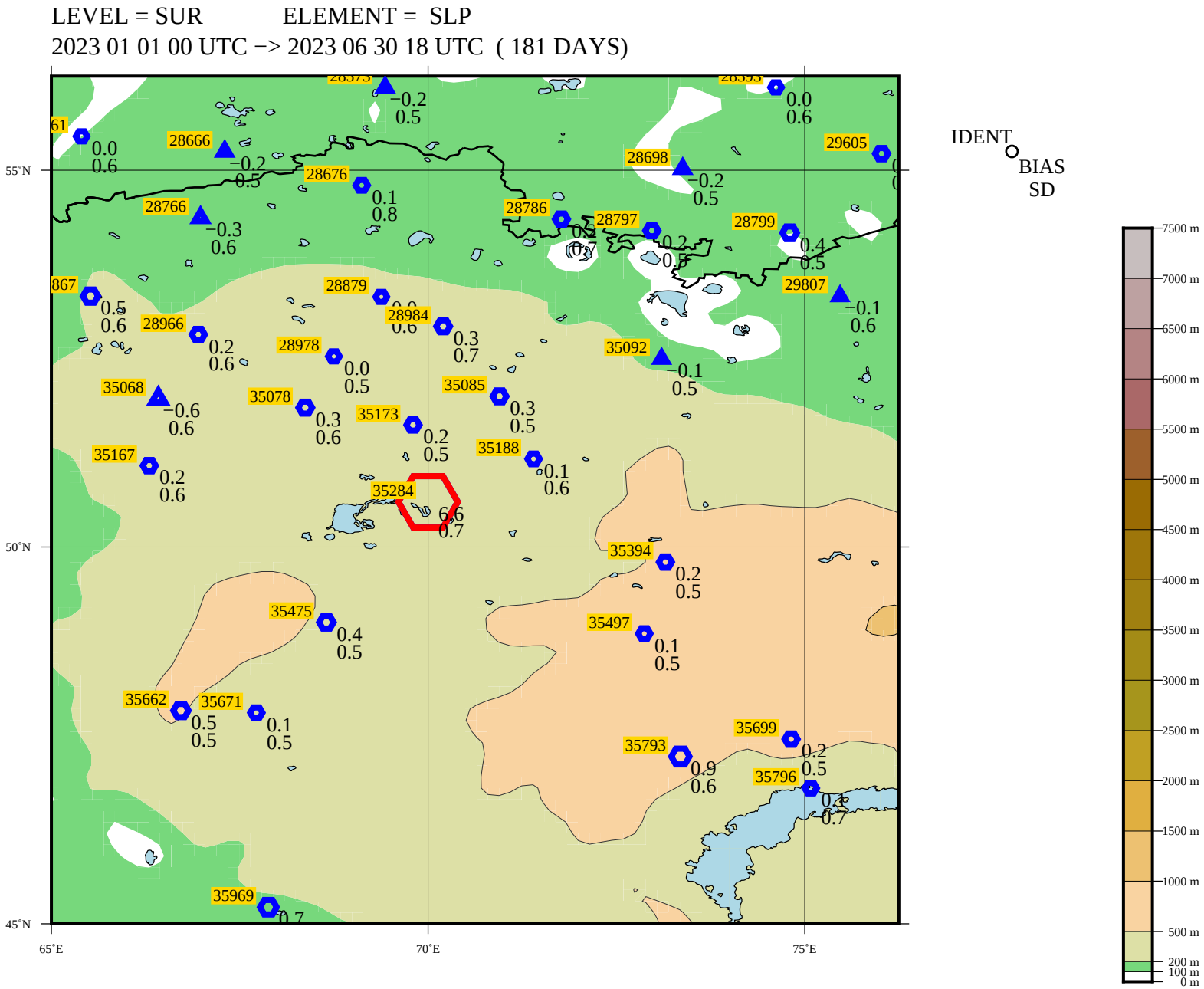

Figure 4 BIAS and SD of SLP for station 35284 (red) and surrounding stations (blue).
The number to the upper left of each symbol is the WMO IDENT, and those to the lower right are the values of BIAS and SD.
The size of each symbol is proportional to the value of BIAS, with hexagonal forms representing positive bias and triangular forms representing negative bias.

Figure 5 Time-series representation of SLP Obs minus FirstGuess for station 35284

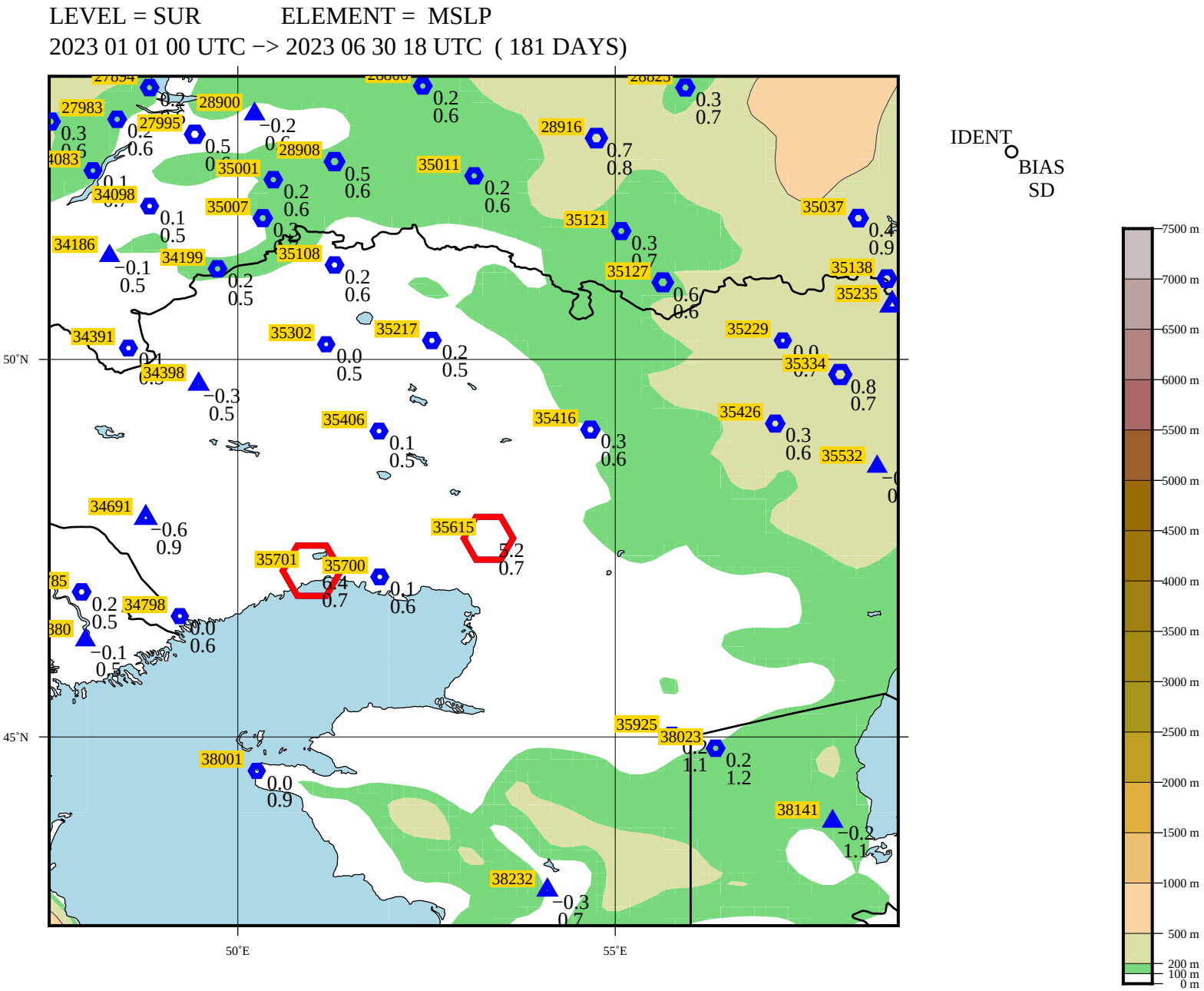

Figure 6 BIAS and SD of MSLP for station 35615, 35701 (red) and surrounding stations (blue).
The number to the upper left of each symbol is the WMO IDENT, and those to the lower right are the values of BIAS and SD.
The size of each symbol is proportional to the value of BIAS, with hexagonal forms representing positive bias and triangular forms representing negative bias.

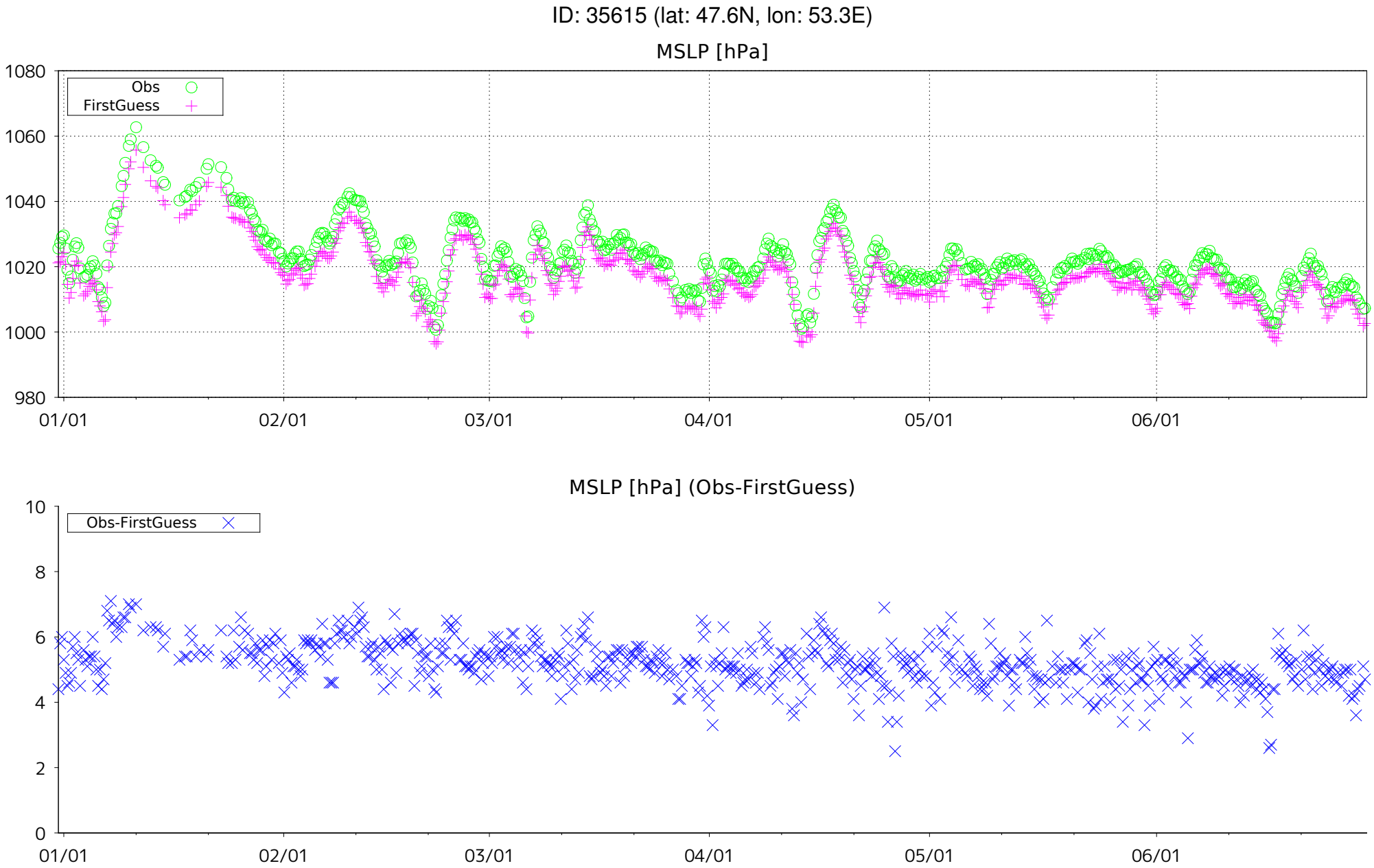

Figure 7 Time-series representation of MSLP Obs minus FirstGuess for station 35615

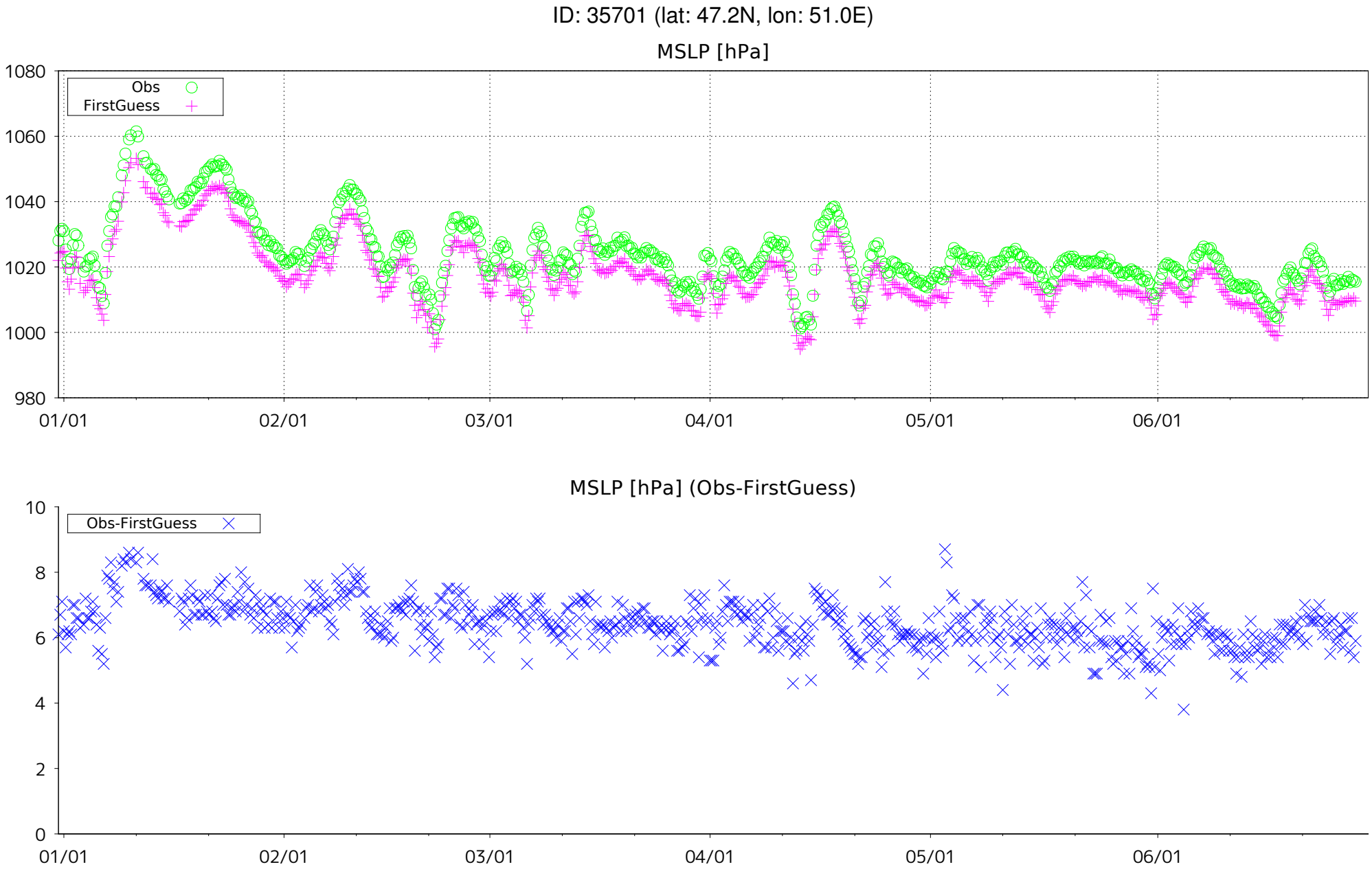

Figure 8 Time-series representation of MSLP Obs minus FirstGuess for station 35701

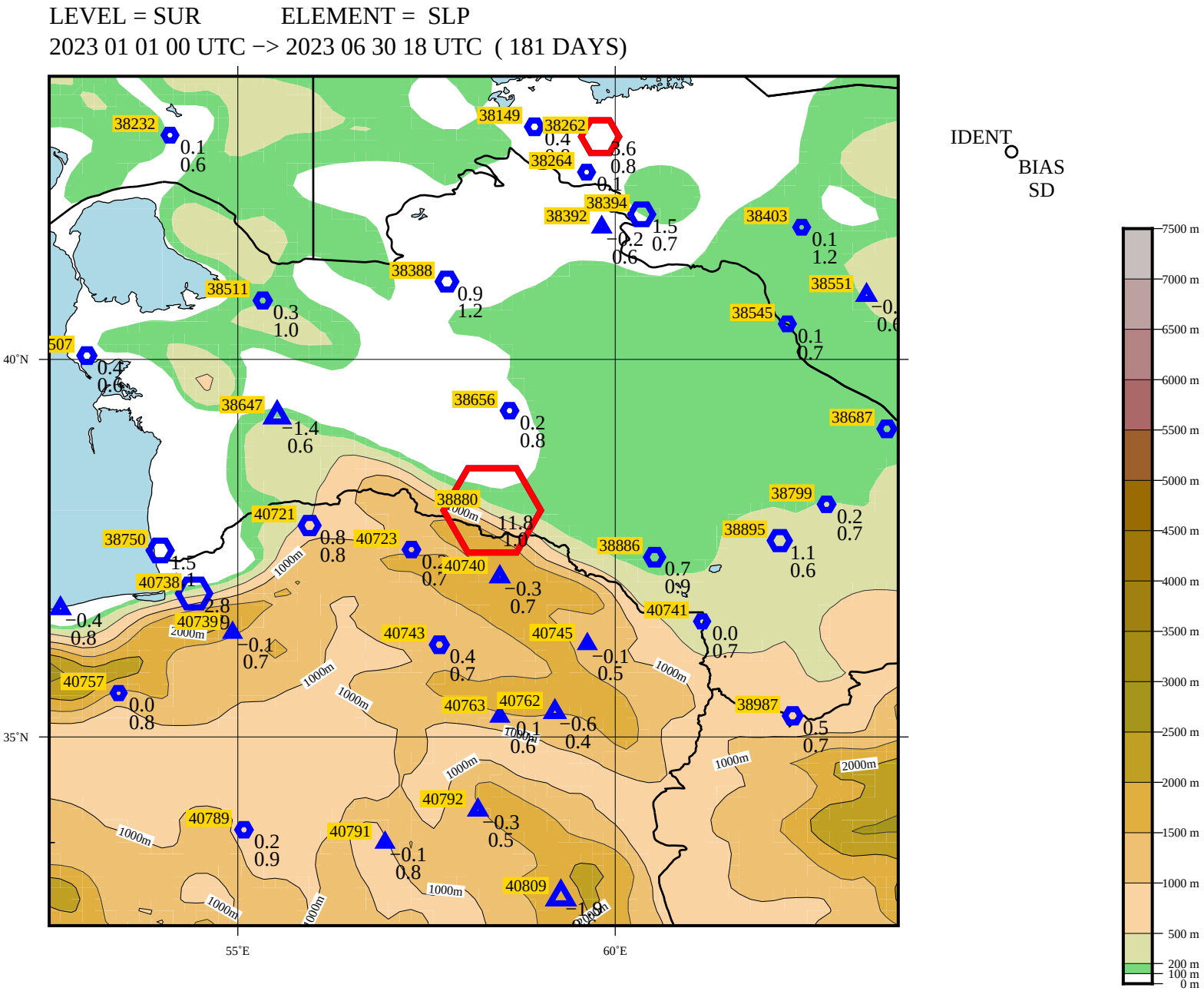

Figure 9 BIAS and SD of SLP for station 38262, 38880 (red) and surrounding stations (blue).
The number to the upper left of each symbol is the WMO IDENT, and those to the lower right are the values of BIAS and SD.
The size of each symbol is proportional to the value of BIAS, with hexagonal forms representing positive bias and triangular forms representing negative bias.

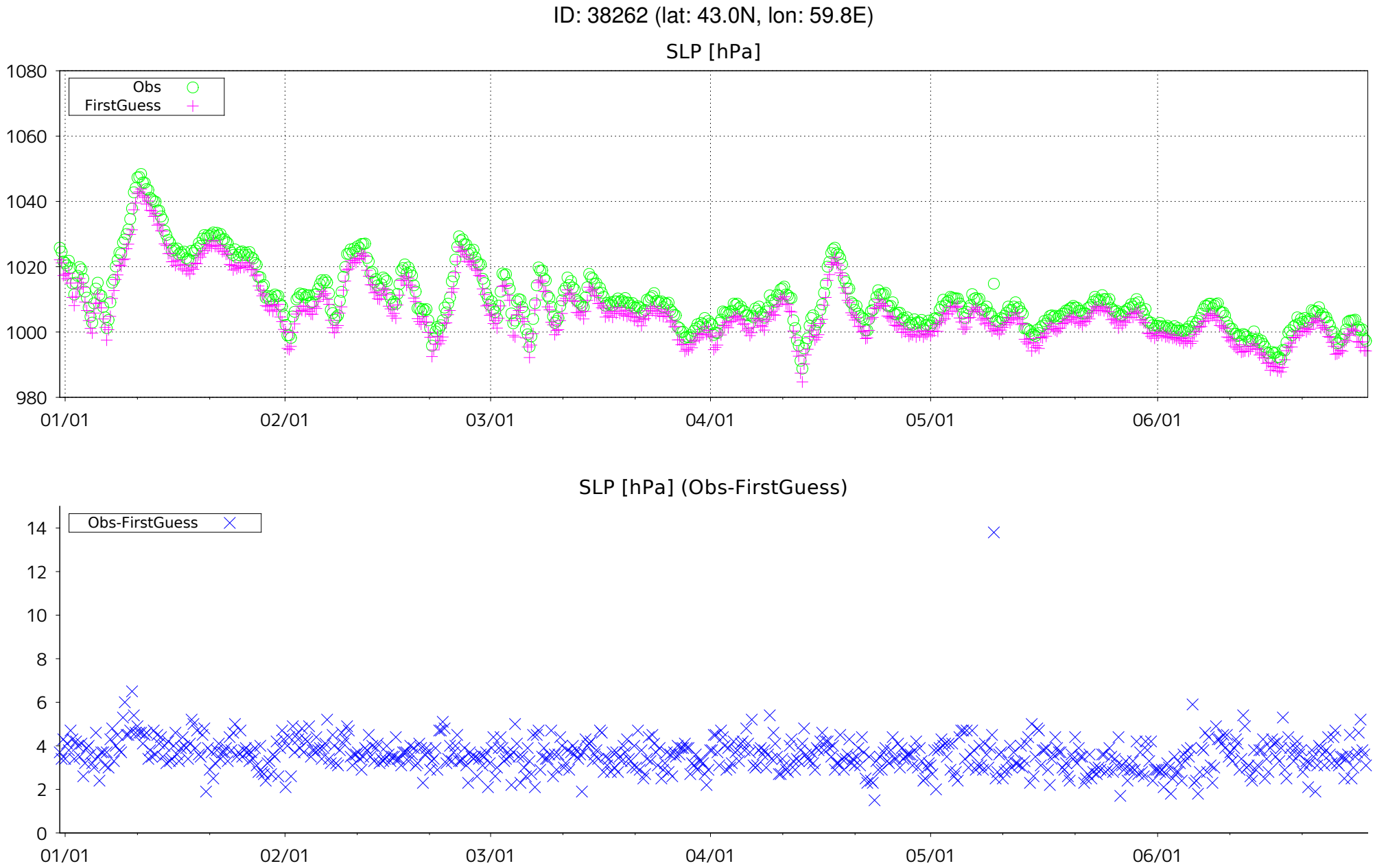

Figure 10 Time-series representation of SLP Obs minus FirstGuess for station 38262

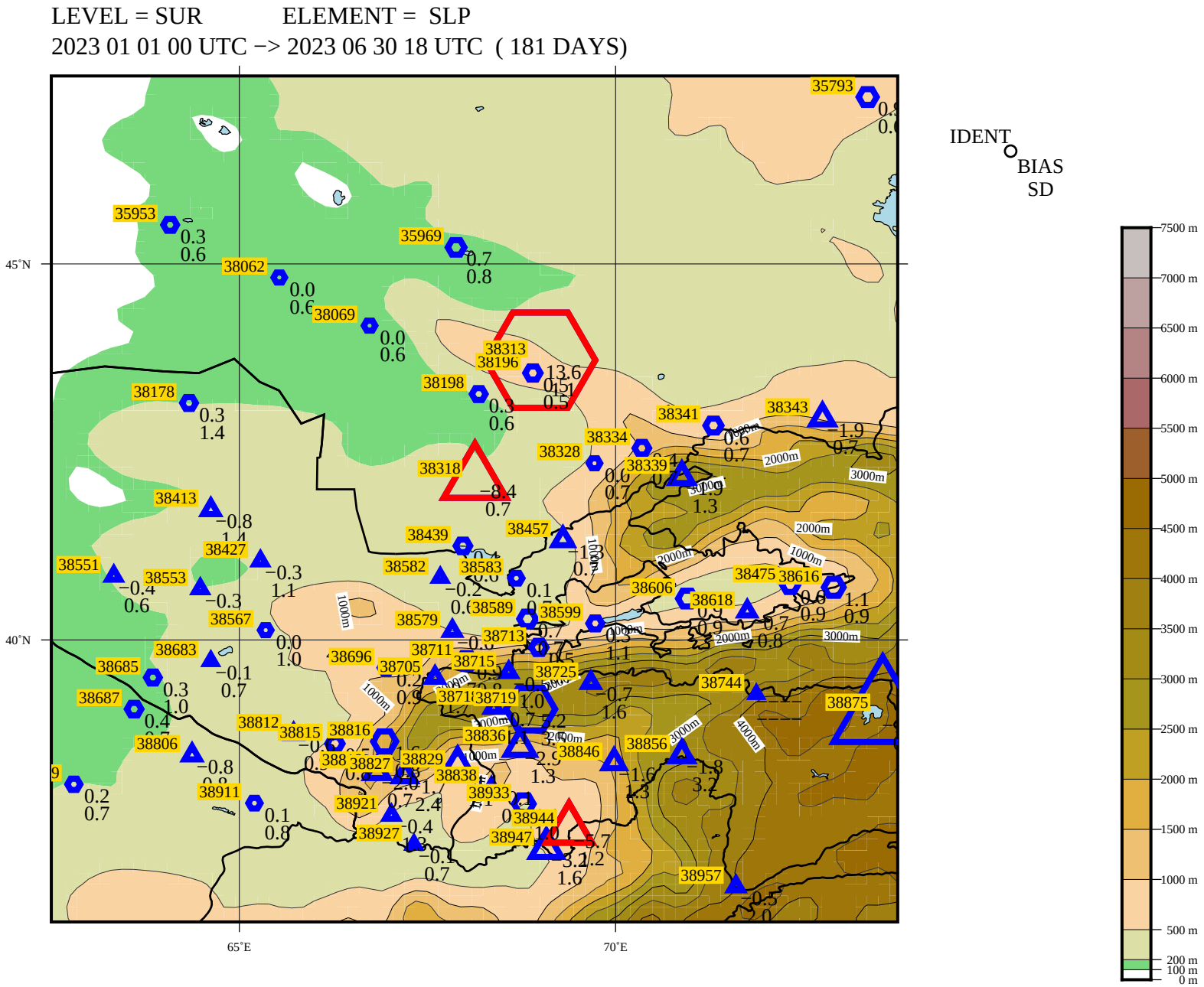

Figure 11 BIAS and SD of SLP for station 38313, 38318, 38944 (red) and surrounding stations (blue).
The number to the upper left of each symbol is the WMO IDENT, and those to the lower right are the values of BIAS and SD.
The size of each symbol is proportional to the value of BIAS, with hexagonal forms representing positive bias and triangular forms representing negative bias.

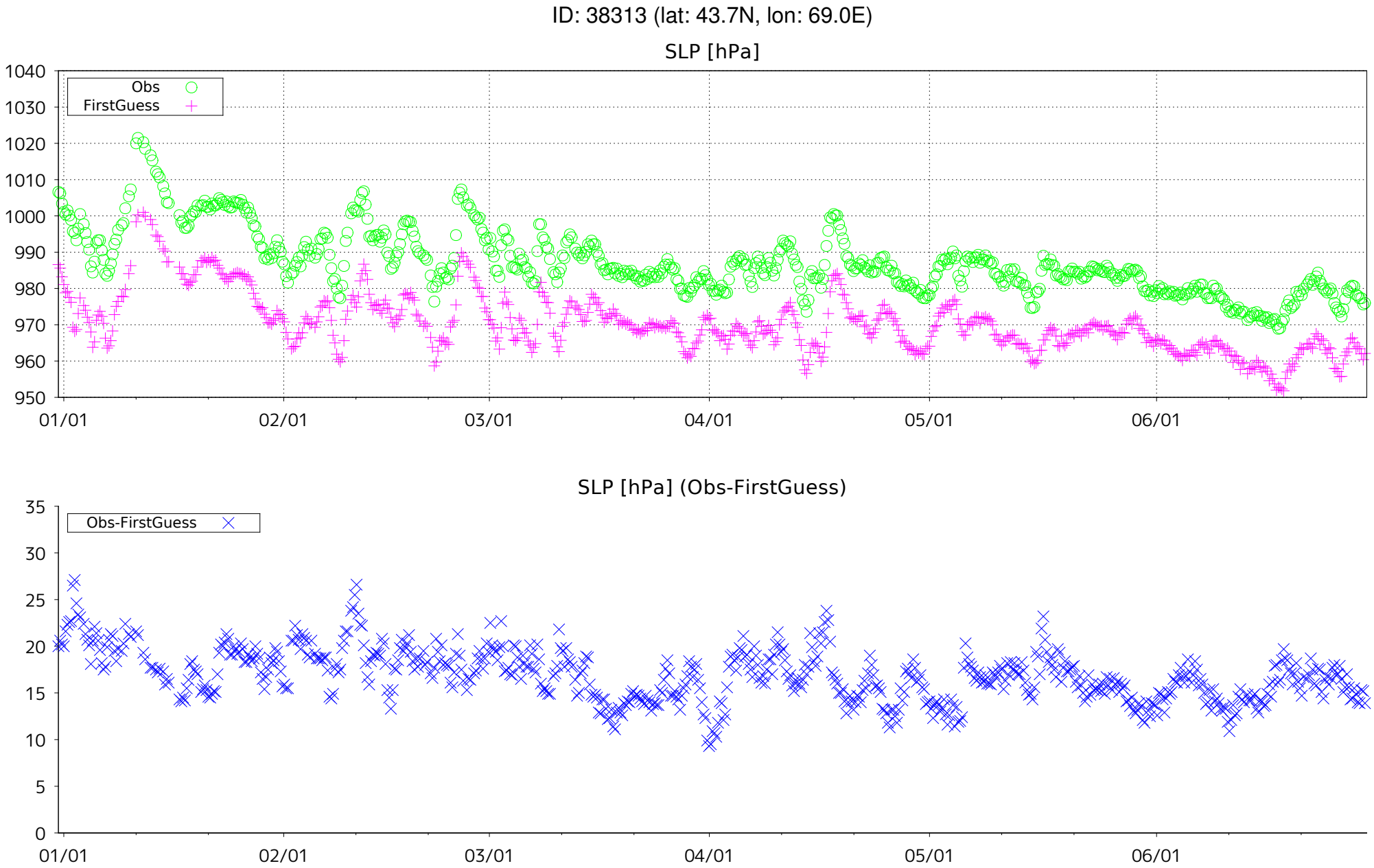

Figure 12 Time-series representation of SLP Obs minus FirstGuess for station 38313

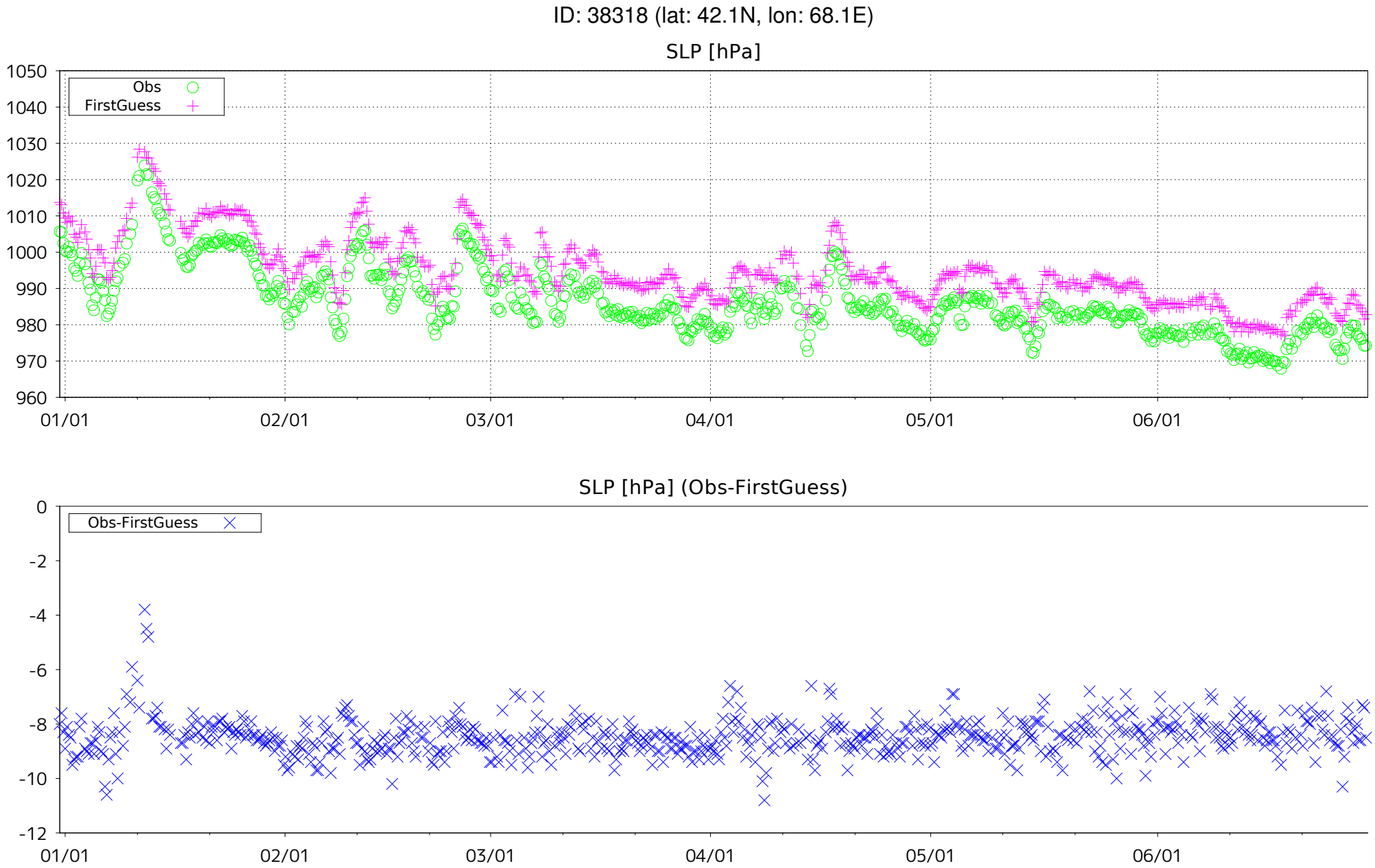

Figure 13 Time-series representation of SLP Obs minus FirstGuess for station 38318

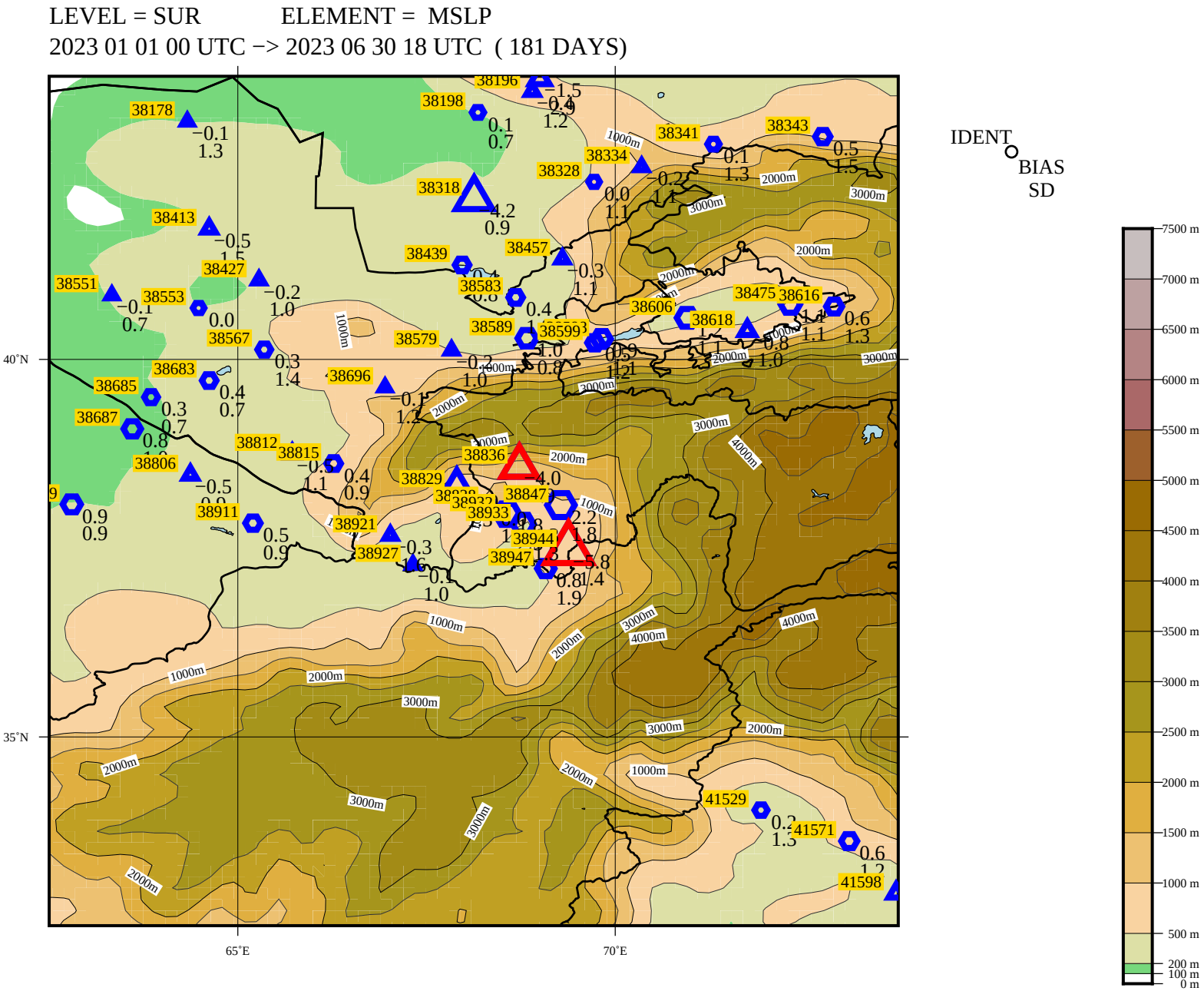

Figure 14 BIAS and SD of MSLP for station 38836, 38944 (red) and surrounding stations (blue).
The number to the upper left of each symbol is the WMO IDENT, and those to the lower right are the values of BIAS and SD.
The size of each symbol is proportional to the value of BIAS, with hexagonal forms representing positive bias and triangular forms representing negative bias.

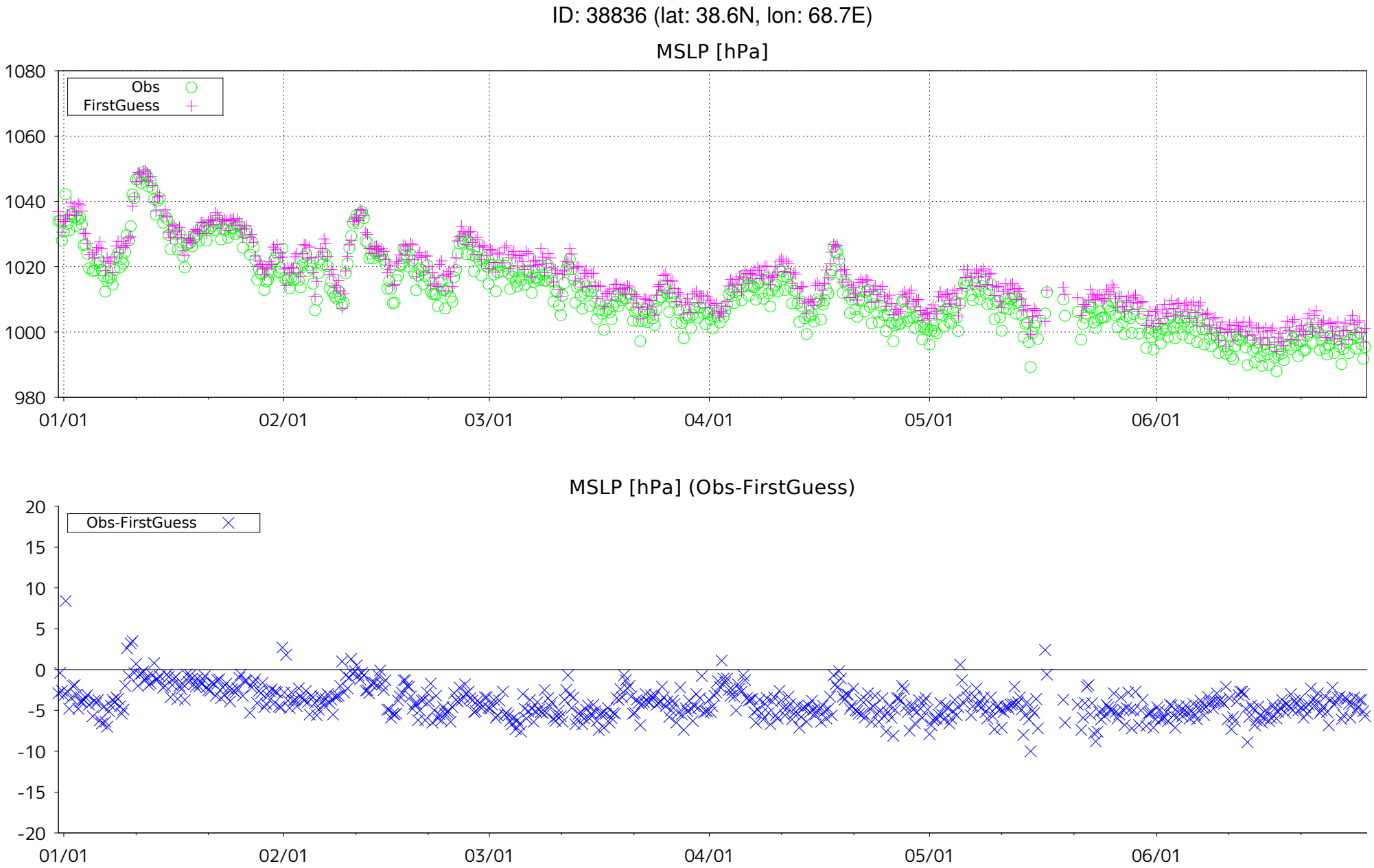

Figure 15 Time-series representation of MSLP Obs minus FirstGuess for station 38836

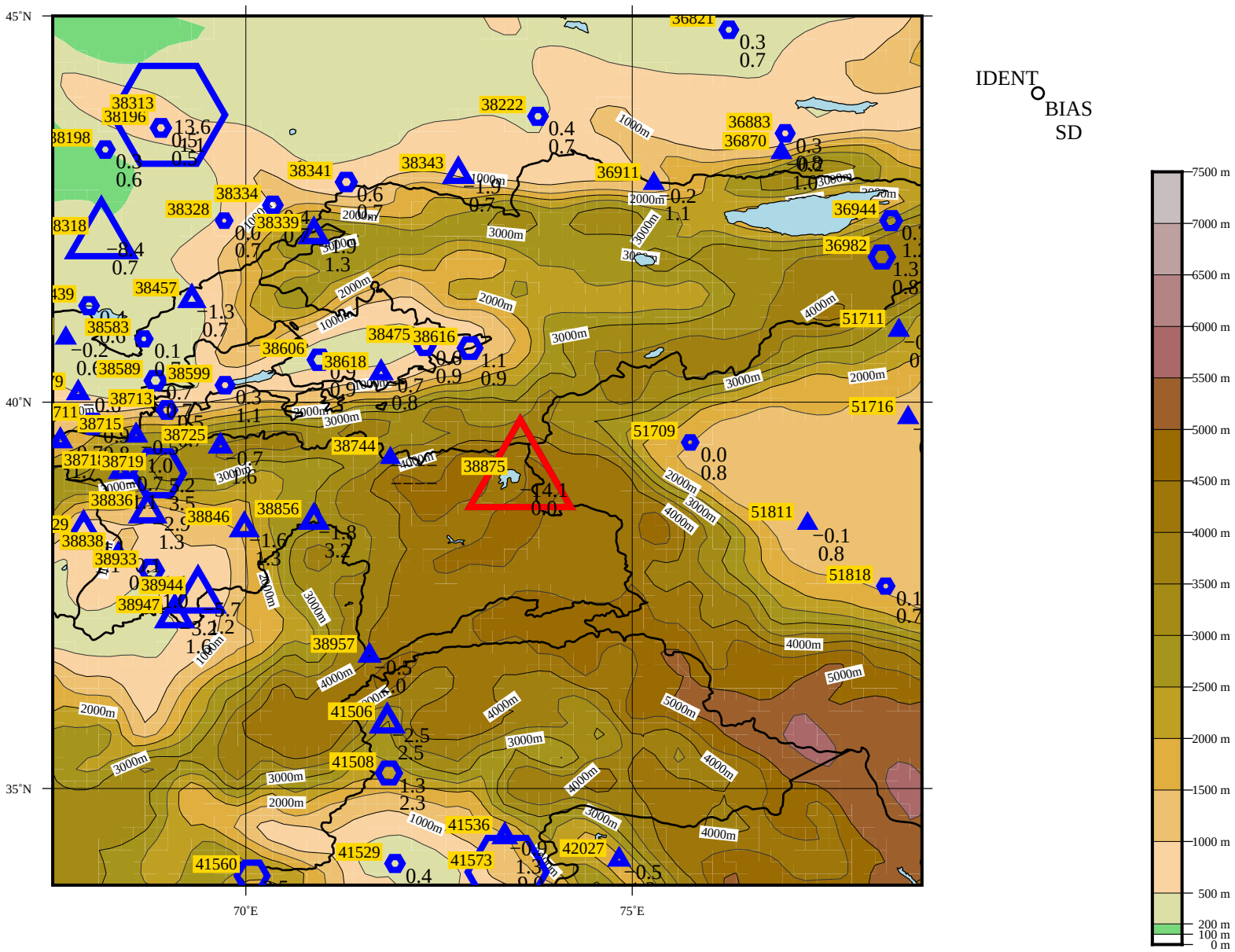

Figure 16 BIAS and SD of SLP for station 38875 (red) and surrounding stations (blue).
The number to the upper left of each symbol is the WMO IDENT, and those to the lower right are the values of BIAS and SD.
The size of each symbol is proportional to the value of BIAS, with hexagonal forms representing positive bias and triangular forms representing negative bias.

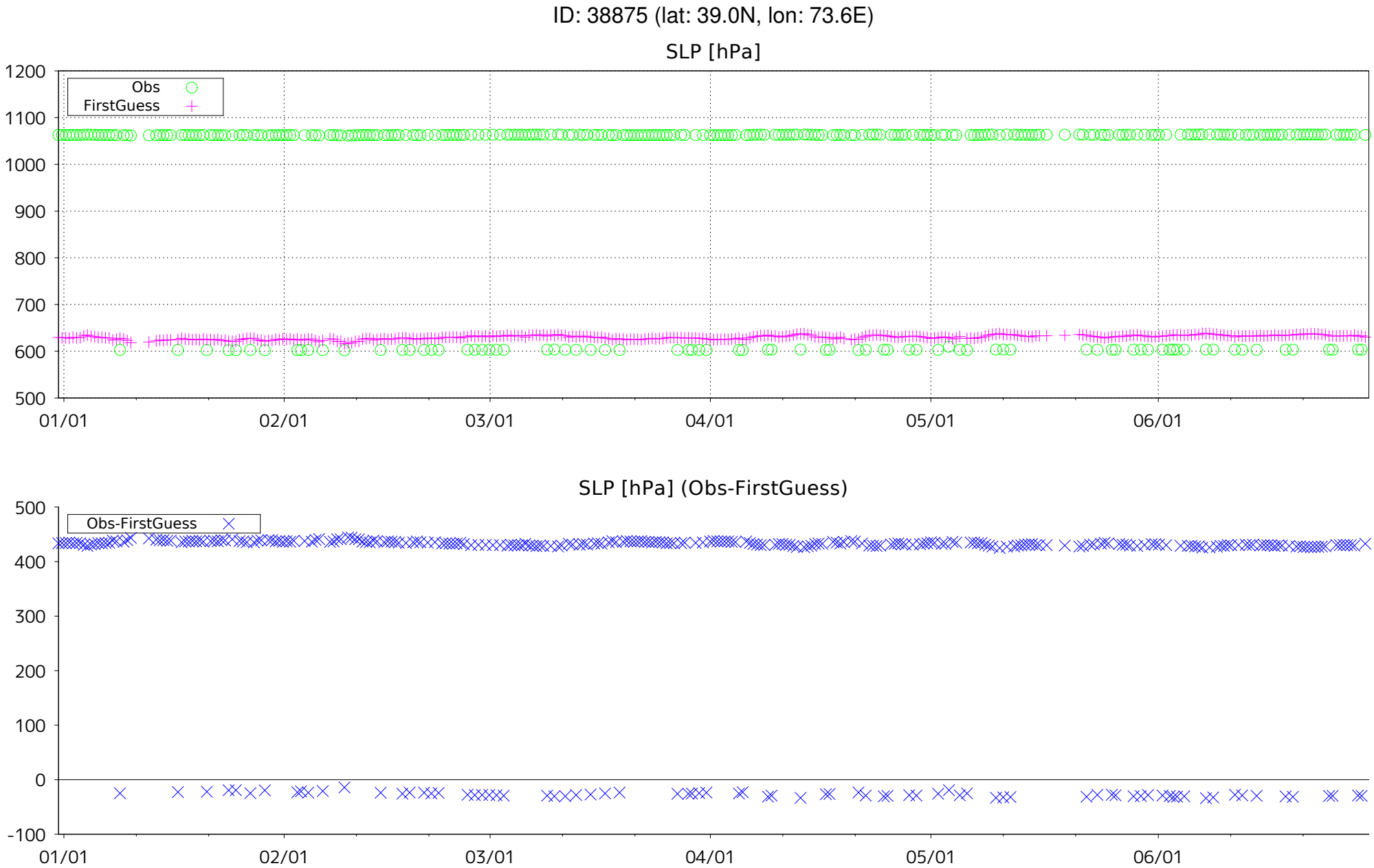

Figure 17 Time-series representation of SLP Obs minus FirstGuess for station 38875

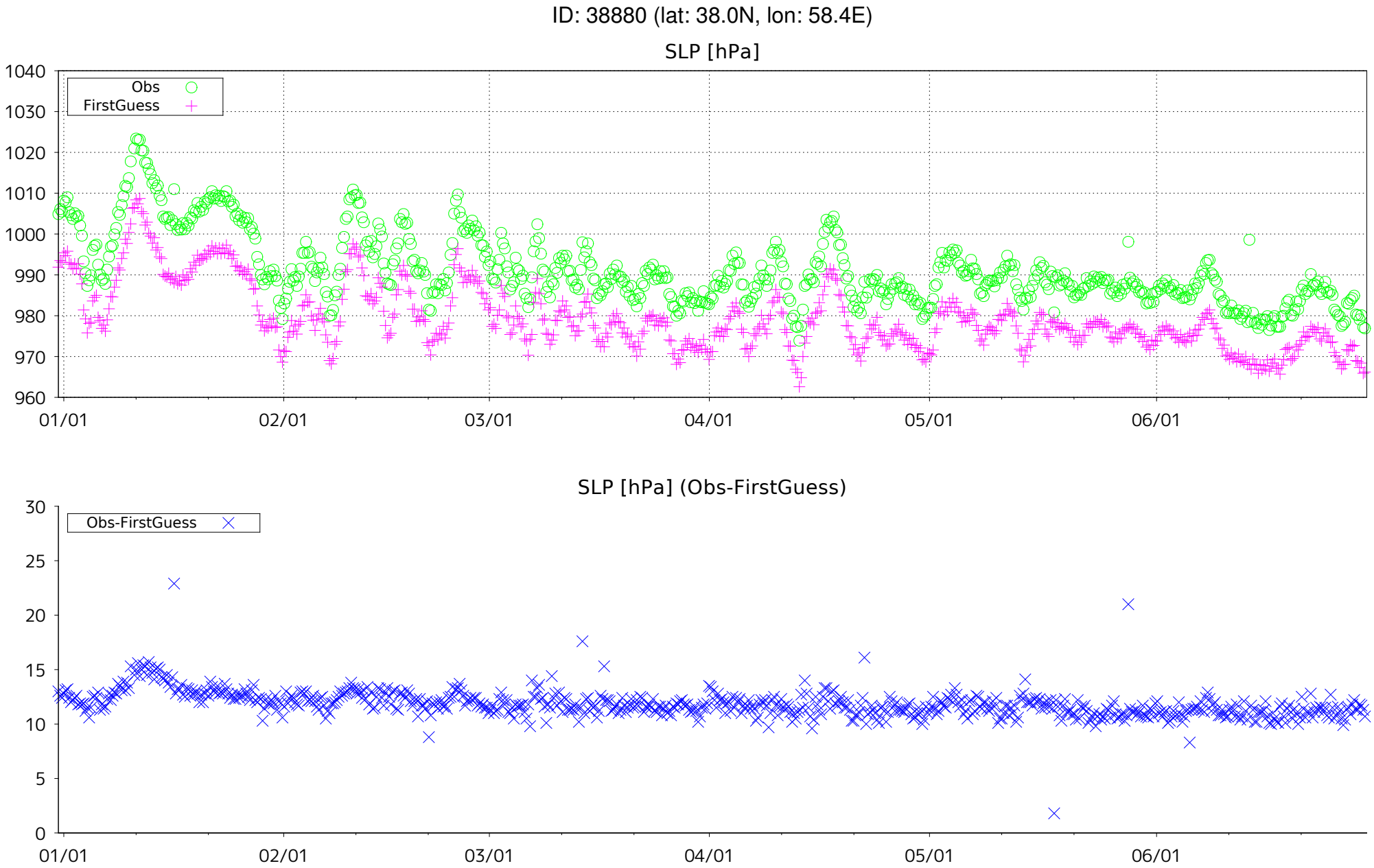

Figure 18 Time-series representation of SLP Obs minus FirstGuess for station 38880

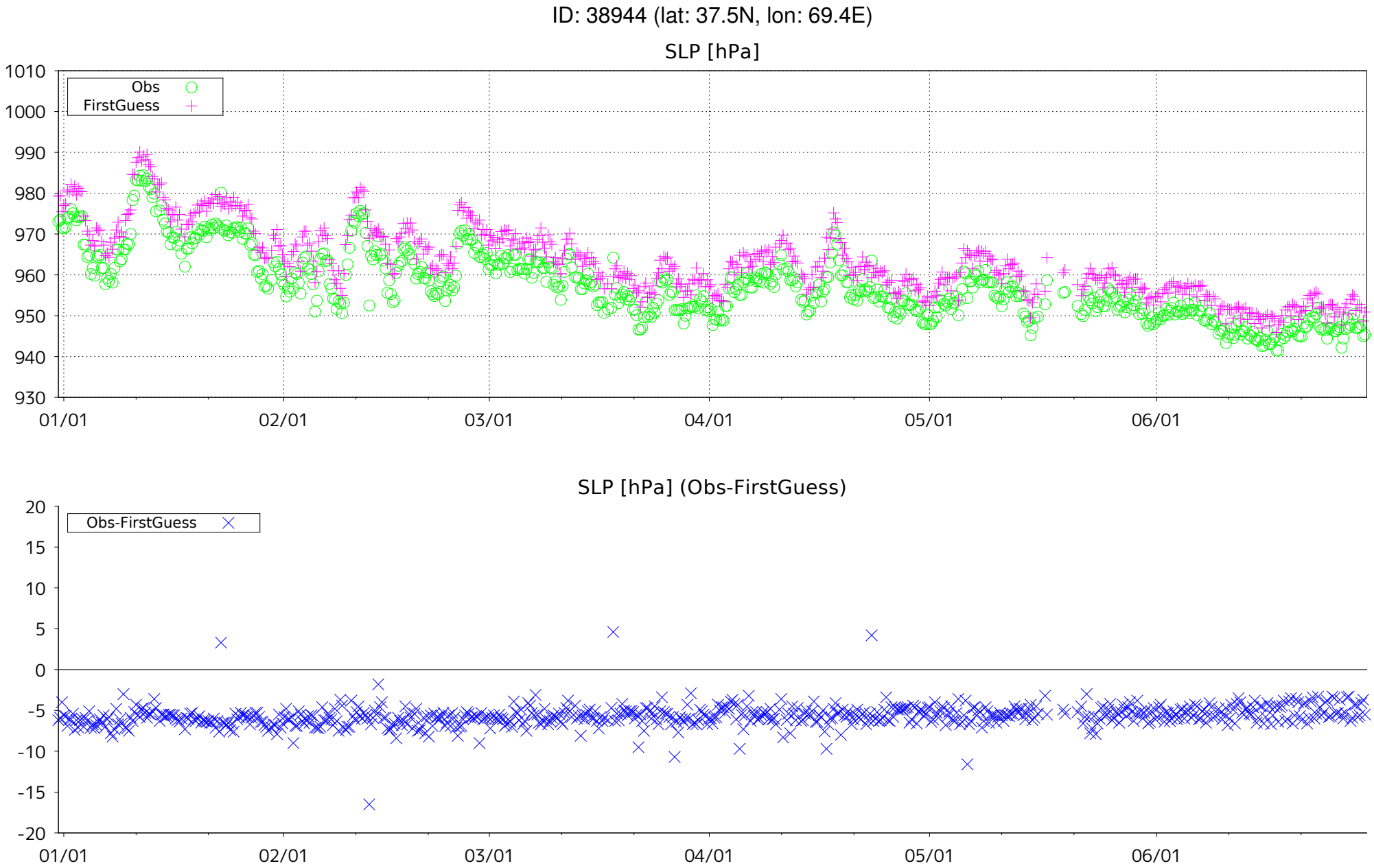

Figure 19(a) Time-series representation of SLP Obs minus FirstGuess for station 38944

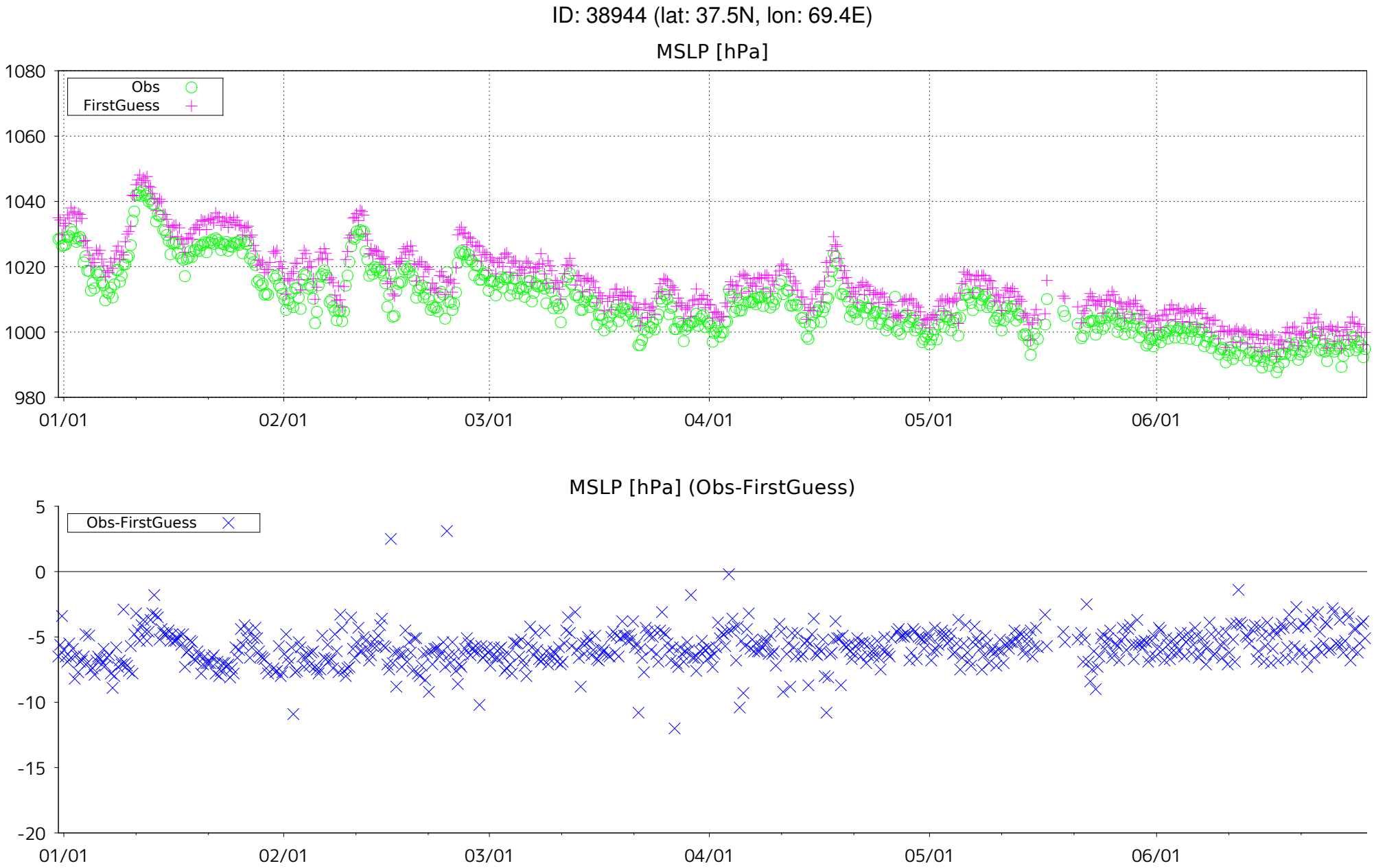

Figure 19(b) Time-series representation of MSLP Obs minus FirstGuess for station 38944

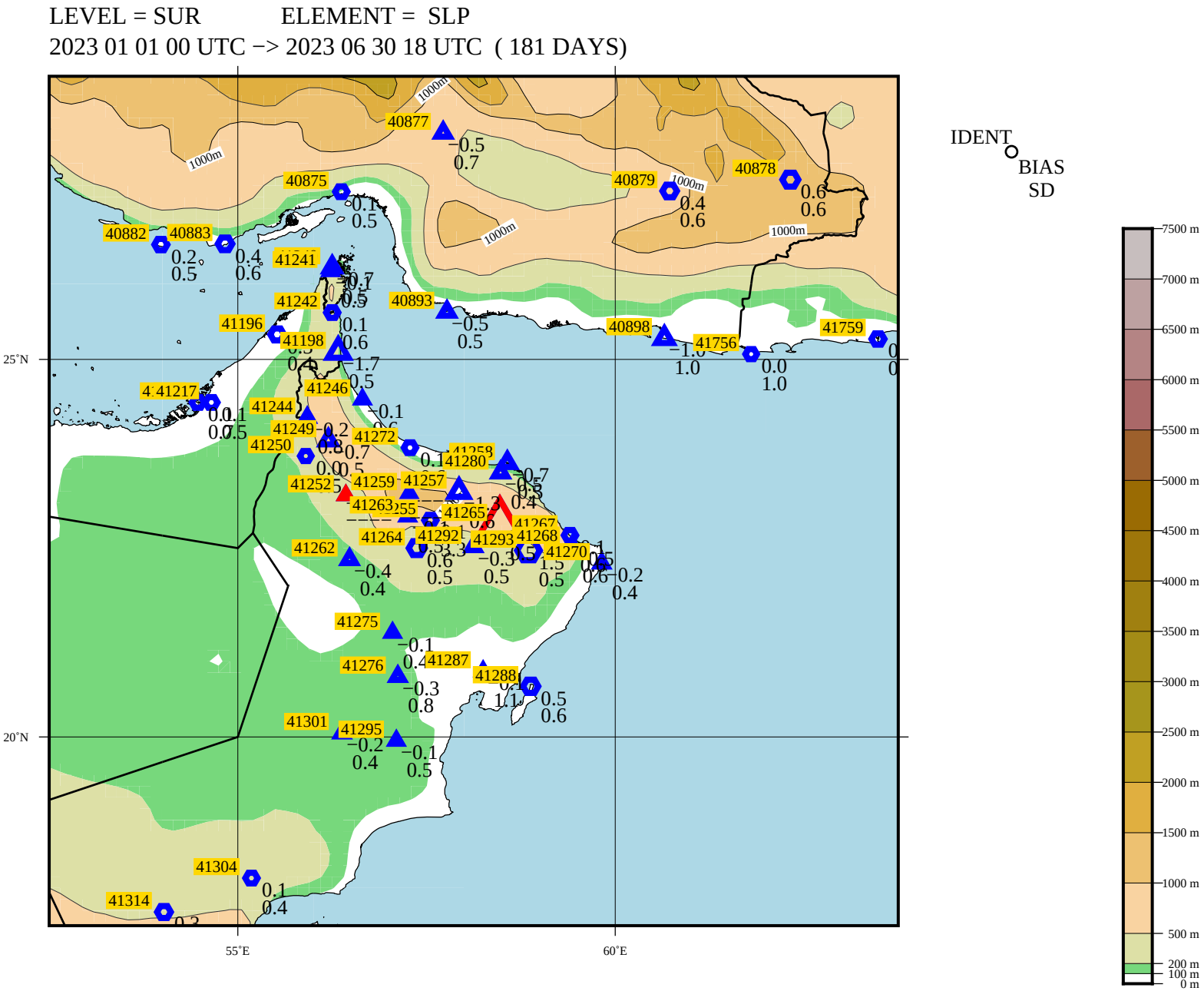

Figure 20 BIAS and SD of SLP for station 41252, 41265 (red) and surrounding stations (blue).
The number to the upper left of each symbol is the WMO IDENT, and those to the lower right are the values of BIAS and SD.
The size of each symbol is proportional to the value of BIAS, with hexagonal forms representing positive bias and triangular forms representing negative bias.

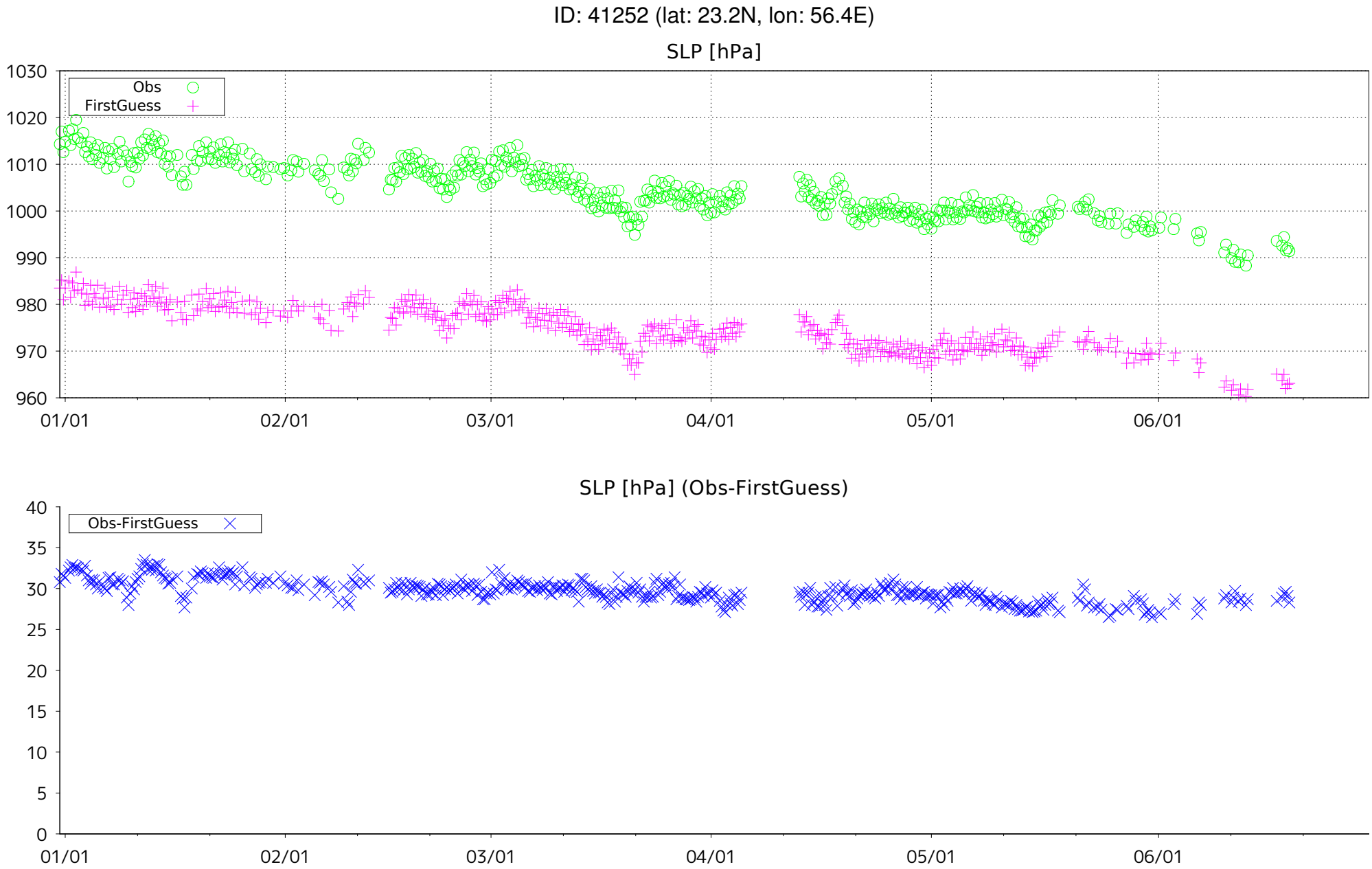

Figure 21 Time-series representation of SLP Obs minus FirstGuess for station 41252

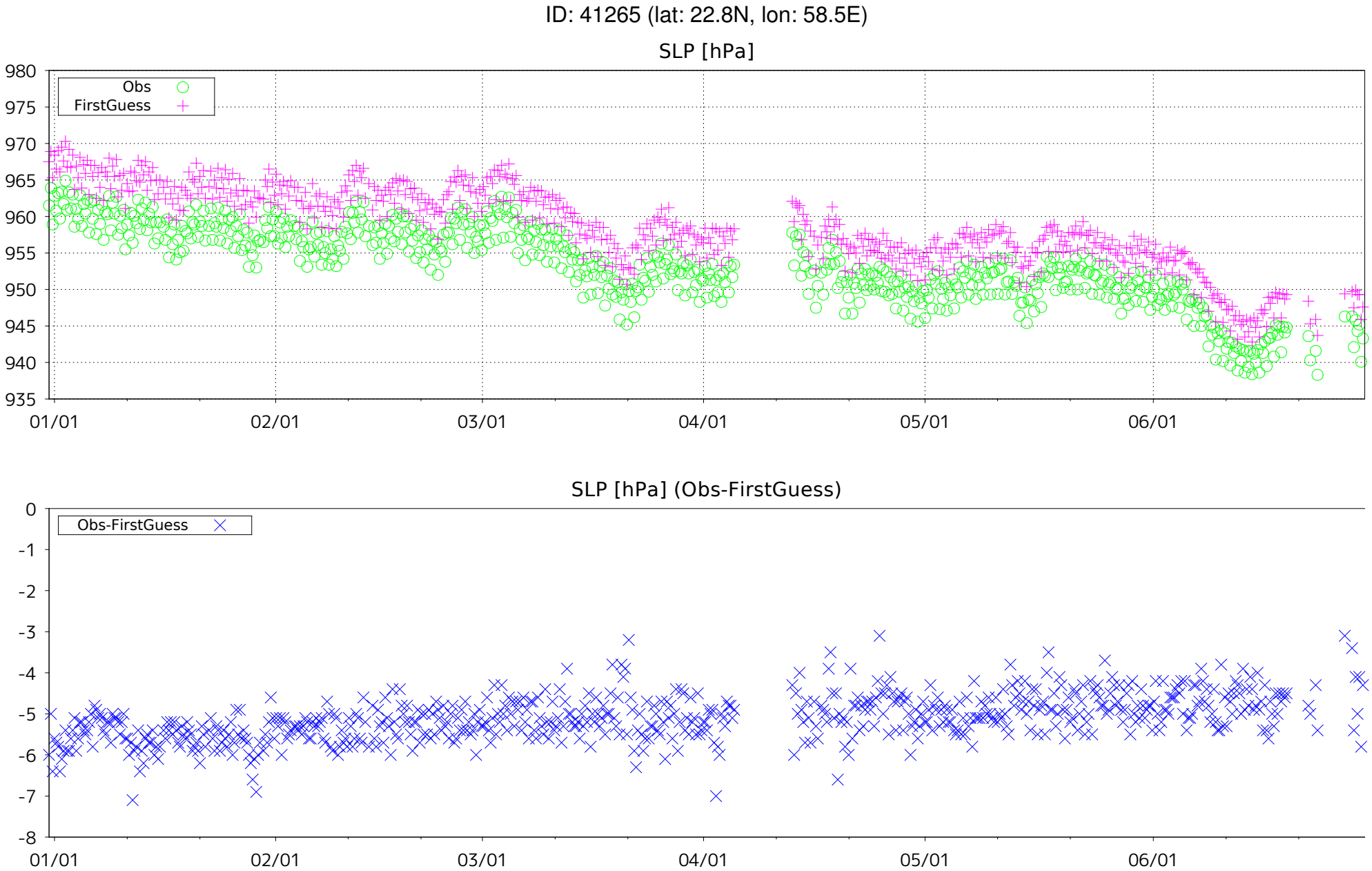

Figure 22 Time-series representation of SLP Obs minus FirstGuess for station 41265

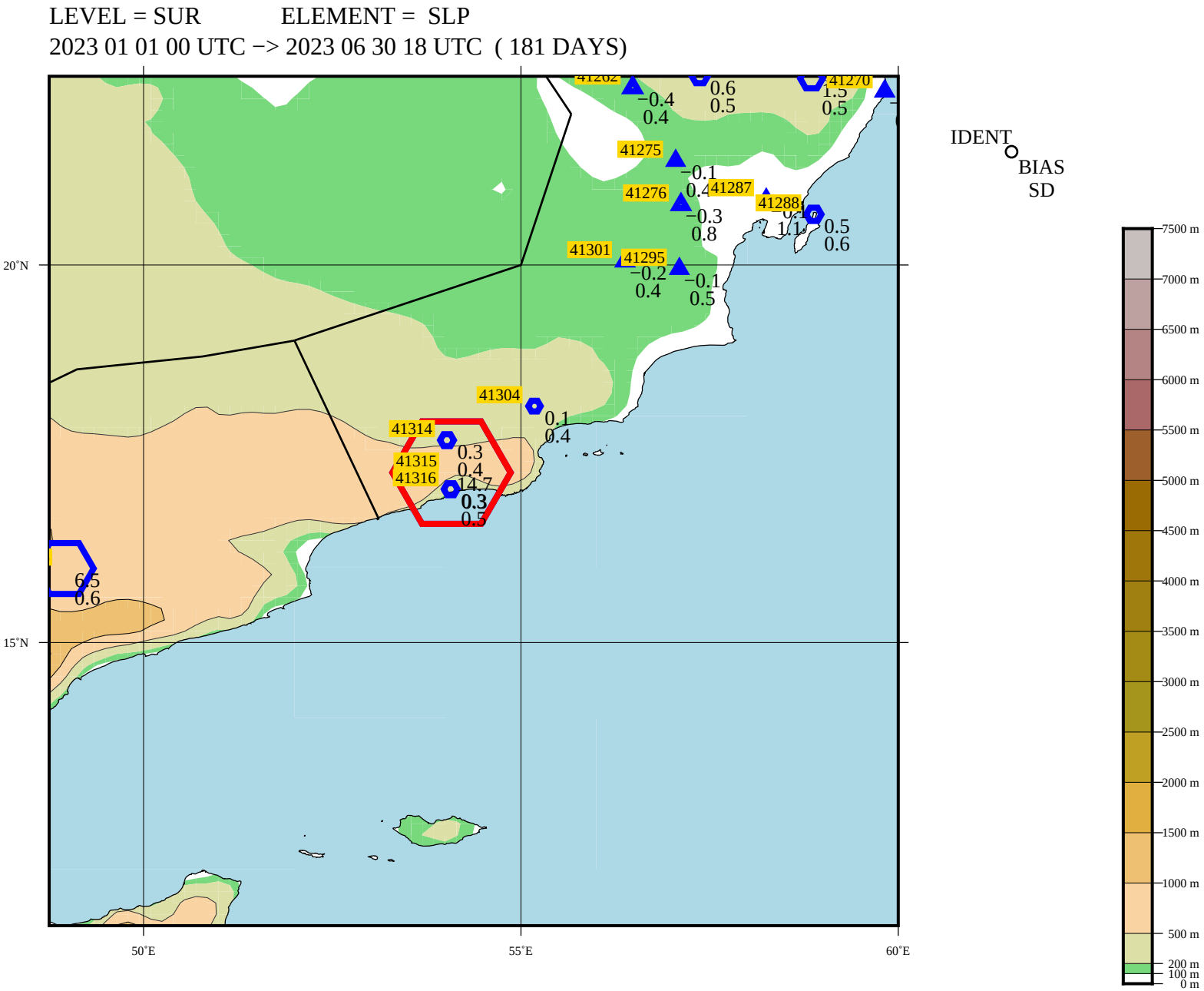

Figure 23 BIAS and SD of SLP for station 41315 (red) and surrounding stations (blue).
The number to the upper left of each symbol is the WMO IDENT, and those to the lower right are the values of BIAS and SD.
The size of each symbol is proportional to the value of BIAS, with hexagonal forms representing positive bias and triangular forms representing negative bias.

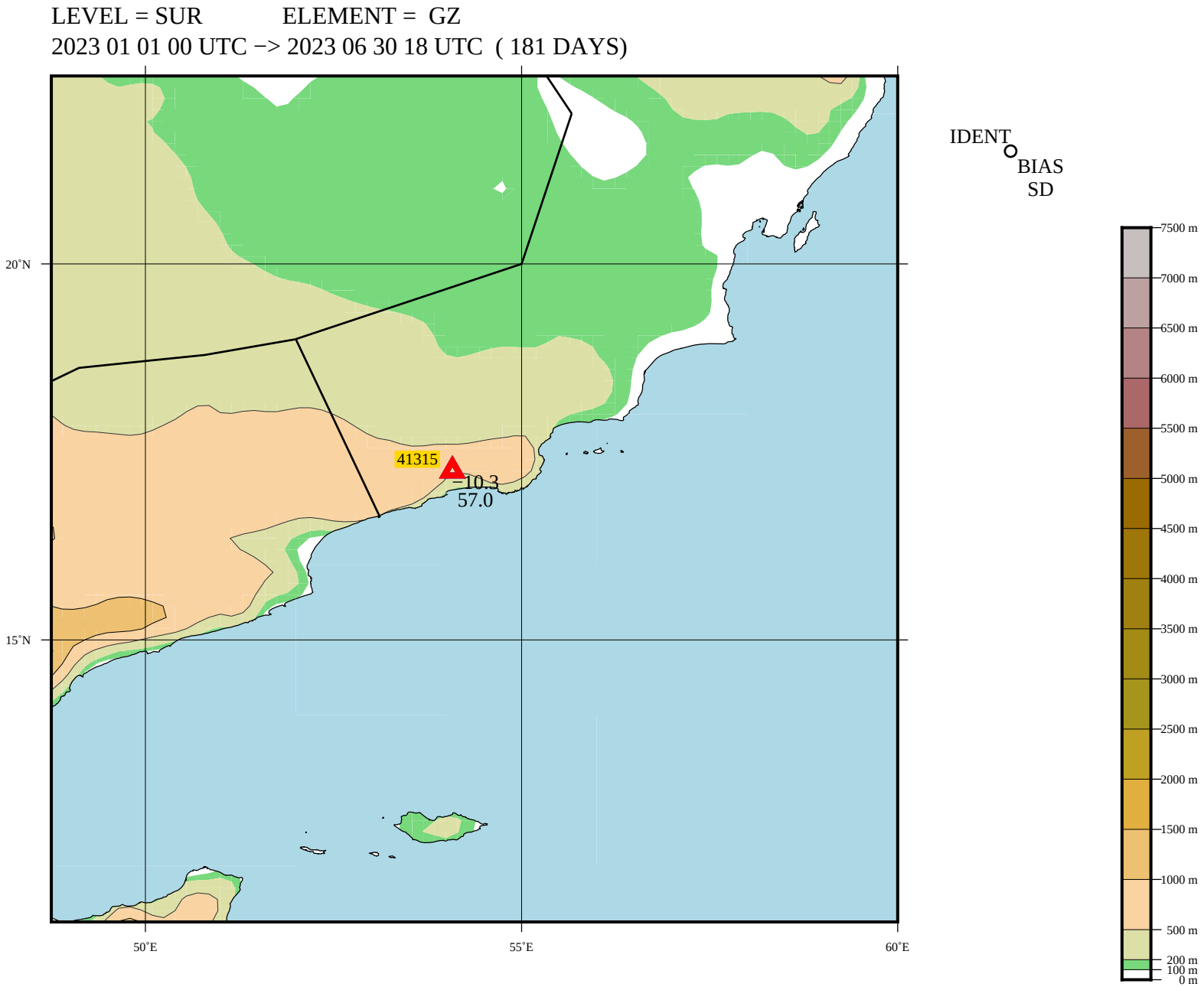

Figure 24 BIAS and SD of GZ for station 41315 (red) and surrounding stations (blue).
The number to the upper left of each symbol is the WMO IDENT, and those to the lower right are the values of BIAS and SD.
The size of each symbol is proportional to the value of BIAS, with hexagonal forms representing positive bias and triangular forms representing negative bias.

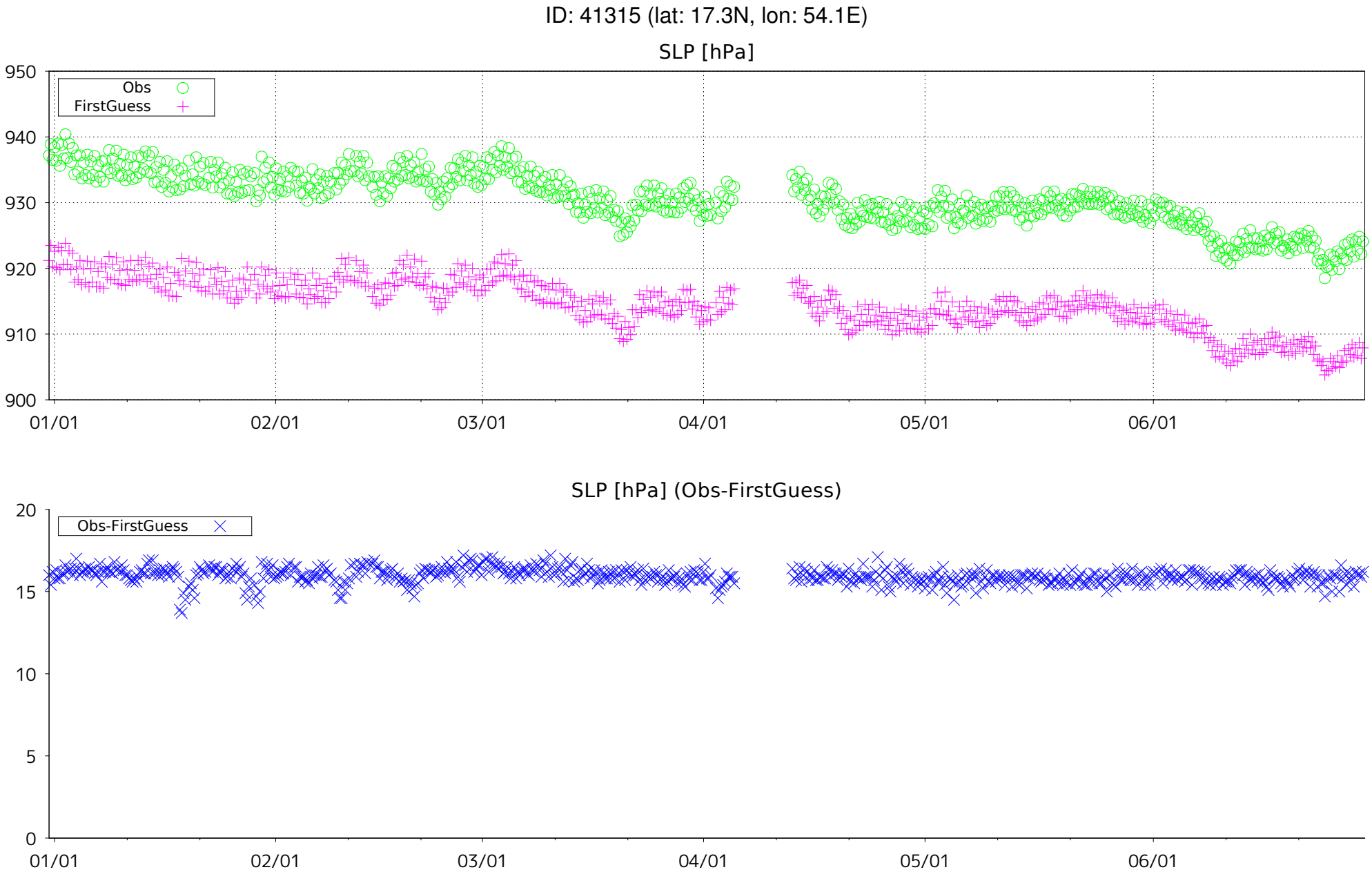

Figure 25(a) Time-series representation of SLP Obs minus FirstGuess for station 41315

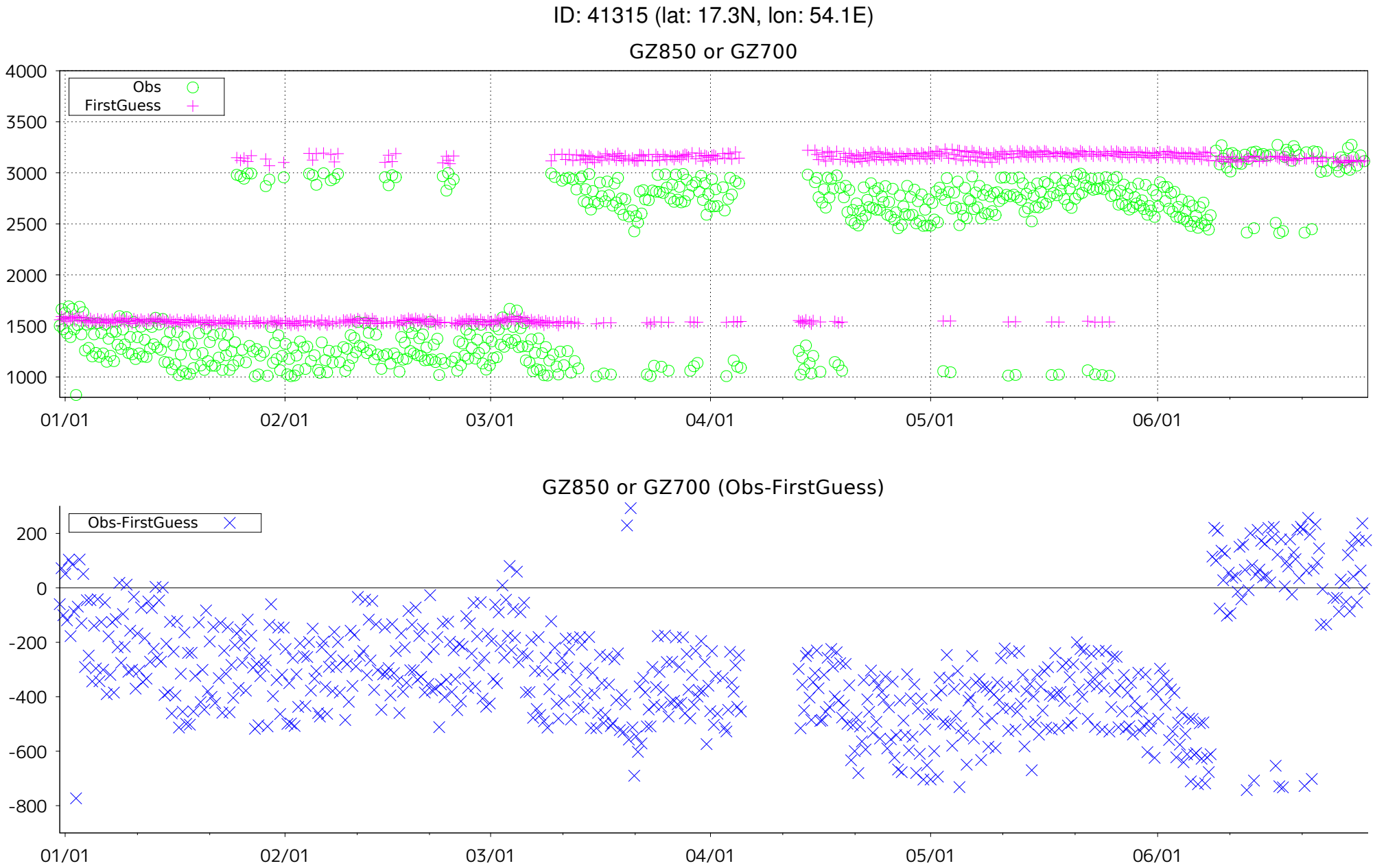

Figure 25(b) Time-series representation of GZ850 or GZ700 Obs minus FirstGuess for station 41315

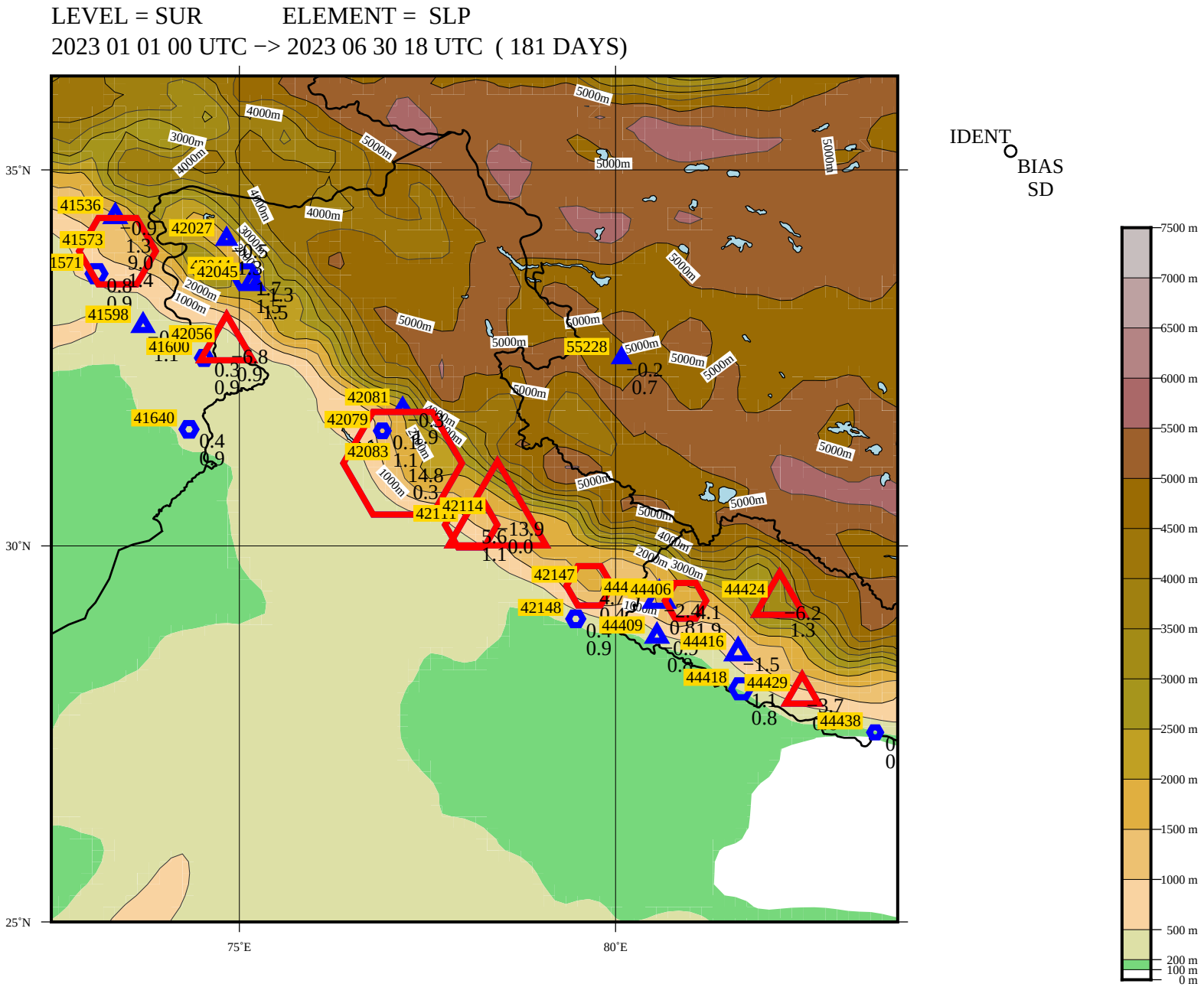

Figure 26 BIAS and SD of SLP for station 41573, 42056, 42083, 42111, 42114, 42147, 44406, 44424, 44429 (red) and surrounding stations (blue).
The number to the upper left of each symbol is the WMO IDENT, and those to the lower right are the values of BIAS and SD.
The size of each symbol is proportional to the value of BIAS, with hexagonal forms representing positive bias and triangular forms representing negative bias.

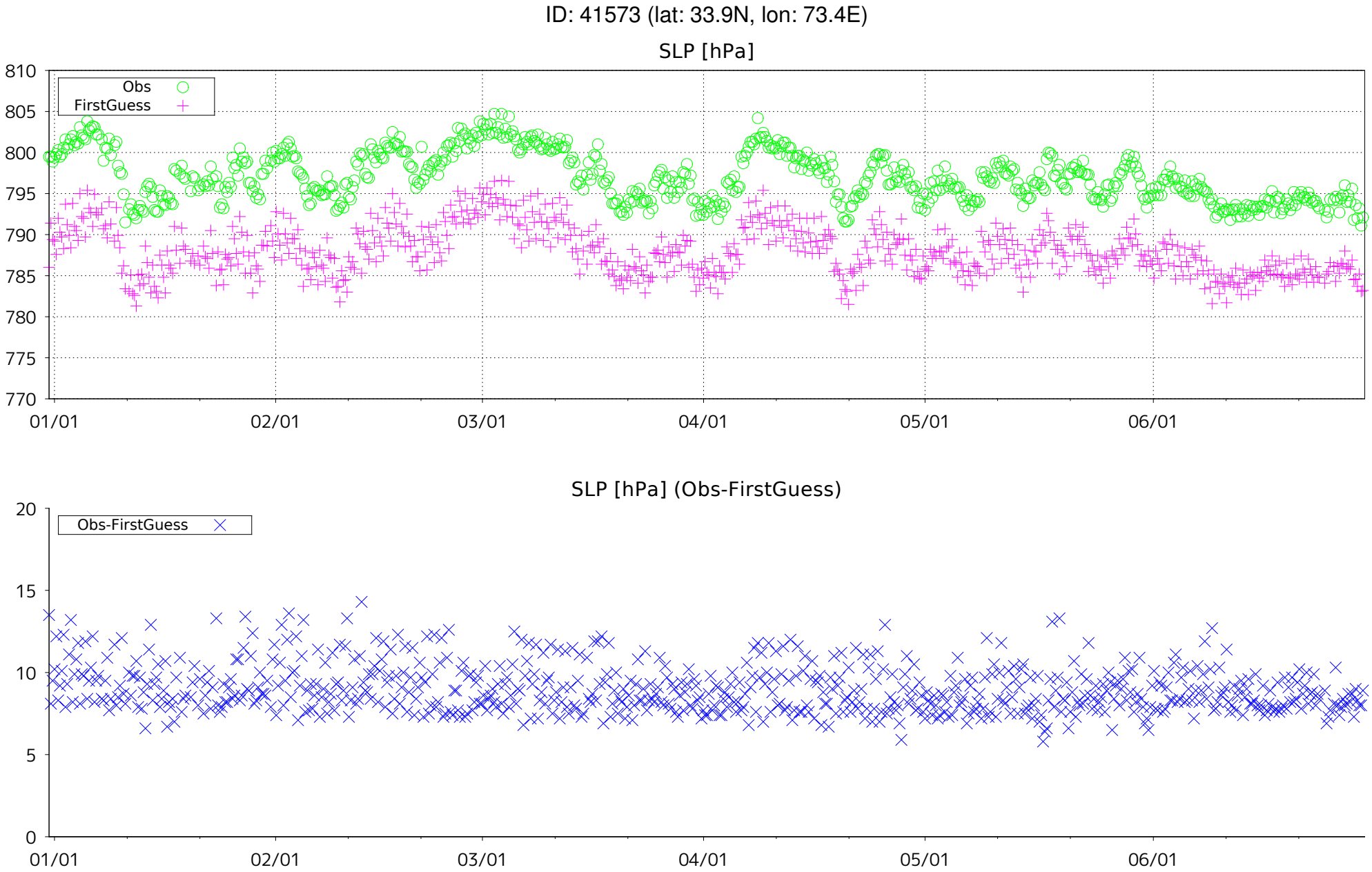

Figure 27 Time-series representation of SLP Obs minus FirstGuess for station 41573

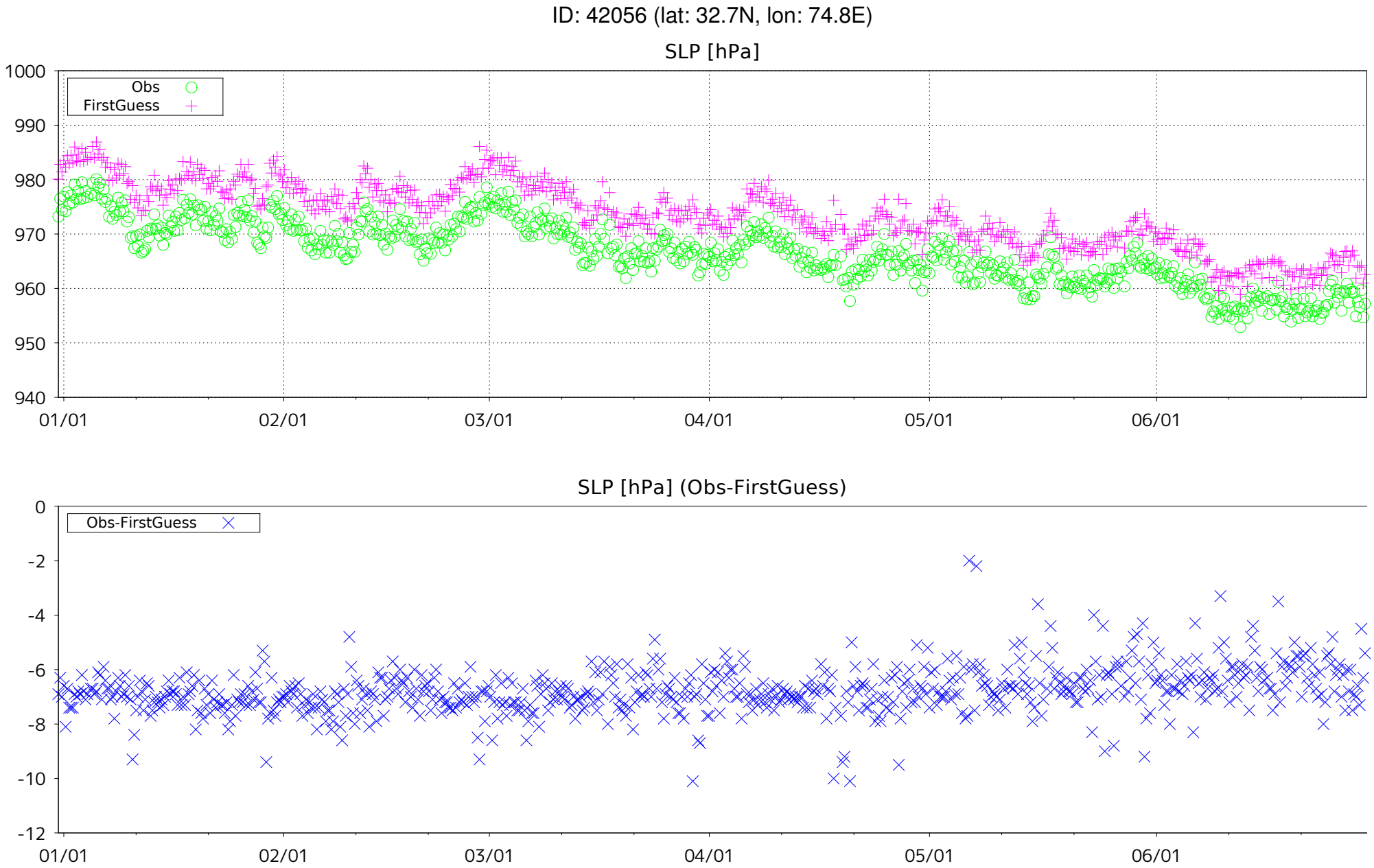

Figure 28 Time-series representation of SLP Obs minus FirstGuess for station 42056

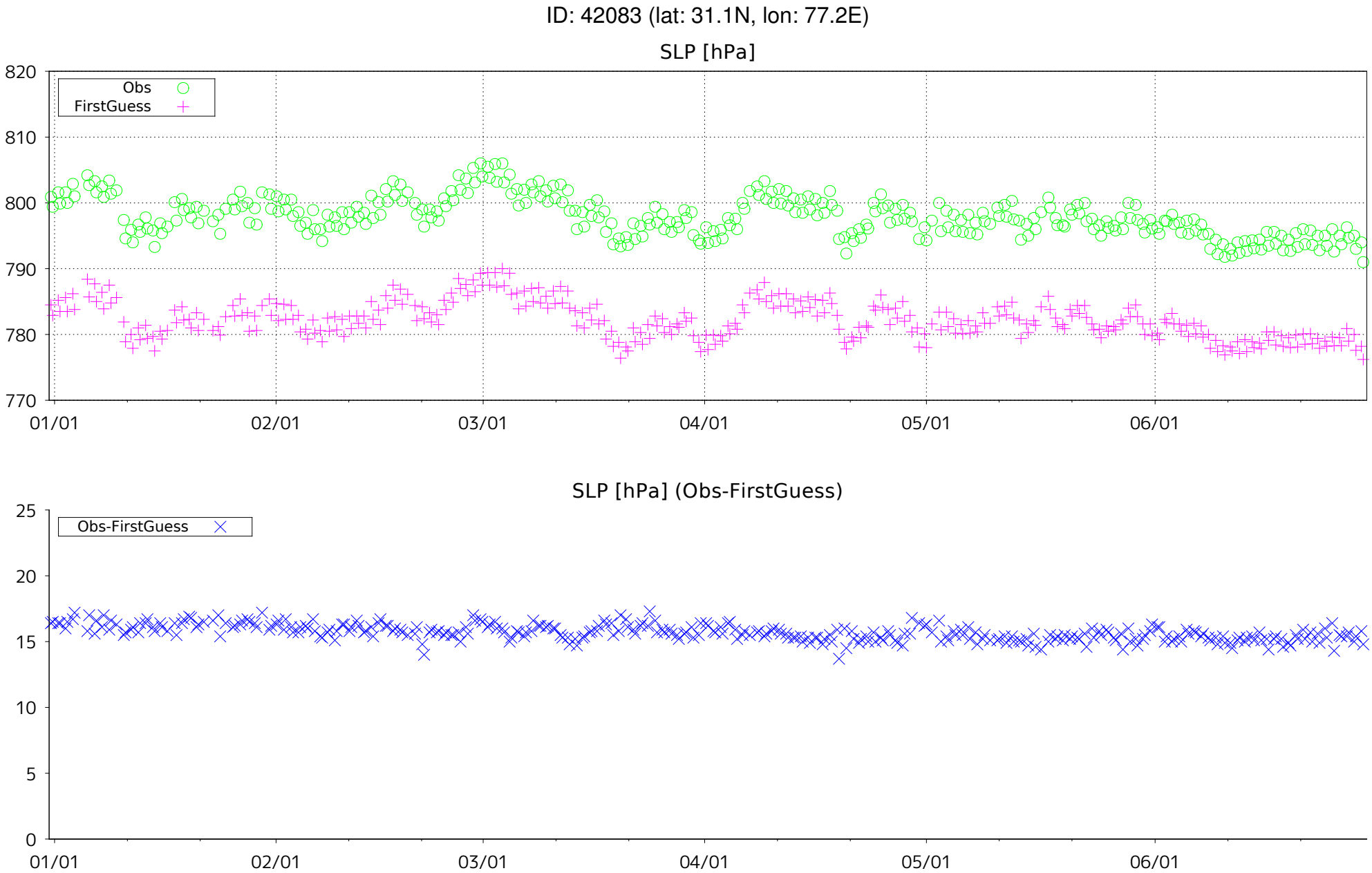

Figure 29 Time-series representation of SLP Obs minus FirstGuess for station 42083

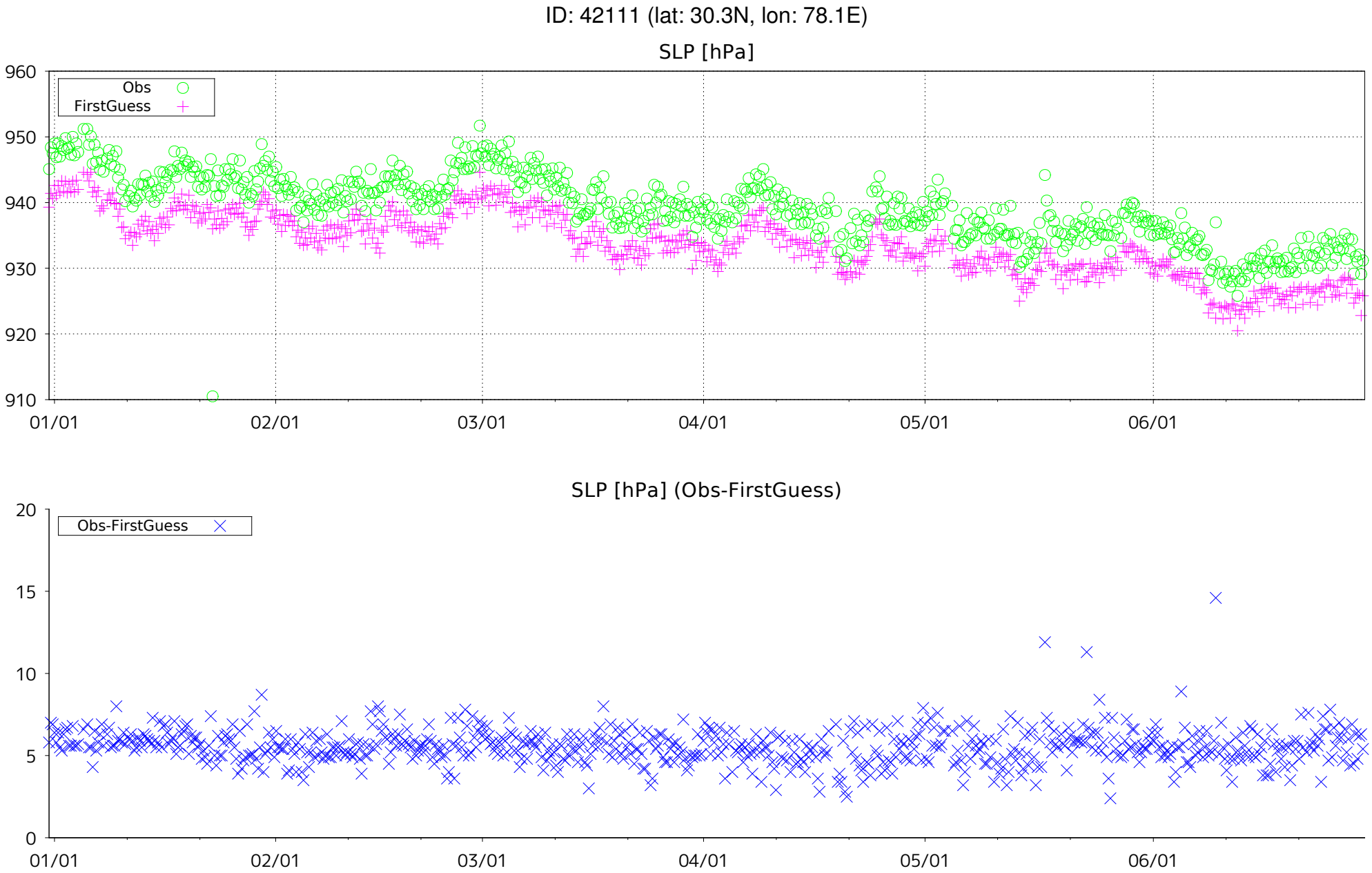

Figure 30 Time-series representation of SLP Obs minus FirstGuess for station 42111

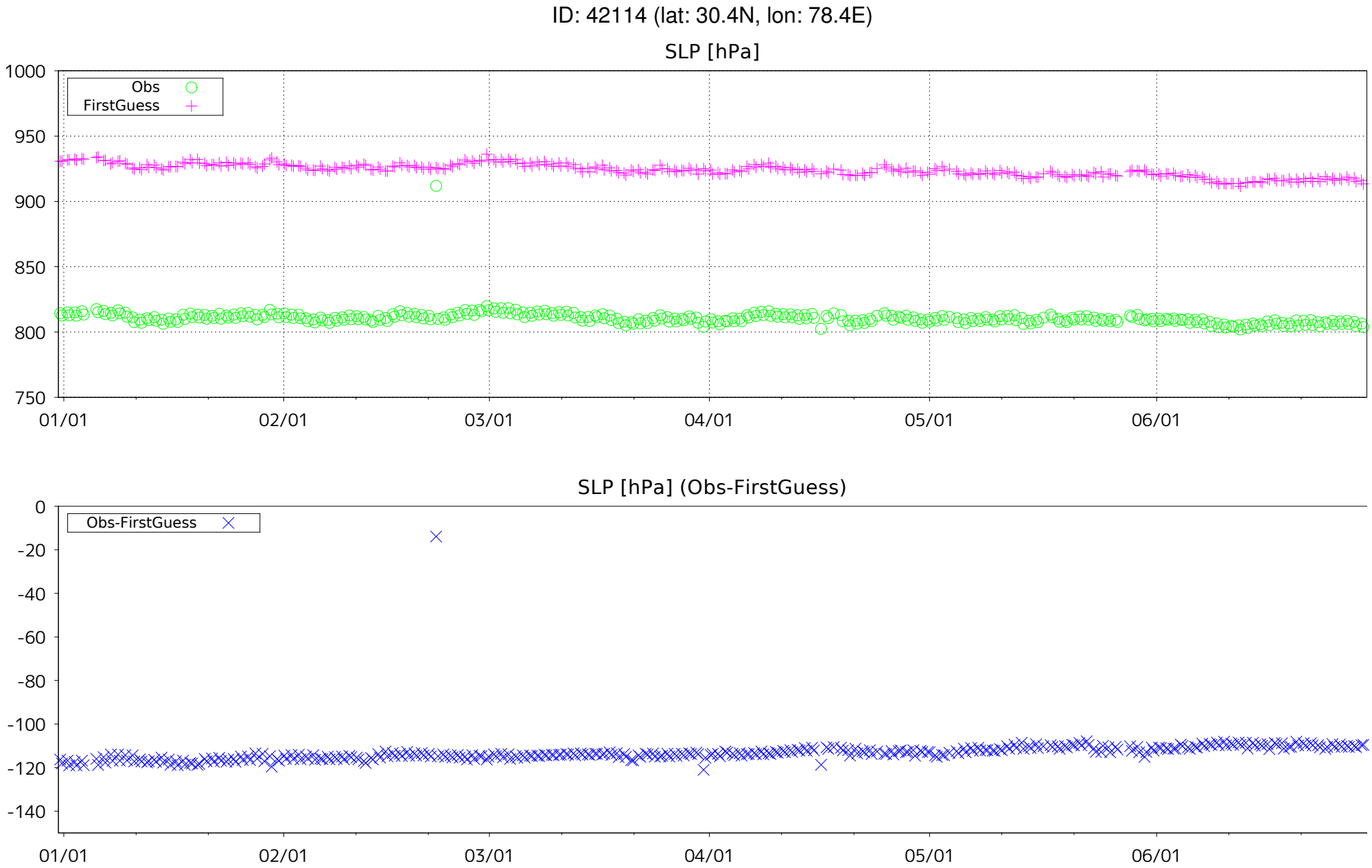

Figure 31 Time-series representation of SLP Obs minus FirstGuess for station 42114

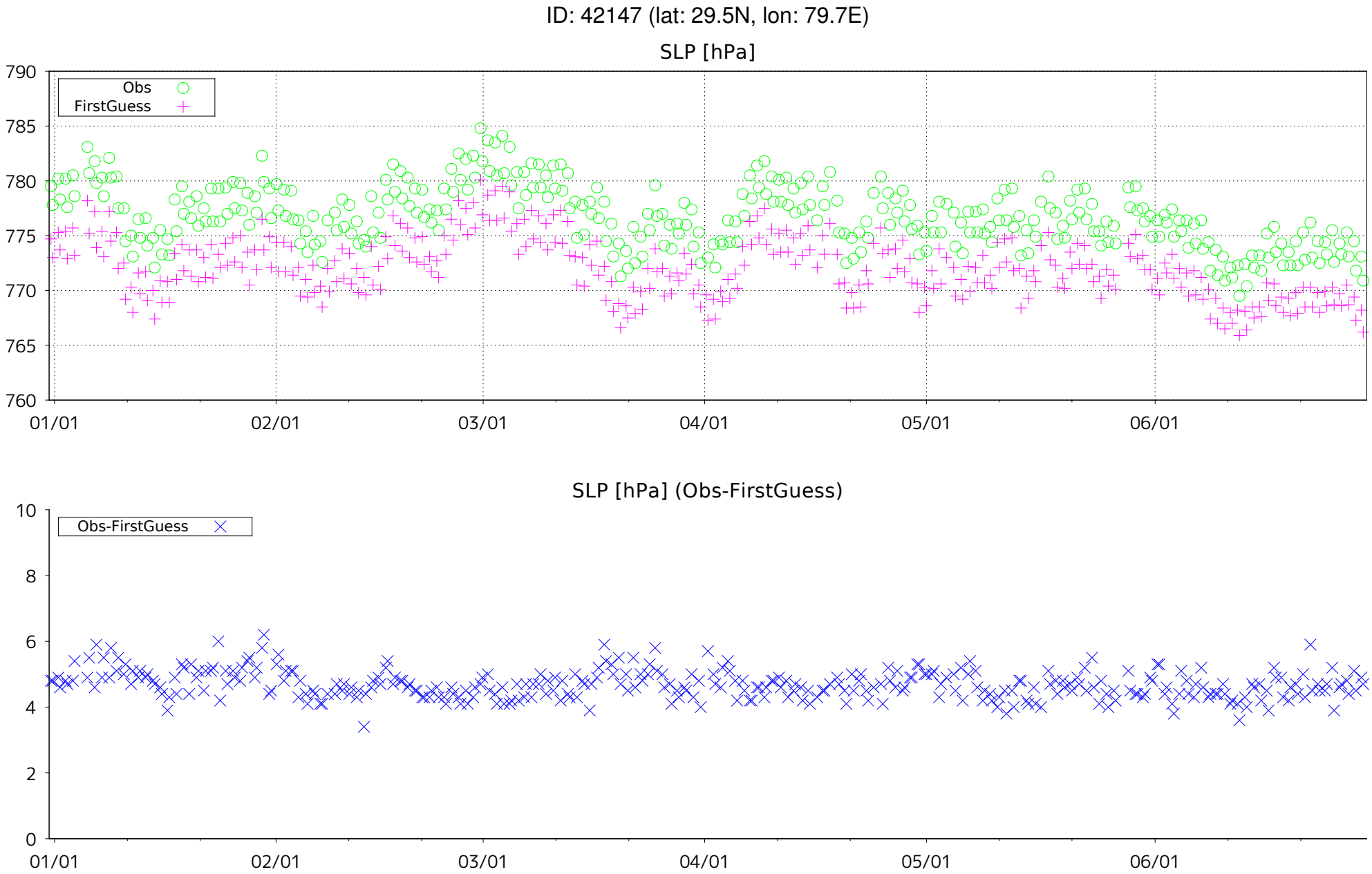

Figure 32 Time-series representation of SLP Obs minus FirstGuess for station 42147

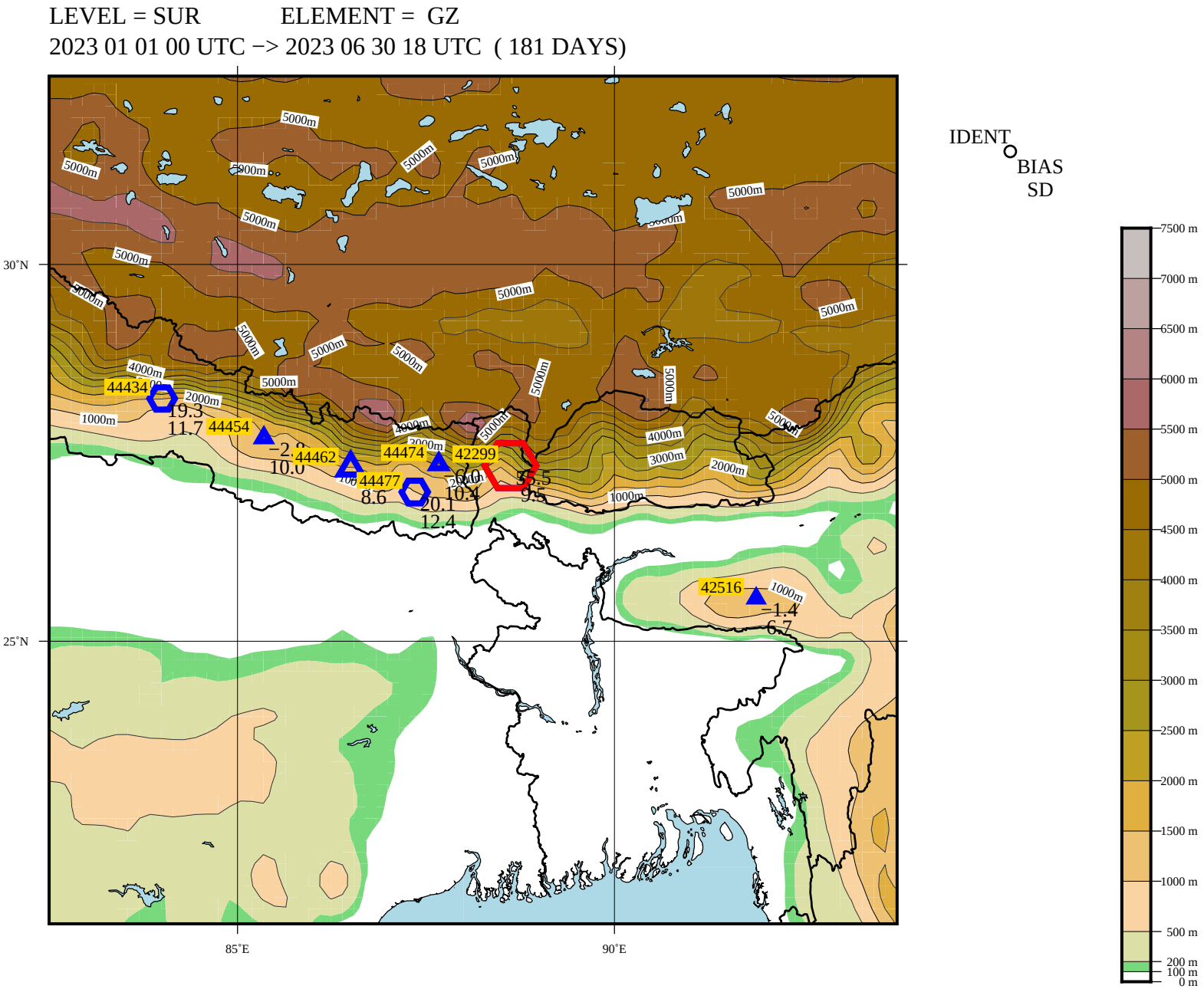

Figure 33 BIAS and SD of GZ for station 42299 (red) and surrounding stations (blue).
The number to the upper left of each symbol is the WMO IDENT, and those to the lower right are the values of BIAS and SD.
The size of each symbol is proportional to the value of BIAS, with hexagonal forms representing positive bias and triangular forms representing negative bias.

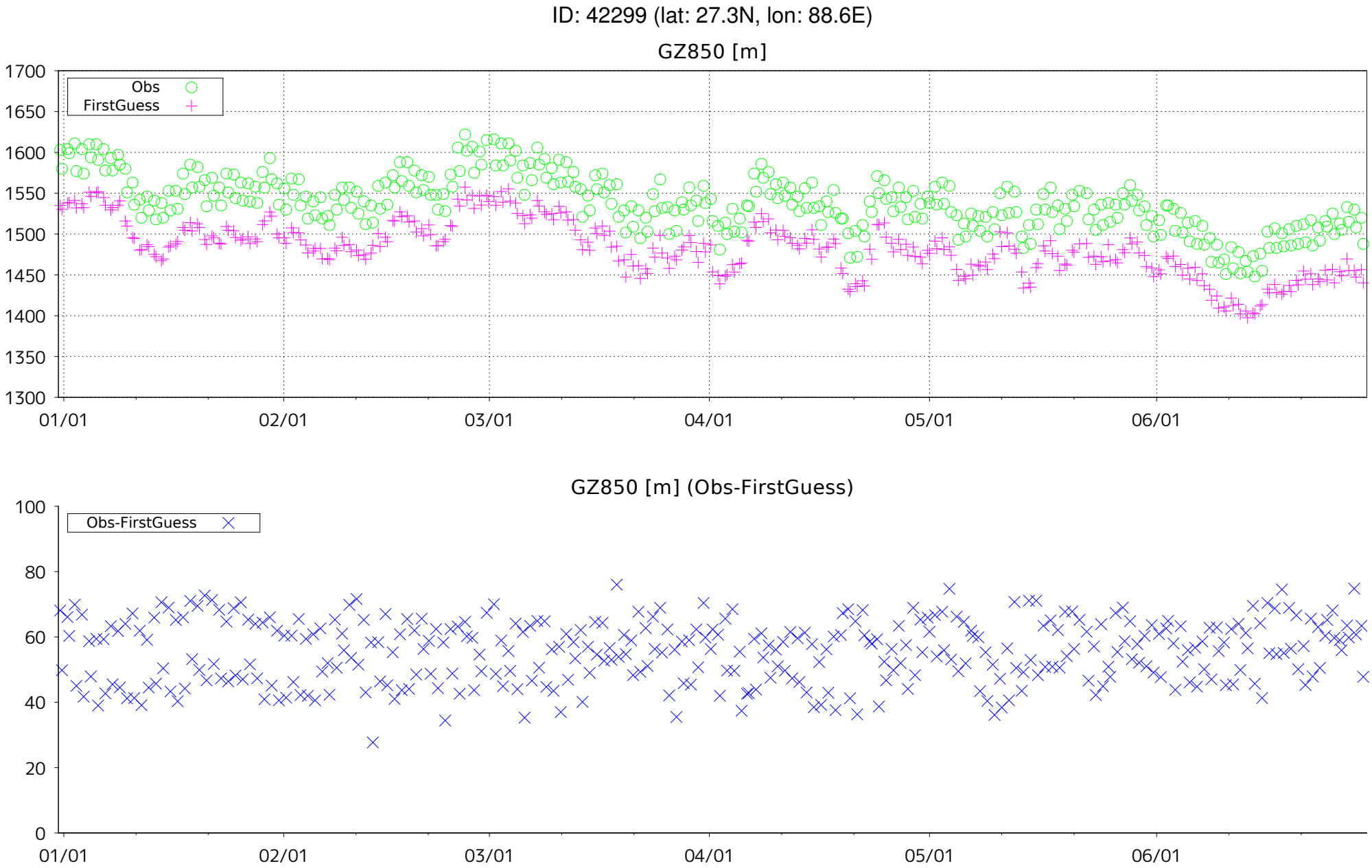

Figure 34 Time-series representation of GZ850 Obs minus FirstGuess for station 42299

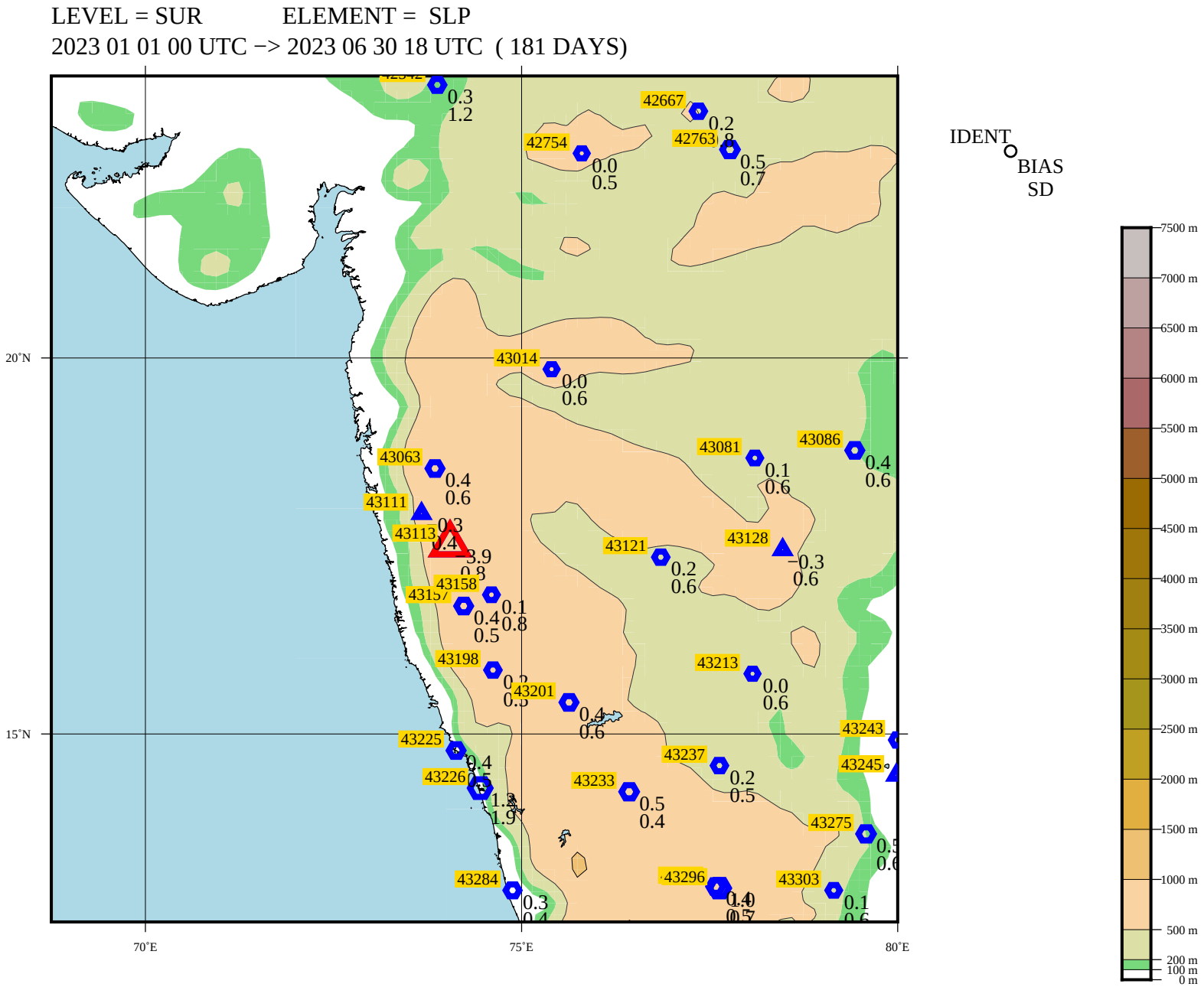

Figure 35 BIAS and SD of SLP for station 43113 (red) and surrounding stations (blue).
The number to the upper left of each symbol is the WMO IDENT, and those to the lower right are the values of BIAS and SD.
The size of each symbol is proportional to the value of BIAS, with hexagonal forms representing positive bias and triangular forms representing negative bias.

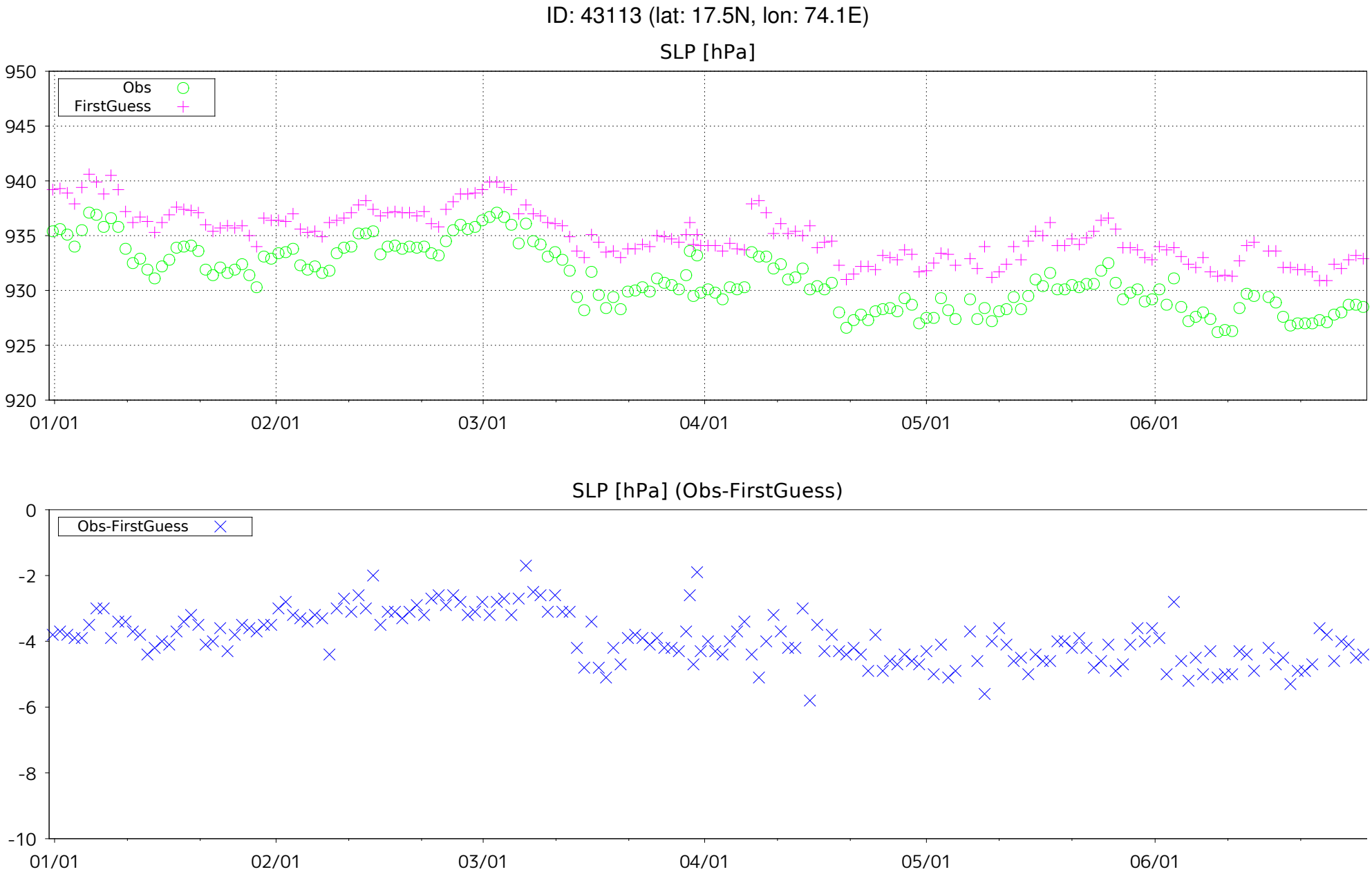

Figure 36 Time-series representation of SLP Obs minus FirstGuess for station 43113

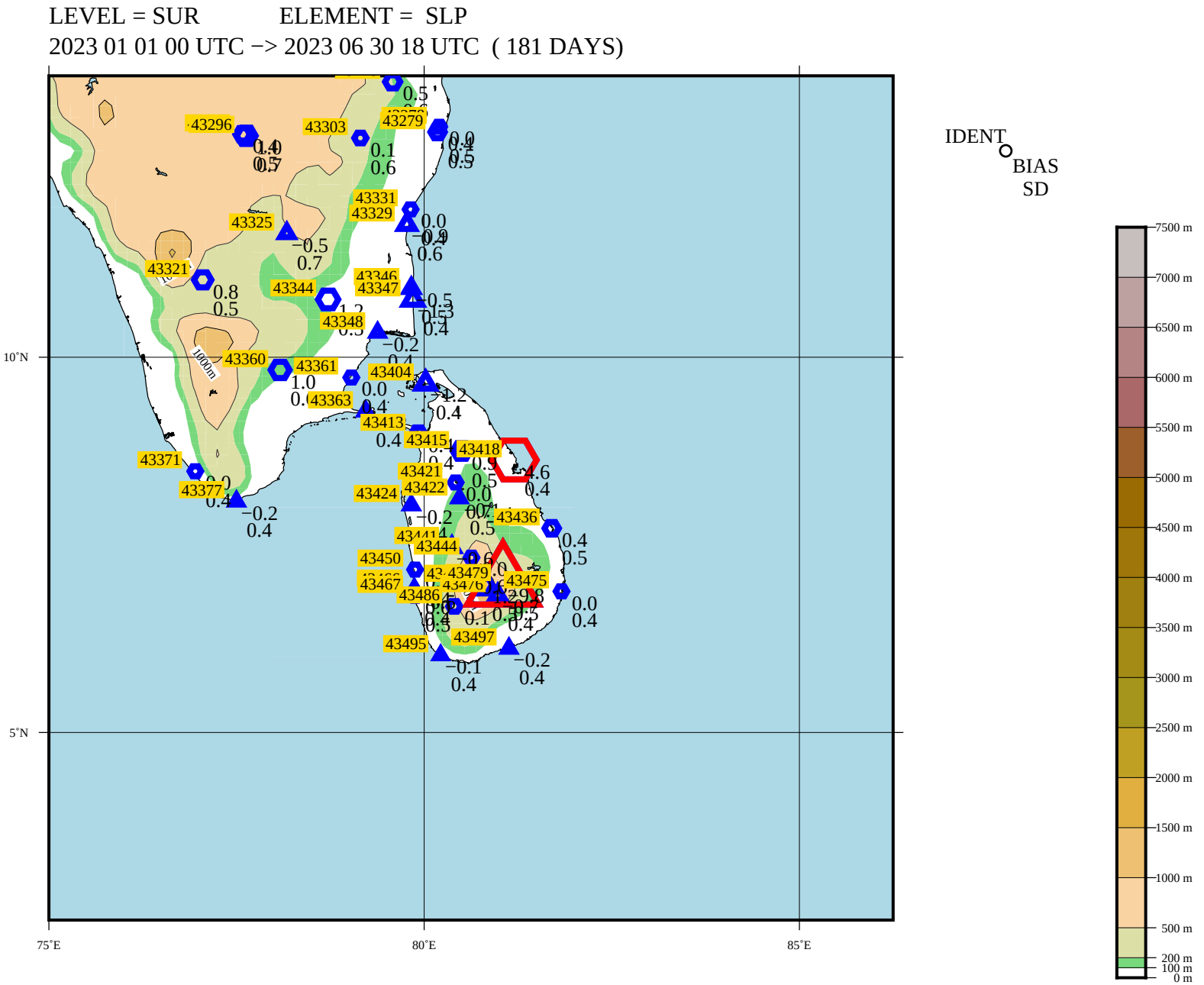

Figure 37 BIAS and SD of SLP for station 43418, 43479 (red) and surrounding stations (blue).
The number to the upper left of each symbol is the WMO IDENT, and those to the lower right are the values of BIAS and SD.
The size of each symbol is proportional to the value of BIAS, with hexagonal forms representing positive bias and triangular forms representing negative bias.

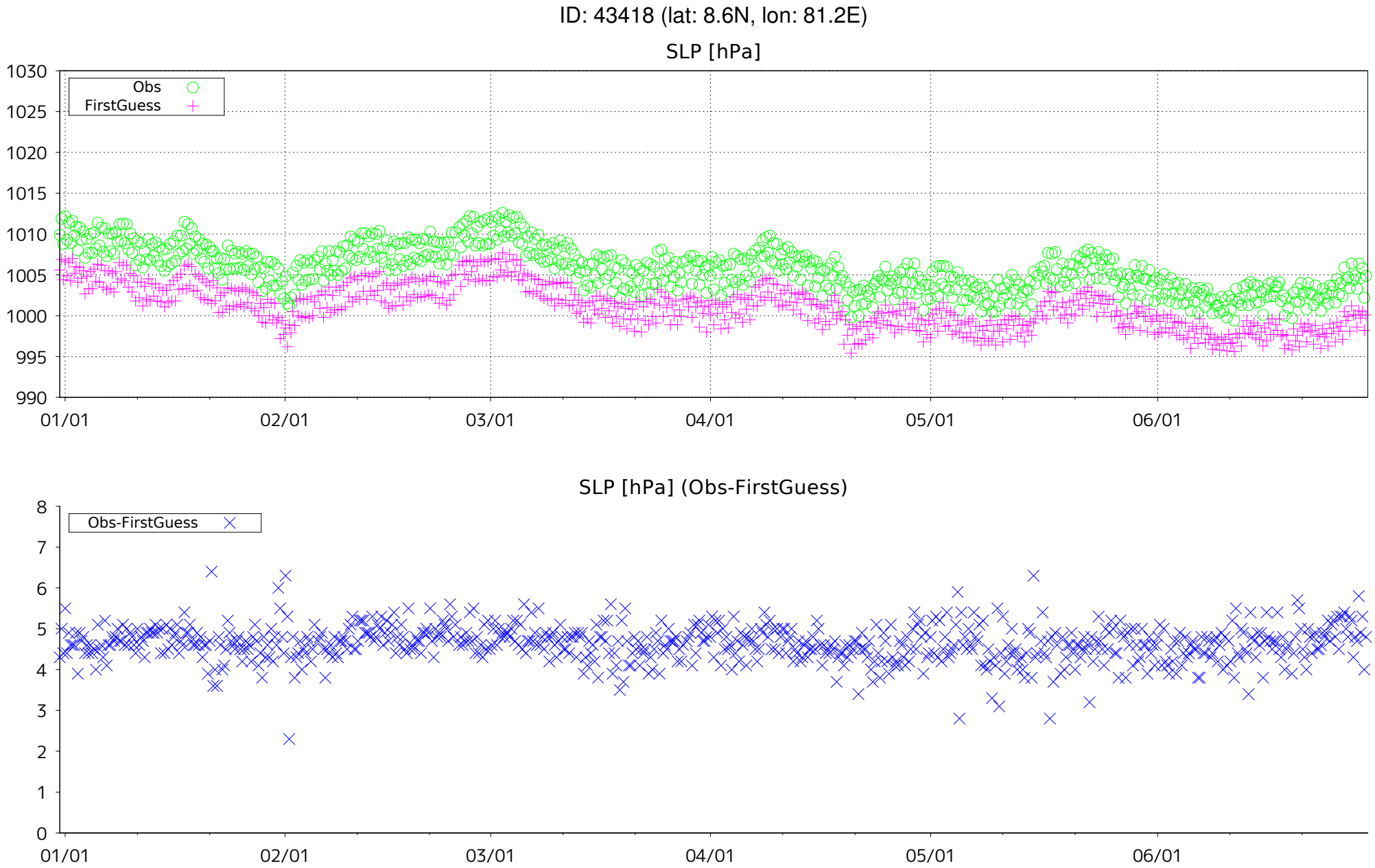

Figure 38 Time-series representation of SLP Obs minus FirstGuess for station 43418

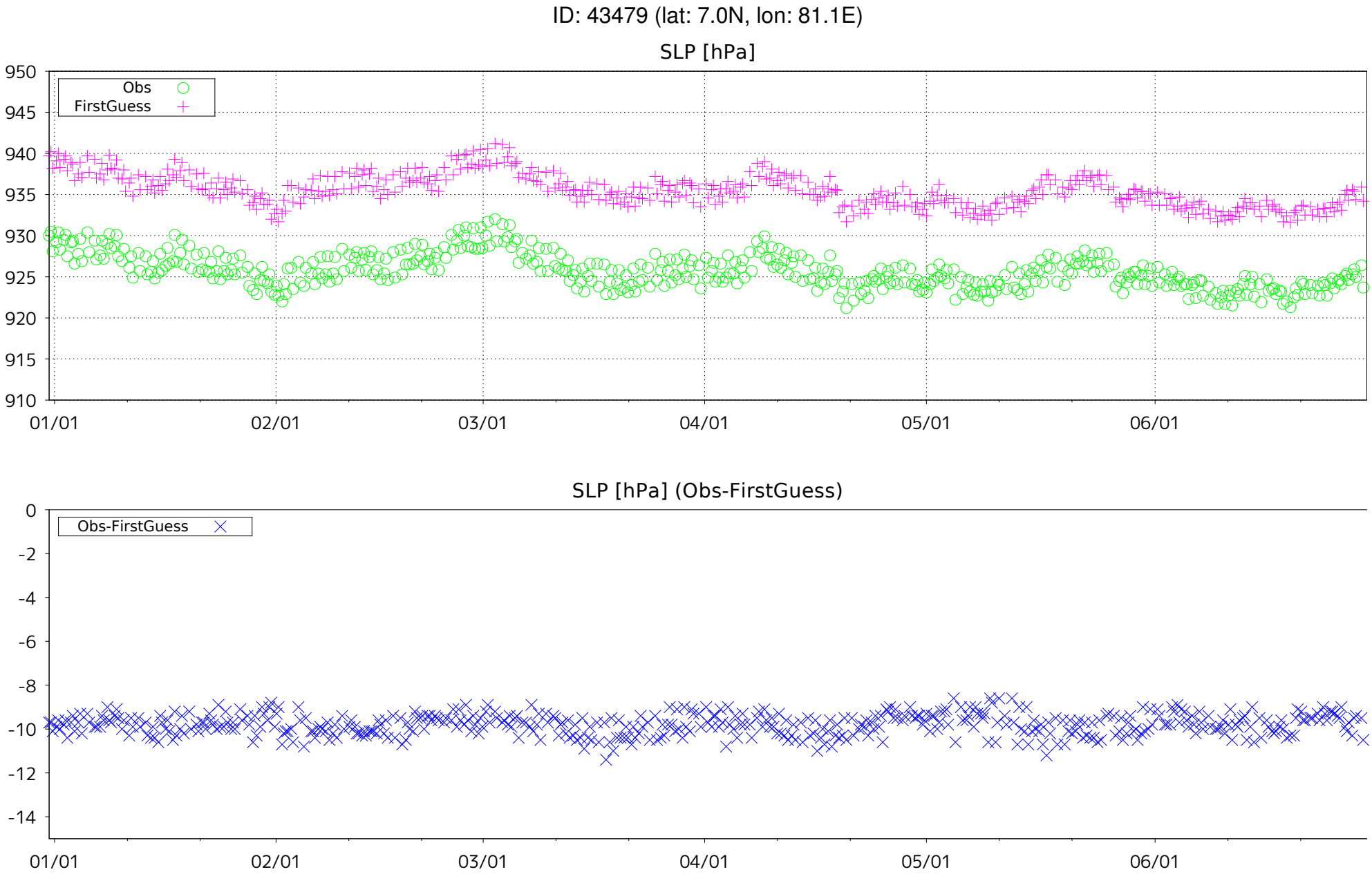

Figure 39 Time-series representation of SLP Obs minus FirstGuess for station 43479

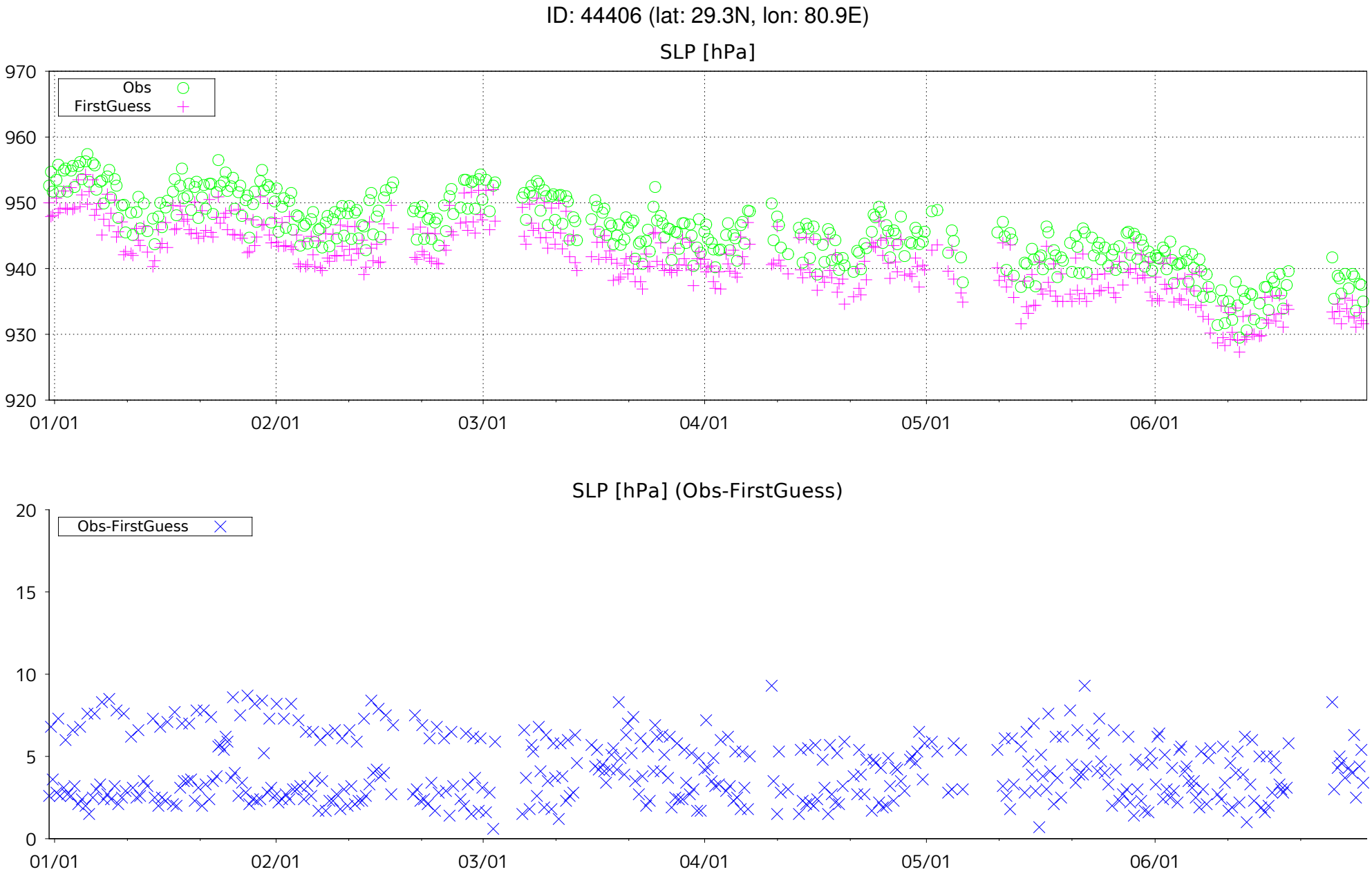

Figure 40 Time-series representation of SLP Obs minus FirstGuess for station 44406

Figure 41 Time-series representation of SLP Obs minus FirstGuess for station 44429

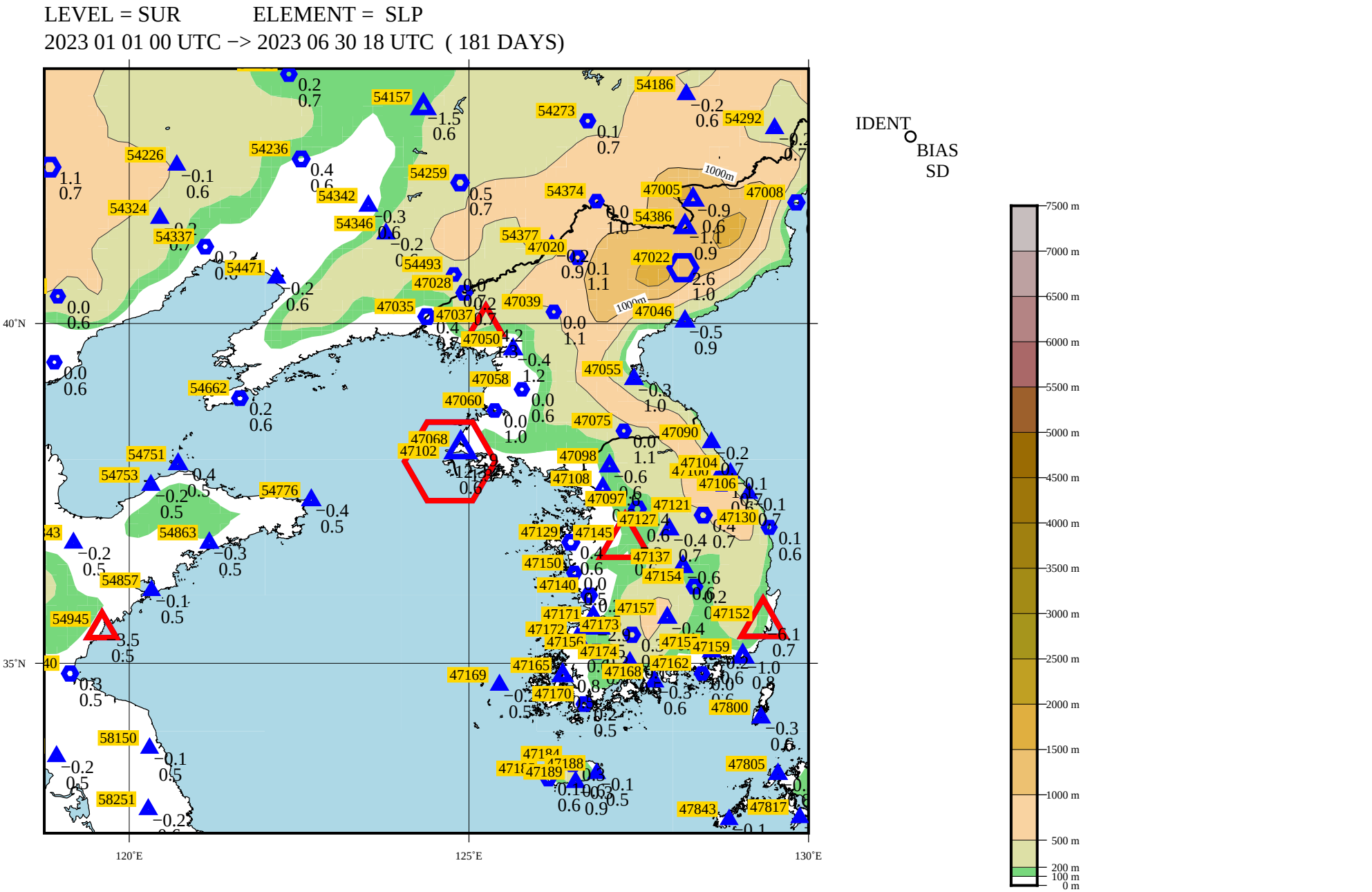

Figure 42 BIAS and SD of SLP for station 47037, 47102, 47145, 47152, 54945 (red) and surrounding stations (blue).
The number to the upper left of each symbol is the WMO IDENT, and those to the lower right are the values of BIAS and SD.
The size of each symbol is proportional to the value of BIAS, with hexagonal forms representing positive bias and triangular forms representing negative bias.

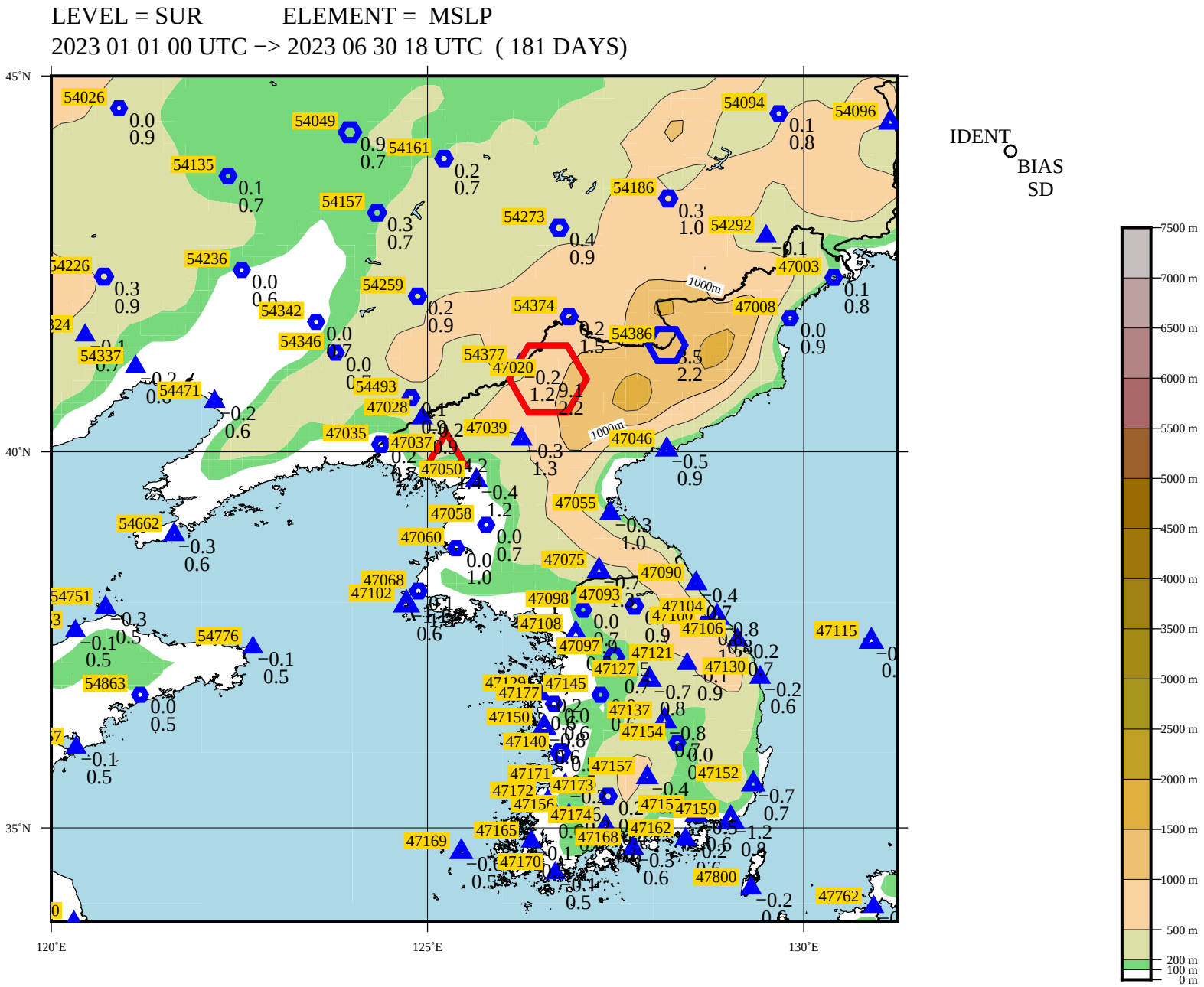

Figure 43 BIAS and SD of MSLP for station 47020, 47037 (red) and surrounding stations (blue).
The number to the upper left of each symbol is the WMO IDENT, and those to the lower right are the values of BIAS and SD.
The size of each symbol is proportional to the value of BIAS, with hexagonal forms representing positive bias and triangular forms representing negative bias.

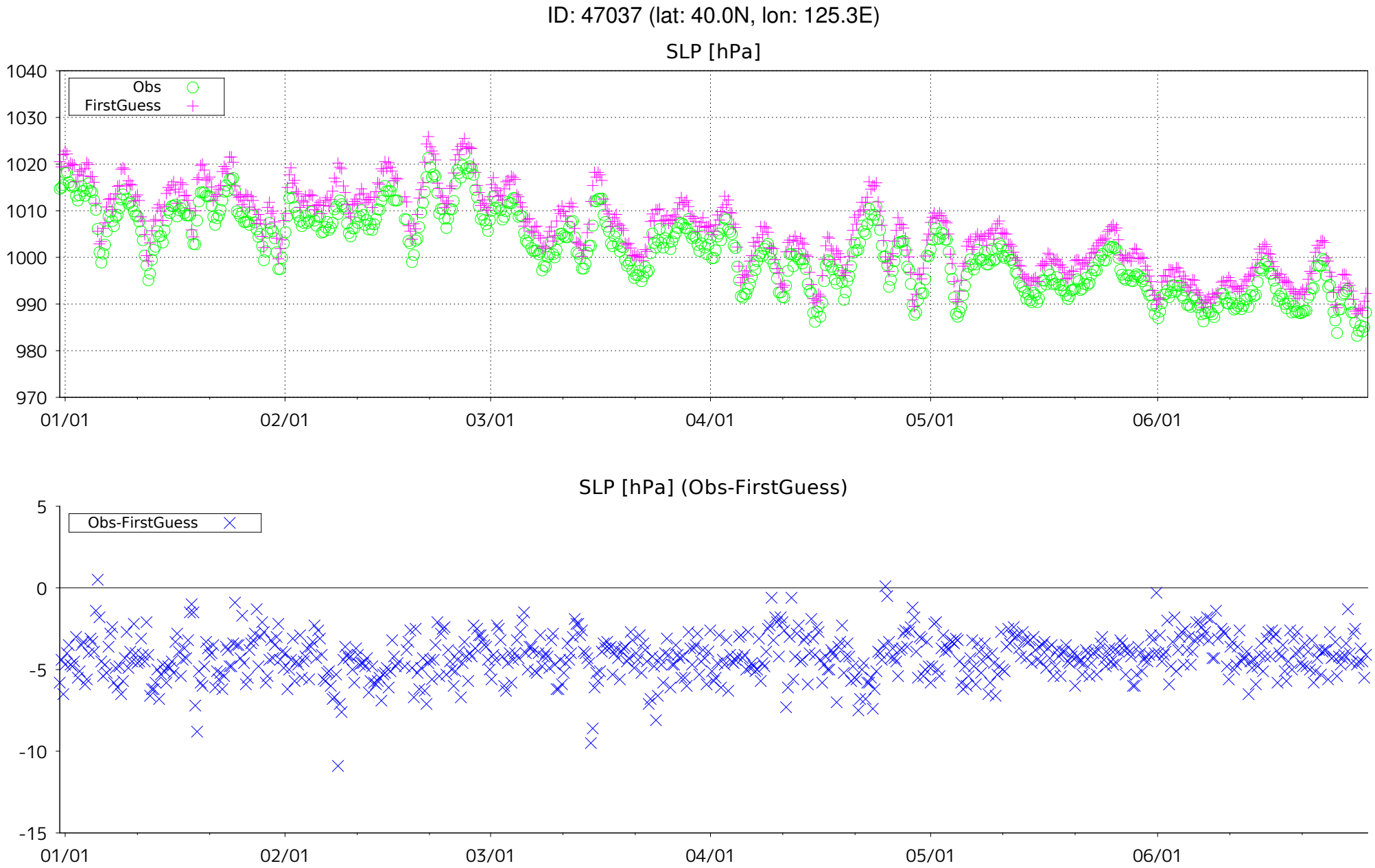

Figure 44(a) Time-series representation of SLP Obs minus FirstGuess for station 47037

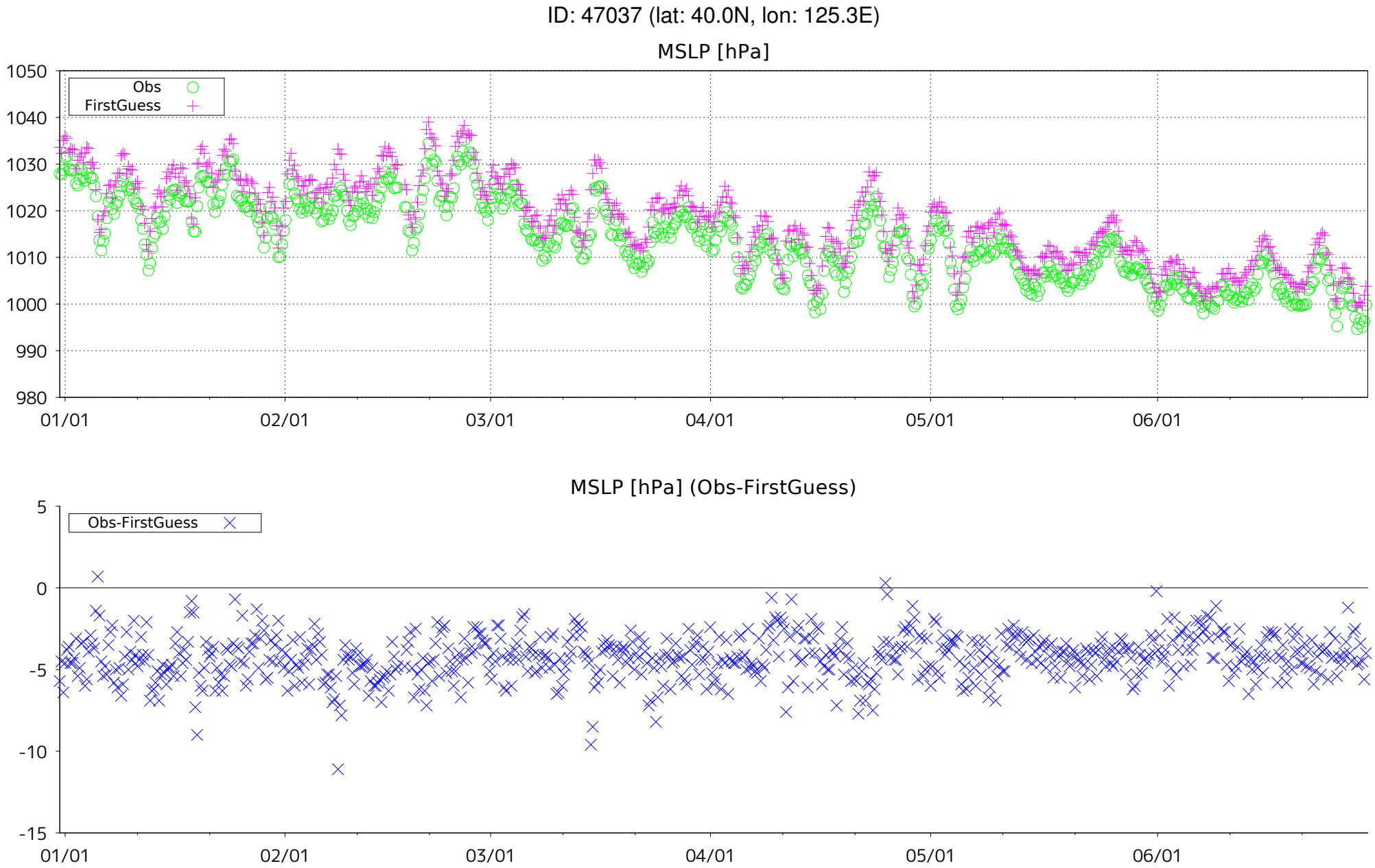

Figure 44(b) Time-series representation of MSLP Obs minus FirstGuess for station 47037

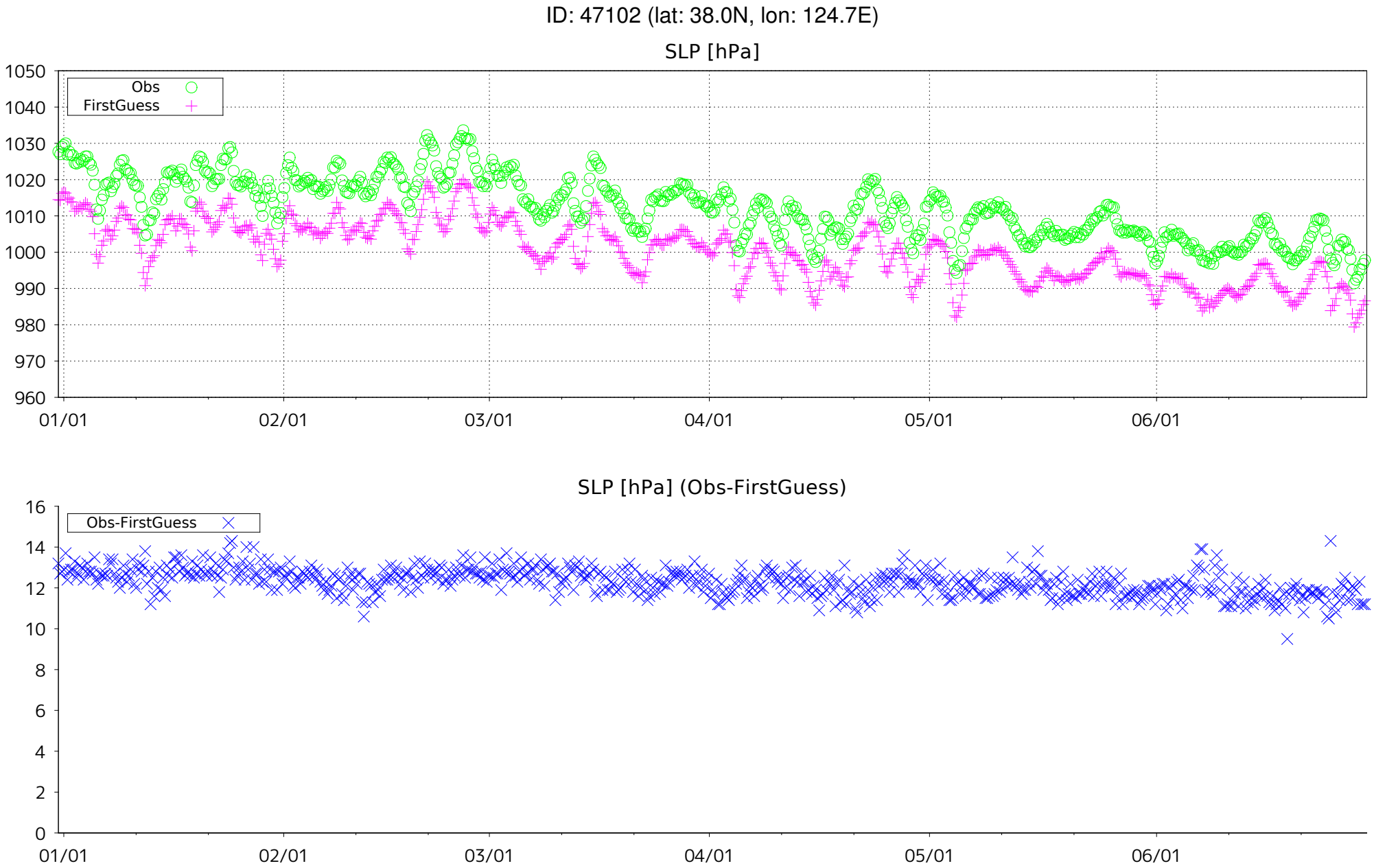

Figure 45 Time-series representation of SLP Obs minus FirstGuess for station 47102

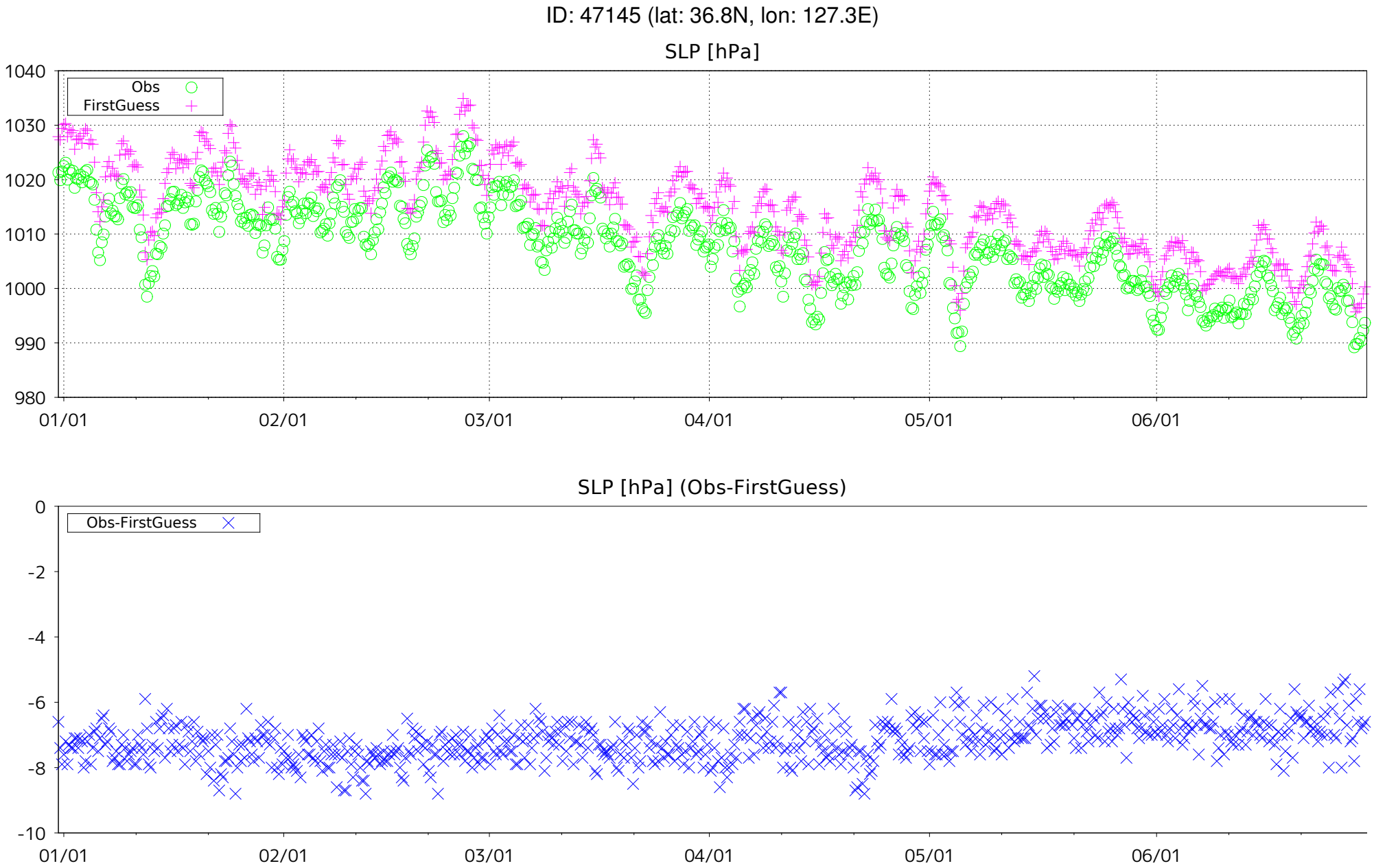

Figure 46 Time-series representation of SLP Obs minus FirstGuess for station 47145

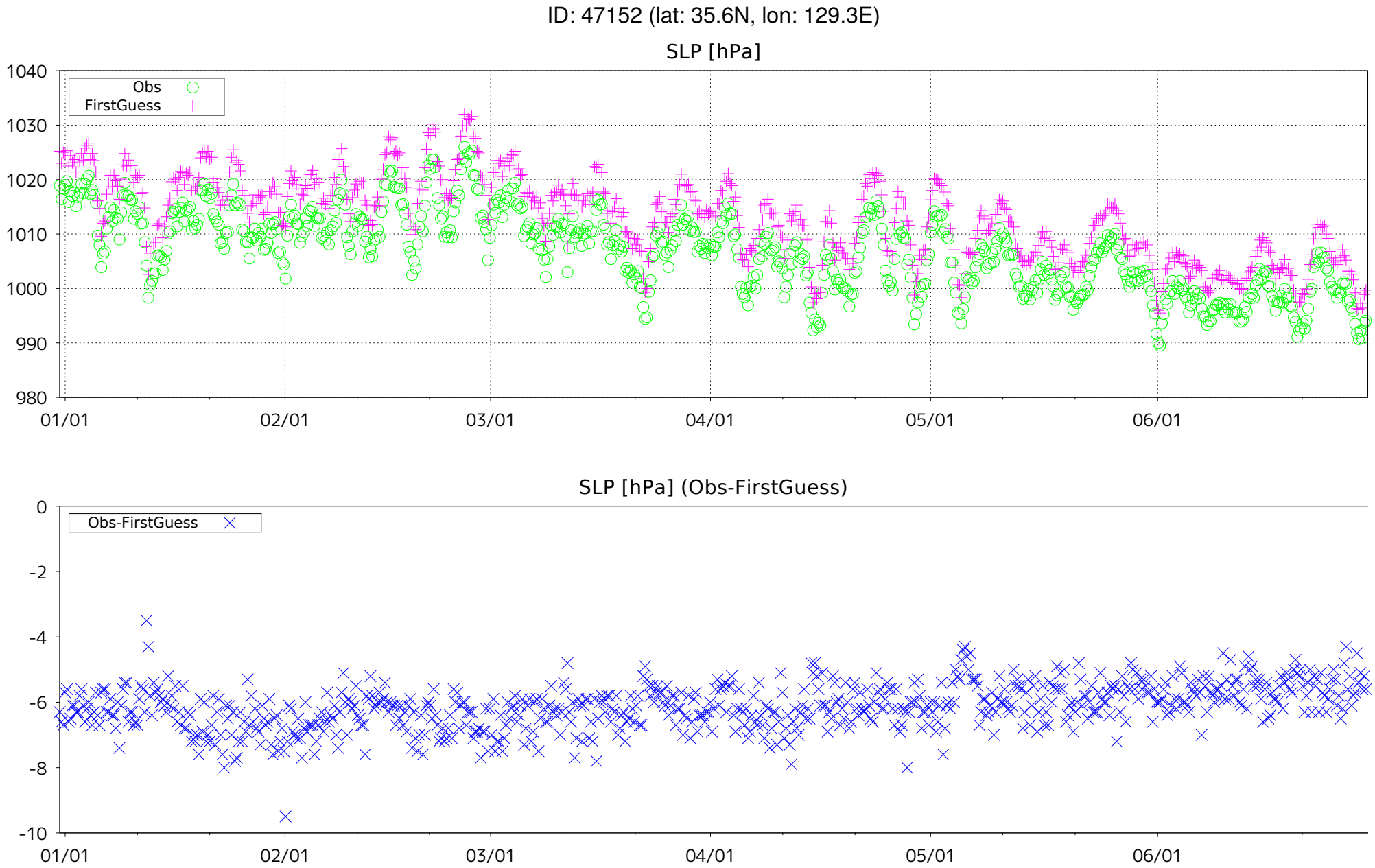

Figure 47 Time-series representation of SLP Obs minus FirstGuess for station 47152

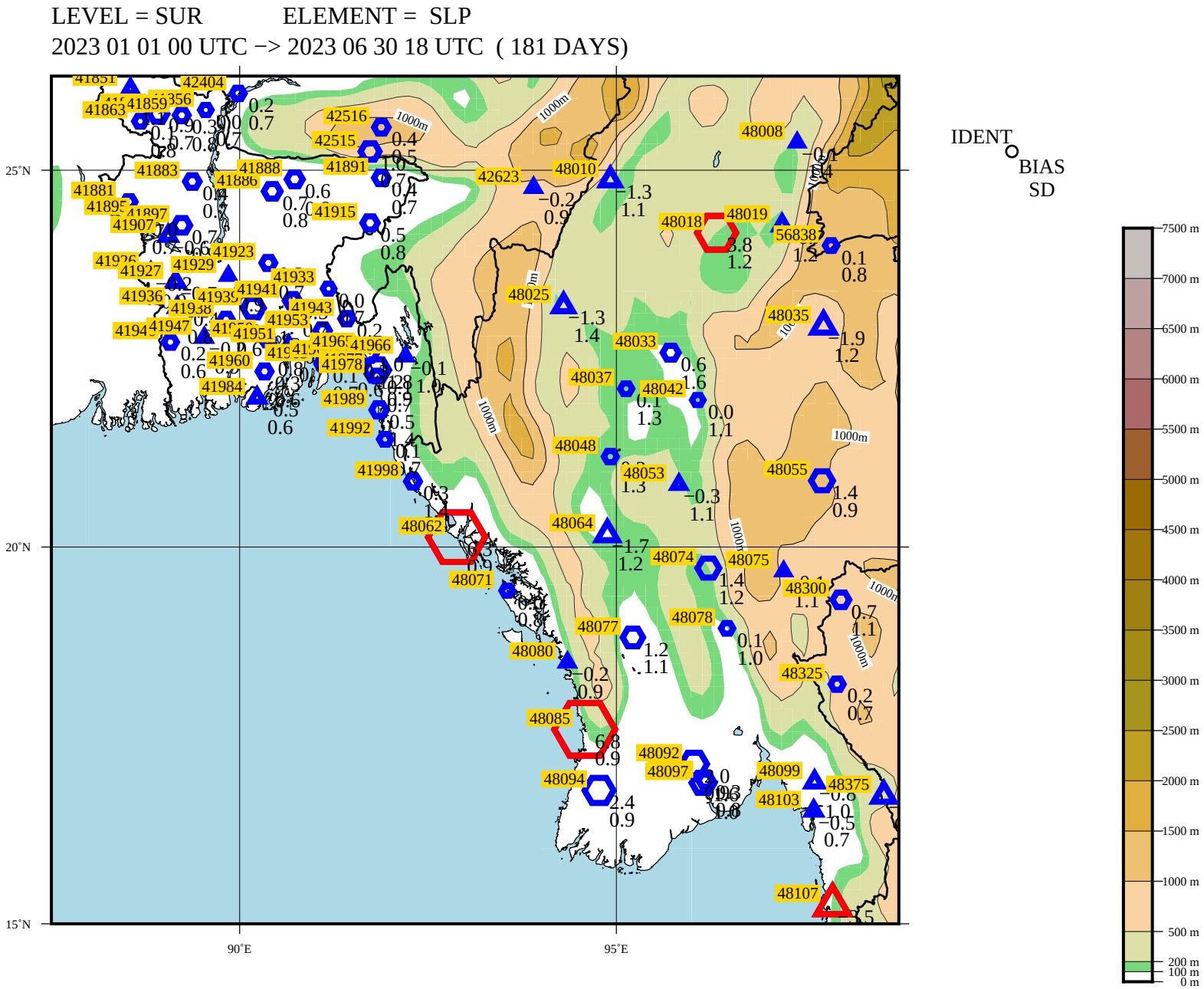

Figure 48 BIAS and SD of SLP for station 48018, 48062, 48085, 48107 (red) and surrounding stations (blue).
The number to the upper left of each symbol is the WMO IDENT, and those to the lower right are the values of BIAS and SD.
The size of each symbol is proportional to the value of BIAS, with hexagonal forms representing positive bias and triangular forms representing negative bias.

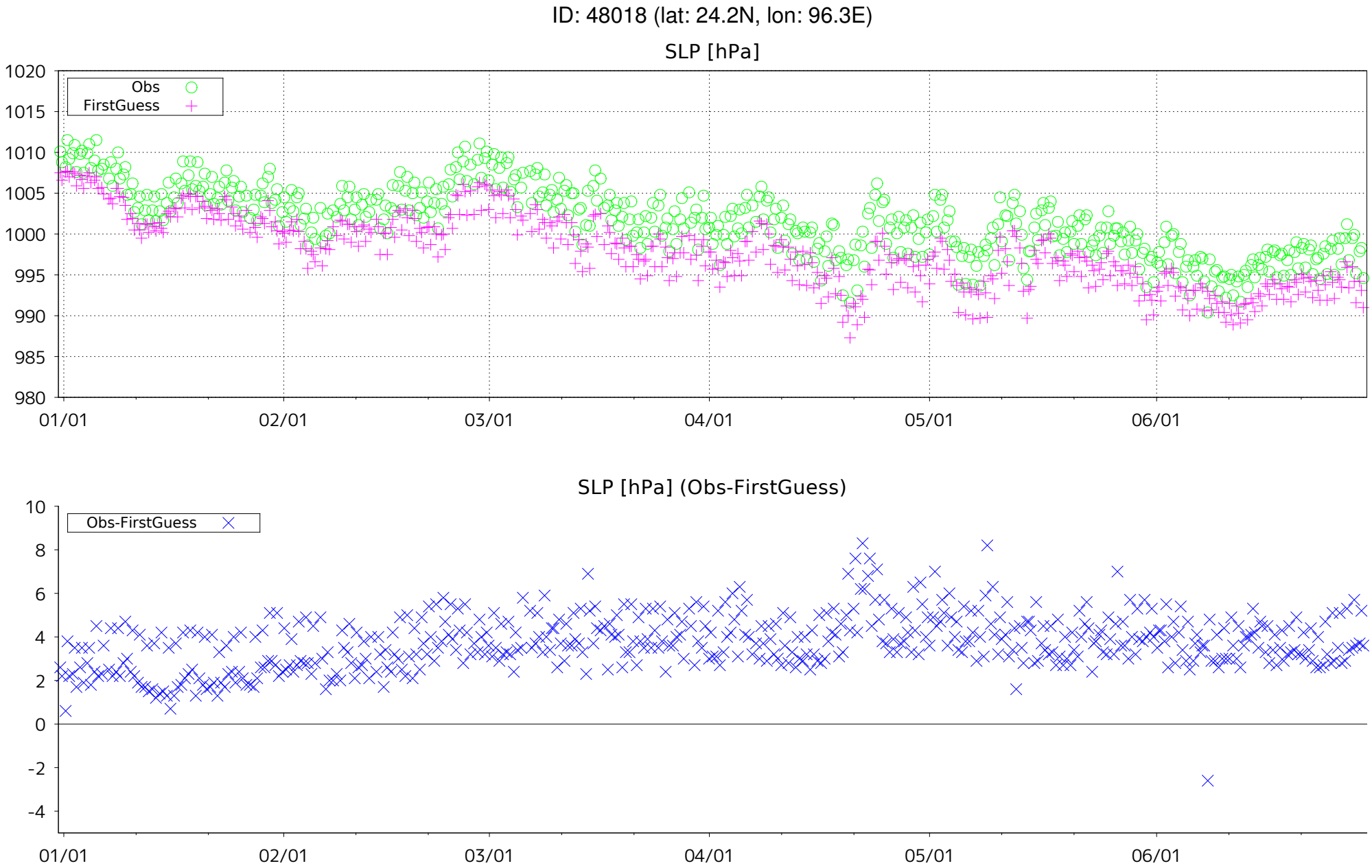

Figure 49 Time-series representation of SLP Obs minus FirstGuess for station 48018

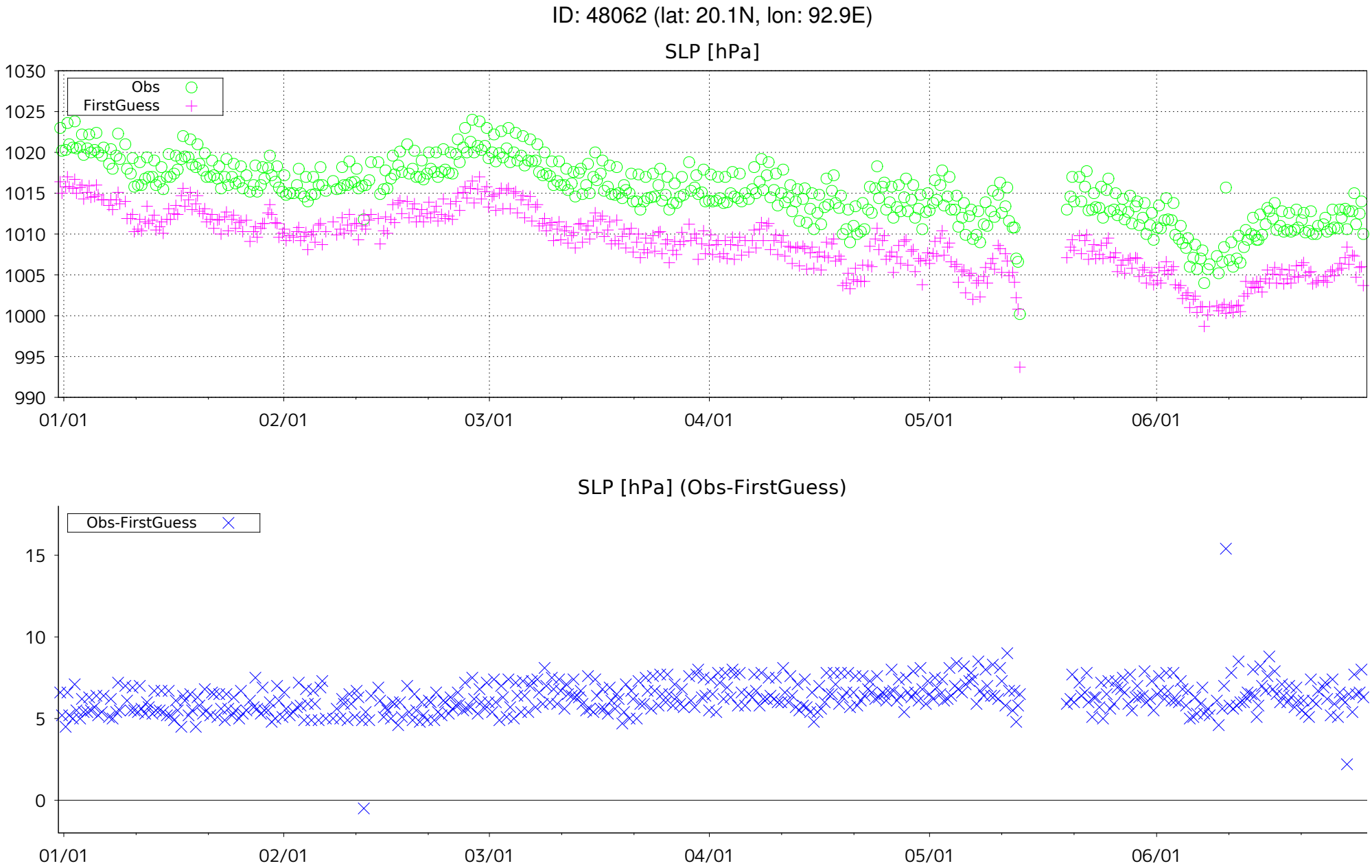

Figure 50 Time-series representation of SLP Obs minus FirstGuess for station 48062

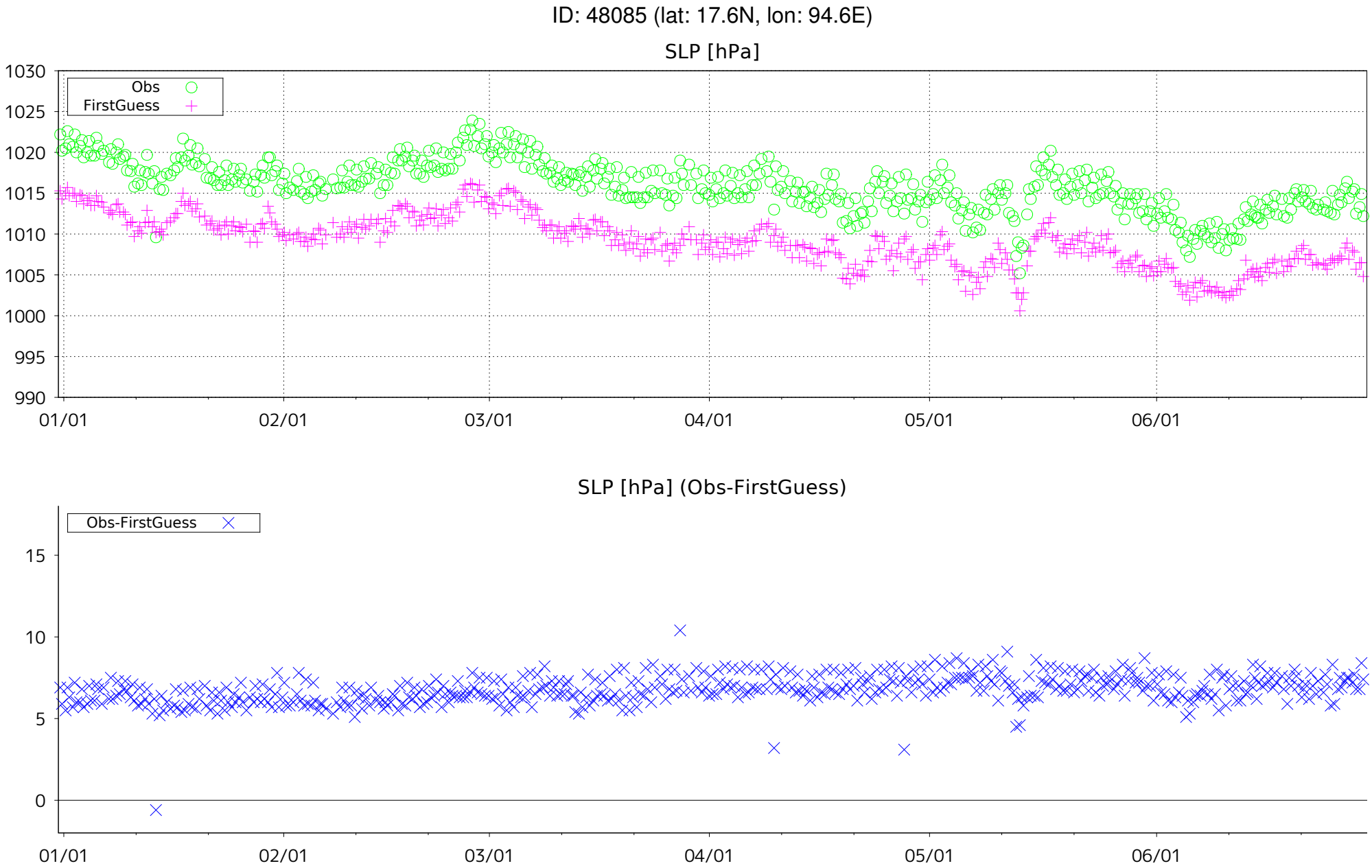

Figure 51 Time-series representation of SLP Obs minus FirstGuess for station 48085

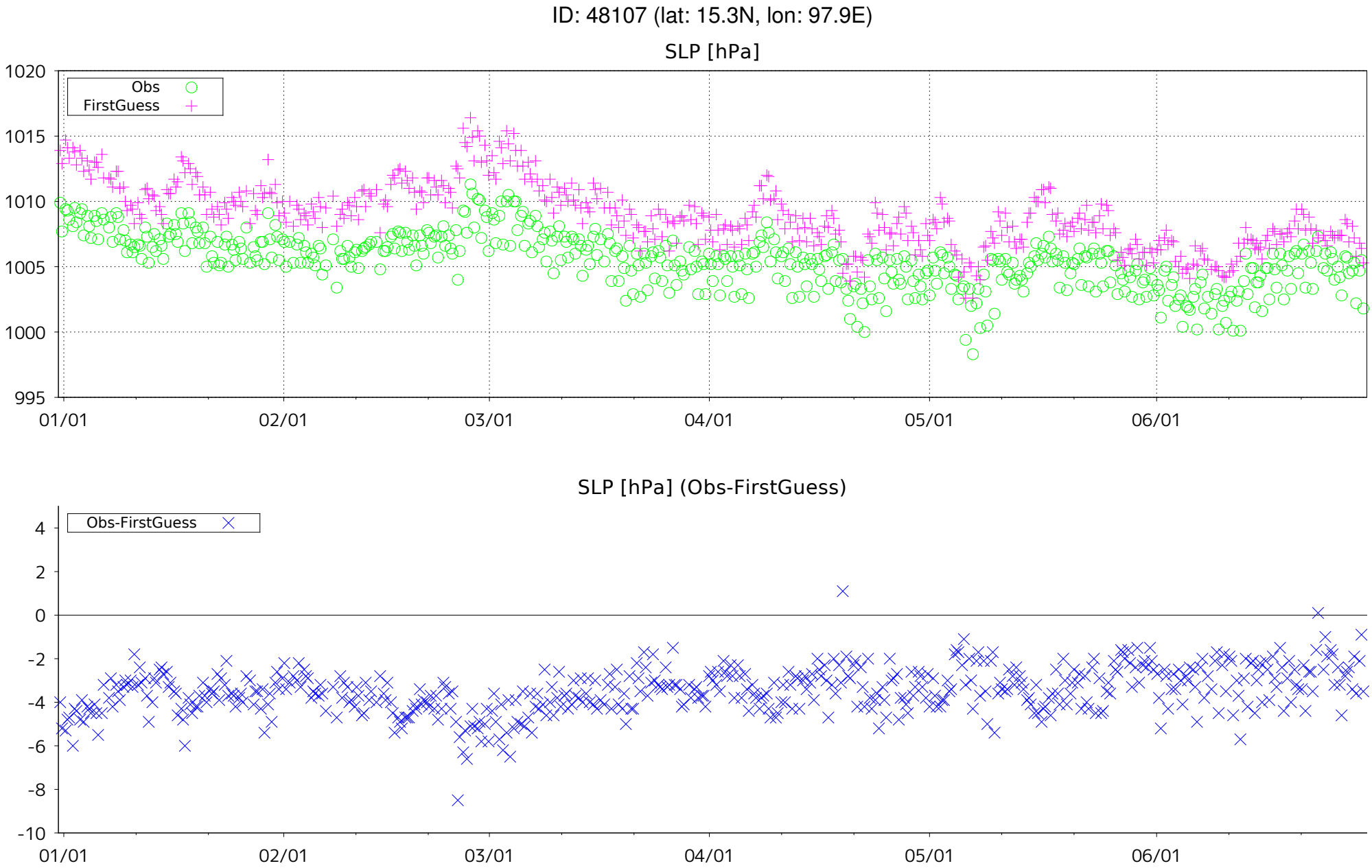

Figure 52 Time-series representation of SLP Obs minus FirstGuess for station 48107

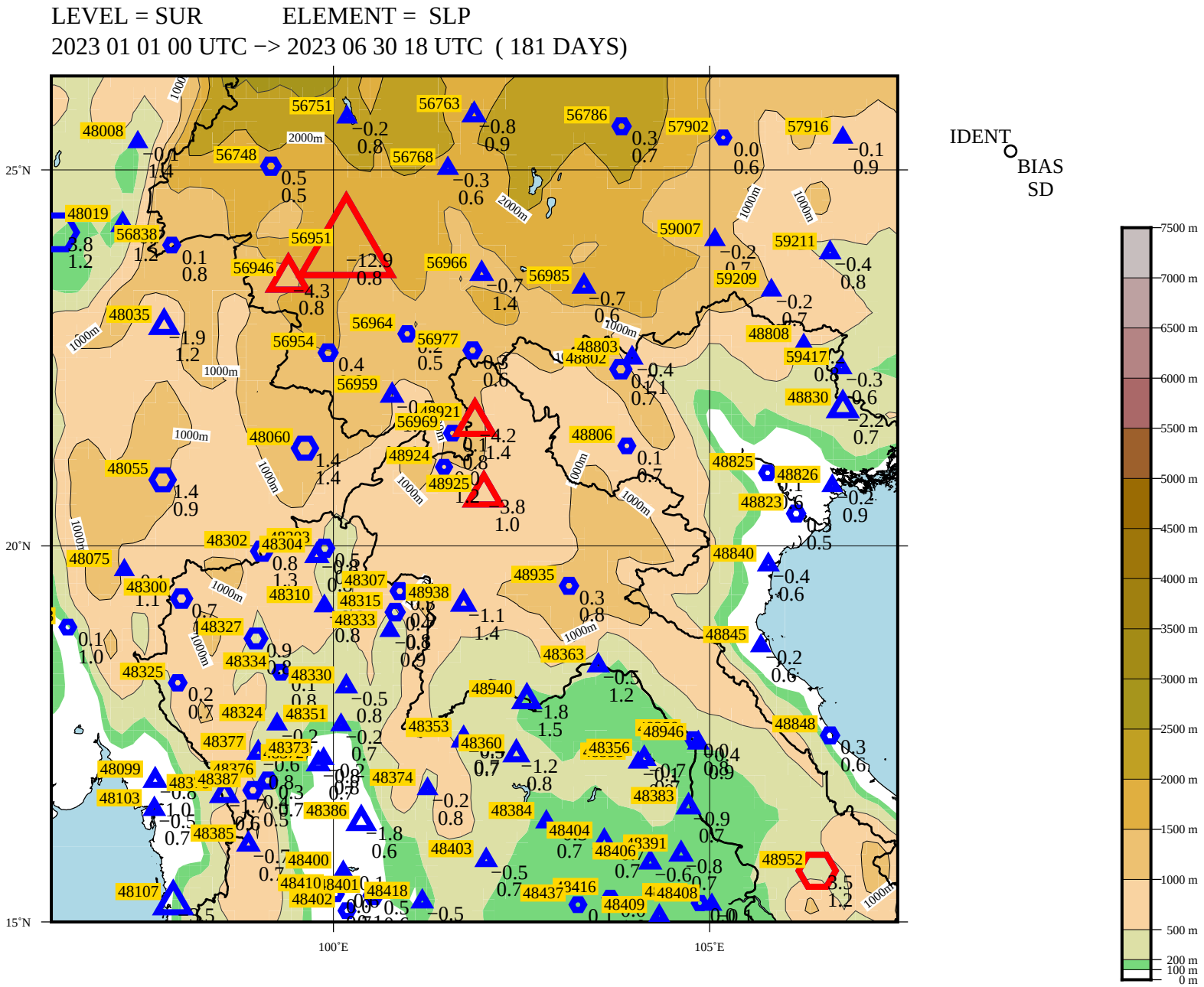

Figure 53 BIAS and SD of SLP for station 48921, 48925, 48952, 56946, 56951 (red) and surrounding stations (blue).
The number to the upper left of each symbol is the WMO IDENT, and those to the lower right are the values of BIAS and SD.
The size of each symbol is proportional to the value of BIAS, with hexagonal forms representing positive bias and triangular forms representing negative bias.

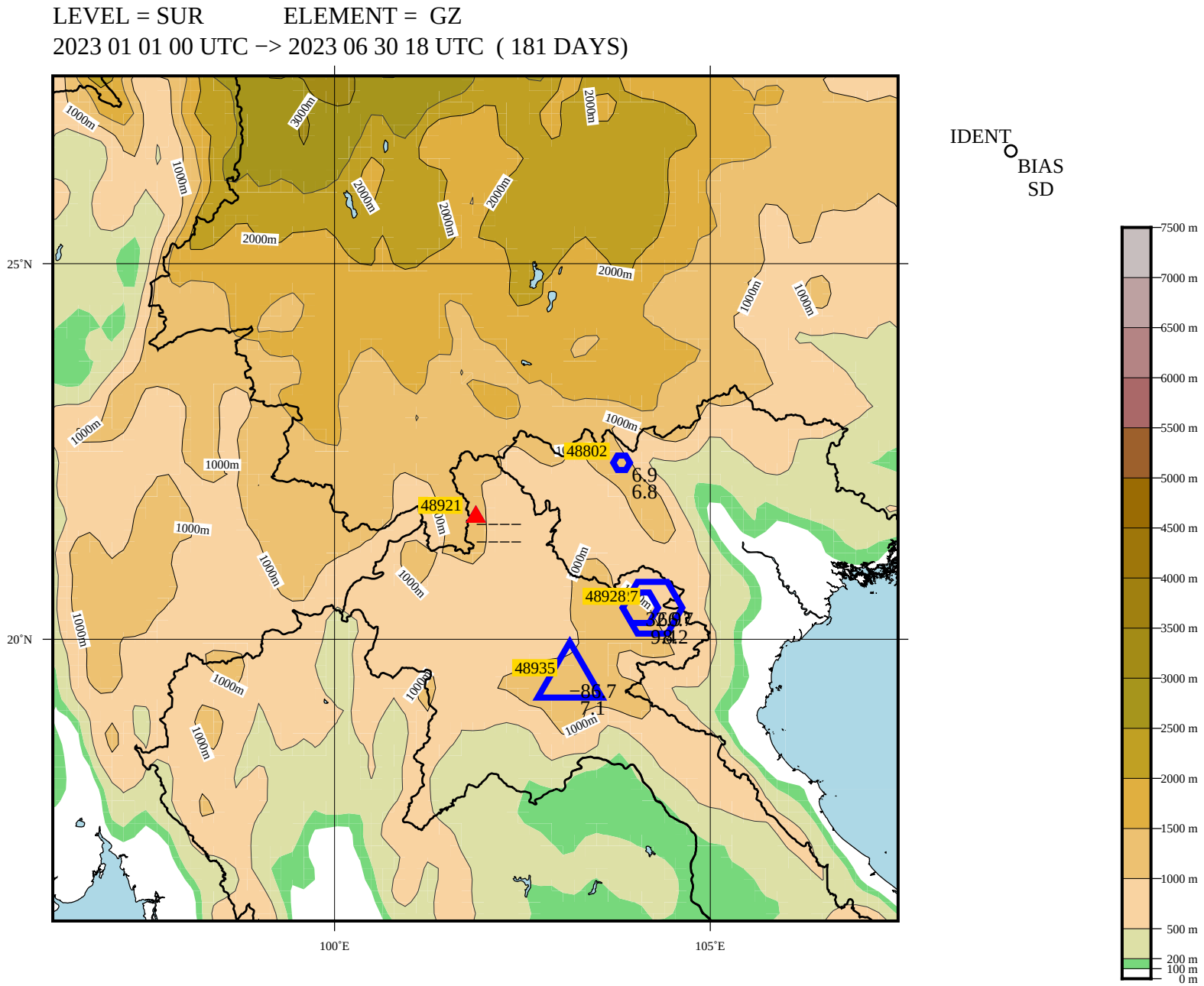

Figure 54 BIAS and SD of GZ for station 48921 (red) and surrounding stations (blue).
The number to the upper left of each symbol is the WMO IDENT, and those to the lower right are the values of BIAS and SD.
The size of each symbol is proportional to the value of BIAS, with hexagonal forms representing positive bias and triangular forms representing negative bias.

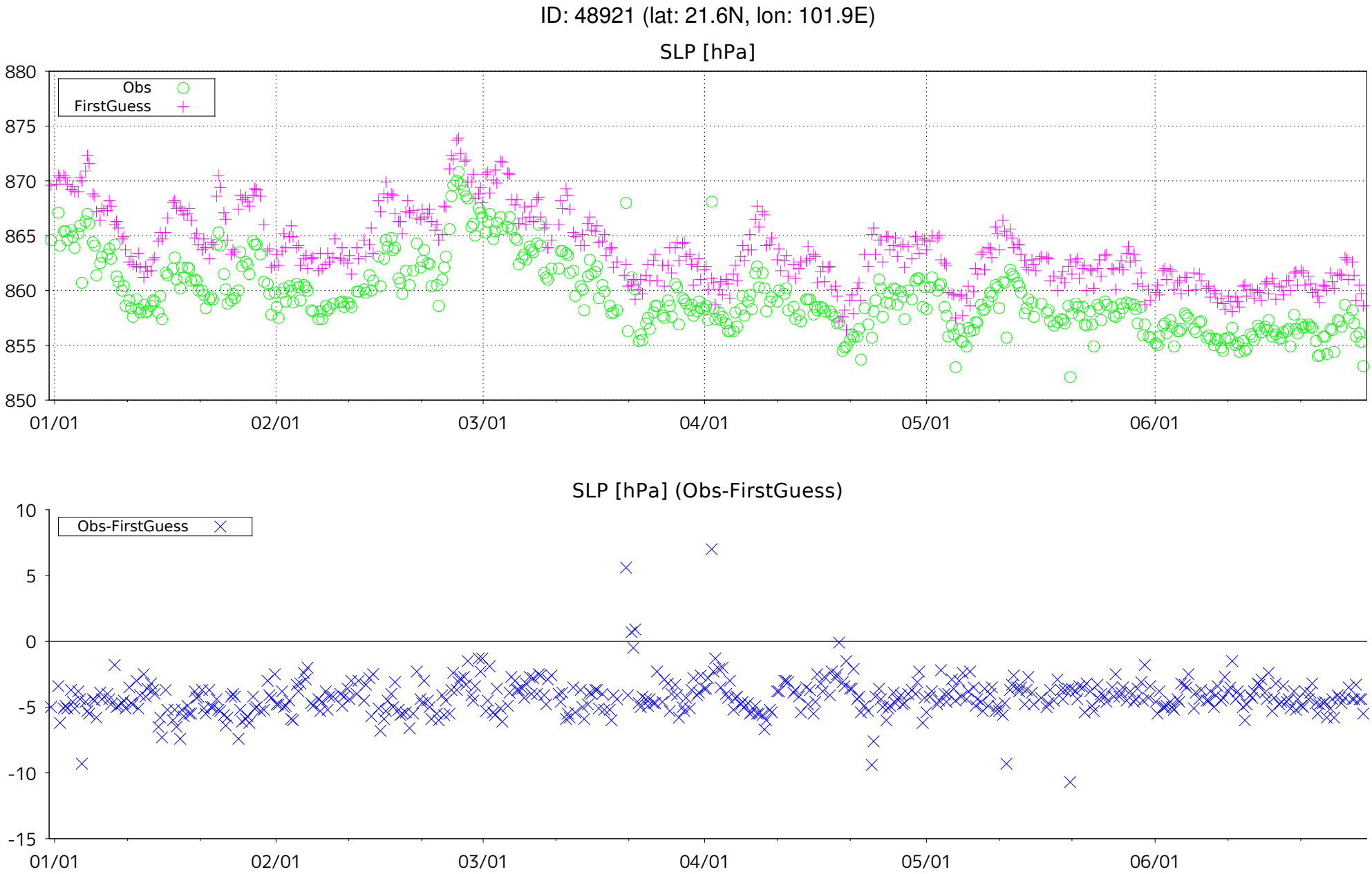

Figure 55(a) Time-series representation of SLP Obs minus FirstGuess for station 48921

Figure 55(b) Time-series representation of GZ850 Obs minus FirstGuess for station 48921

Figure 56 Time-series representation of SLP Obs minus FirstGuess for station 48925

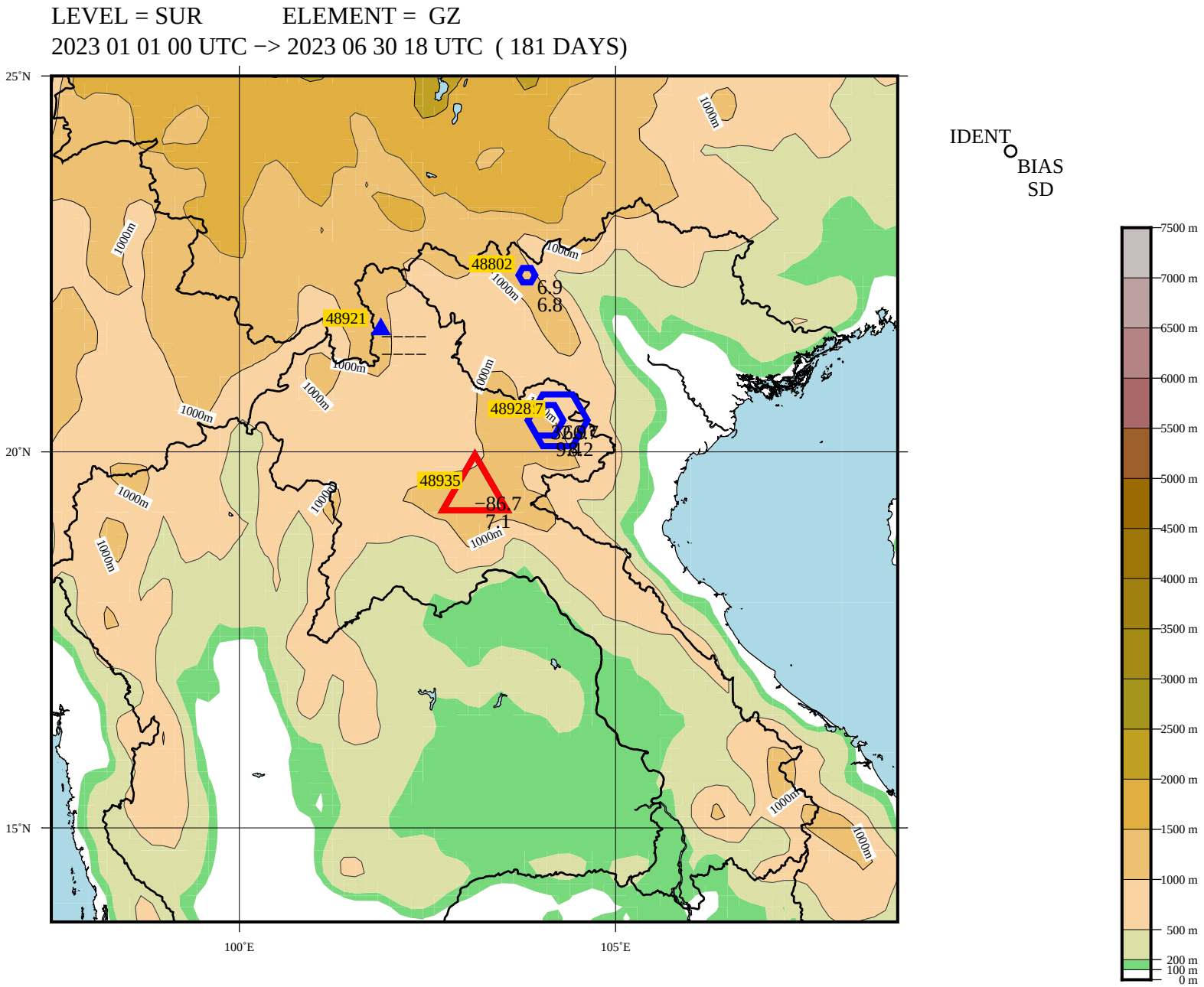

Figure 57 BIAS and SD of GZ for station 48935 (red) and surrounding stations (blue).
The number to the upper left of each symbol is the WMO IDENT, and those to the lower right are the values of BIAS and SD.
The size of each symbol is proportional to the value of BIAS, with hexagonal forms representing positive bias and triangular forms representing negative bias.

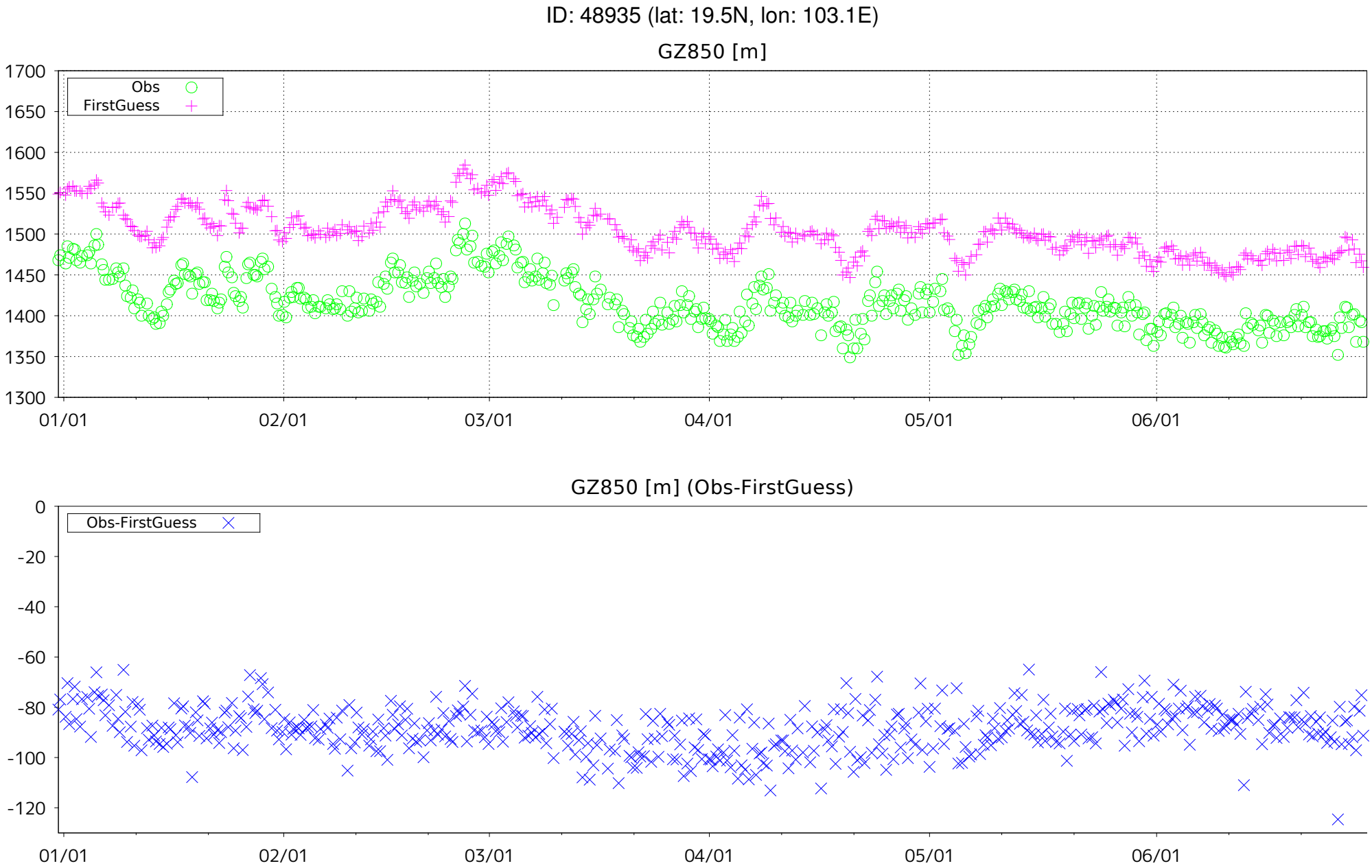

Figure 58 Time-series representation of GZ850 Obs minus FirstGuess for station 48935

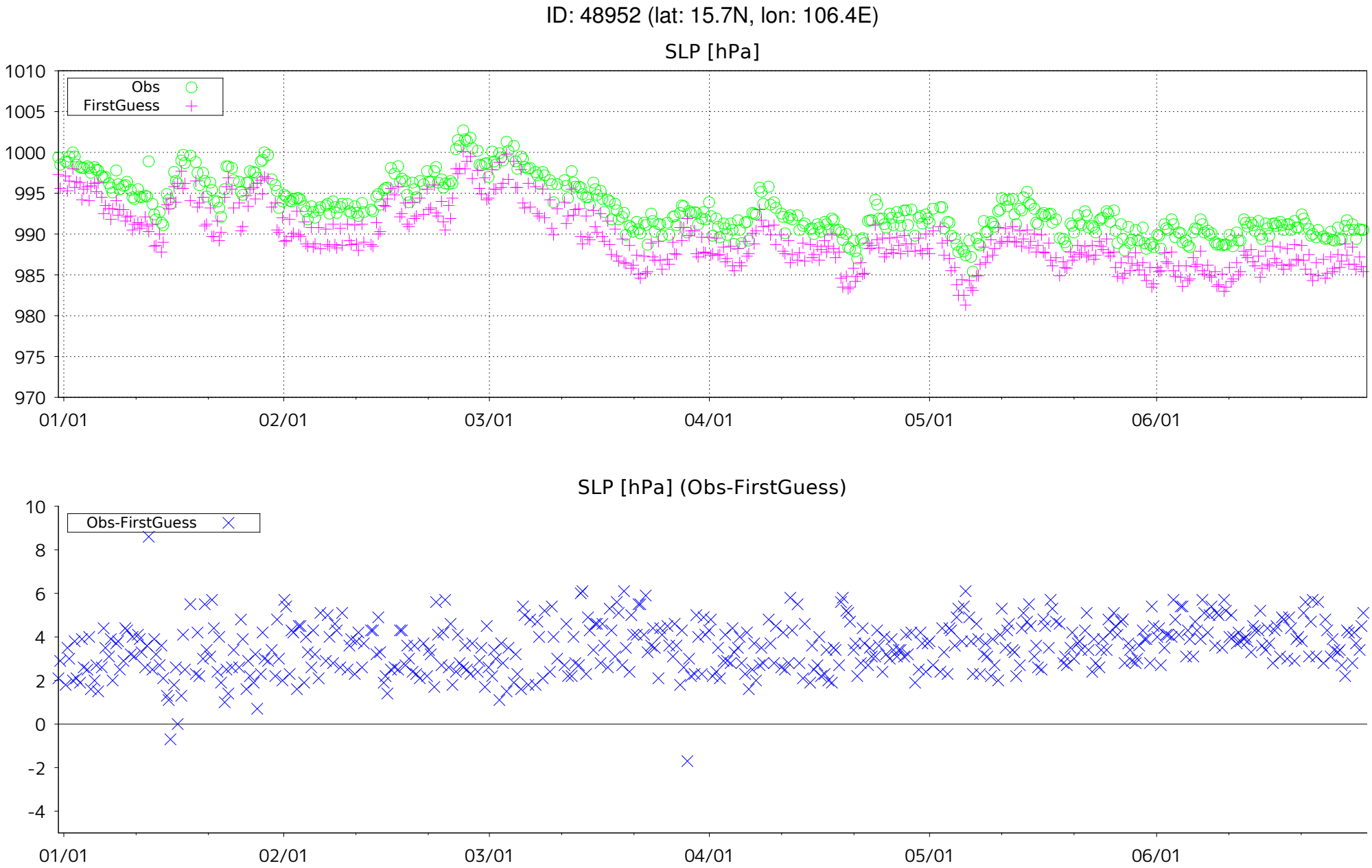

Figure 59 Time-series representation of SLP Obs minus FirstGuess for station 48952

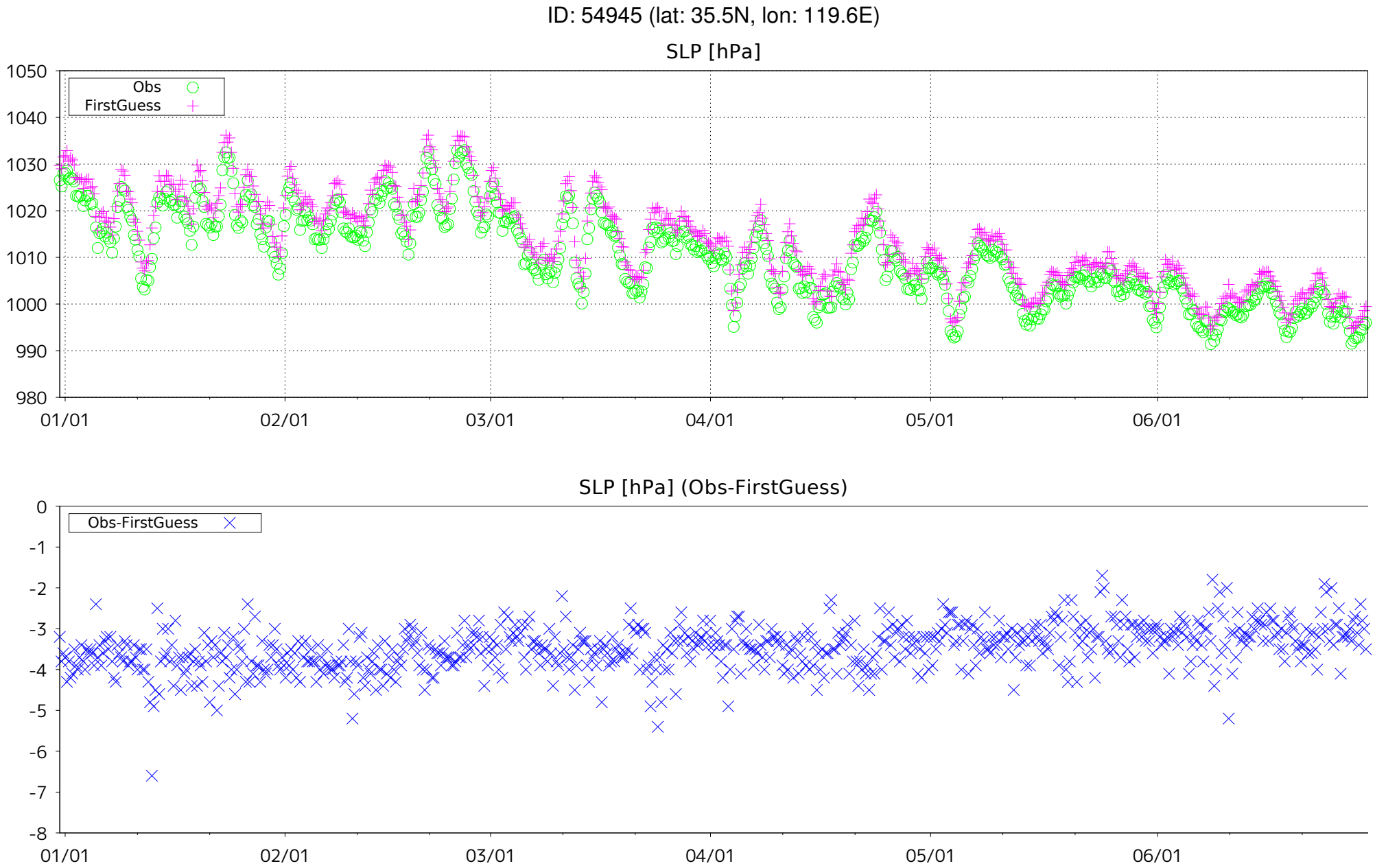

Figure 60 Time-series representation of SLP Obs minus FirstGuess for station 54945

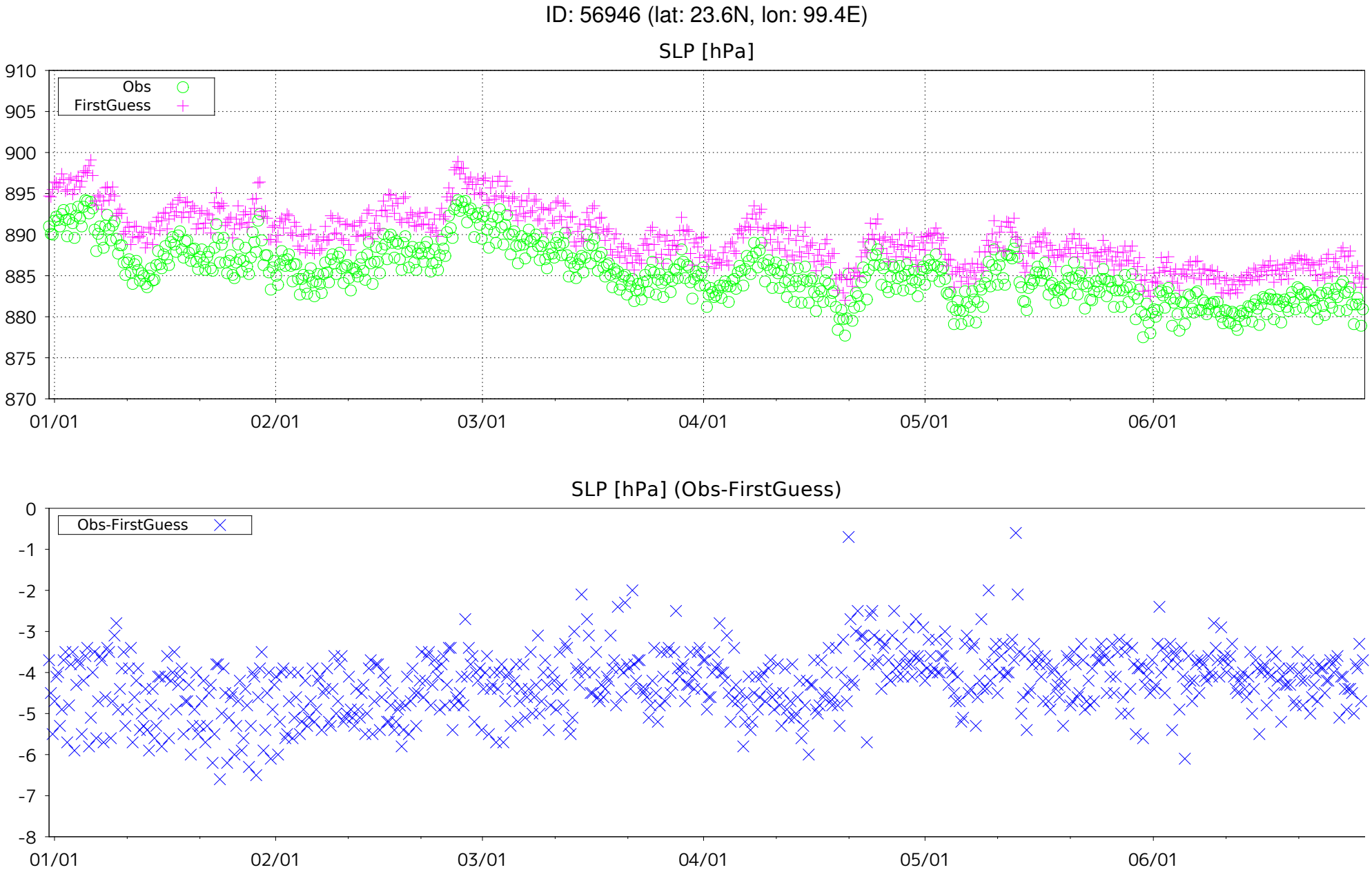

Figure 61 Time-series representation of SLP Obs minus FirstGuess for station 56946

Figure 62 Time-series representation of SLP Obs minus FirstGuess for station 56951

LEVEL = SUR ELEMENT = SLP

2023 01 01 00 UTC -> 2023 06 30 18 UTC (181 DAYS)

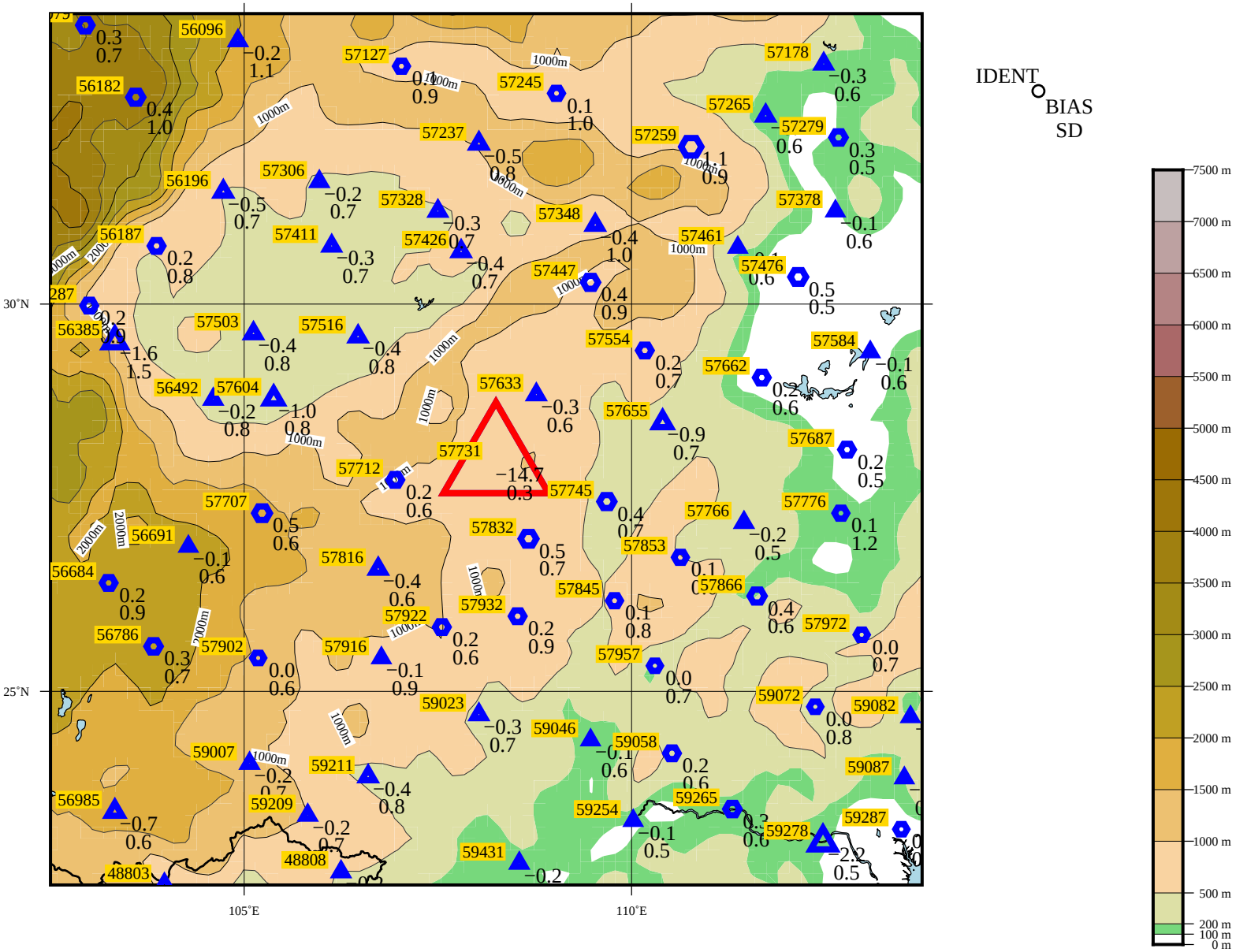

Figure 63 BIAS and SD of SLP for station 57731 (red) and surrounding stations (blue).
The number to the upper left of each symbol is the WMO IDENT, and those to the lower right are the values of BIAS and SD.
The size of each symbol is proportional to the value of BIAS, with hexagonal forms representing positive bias and triangular forms representing negative bias.

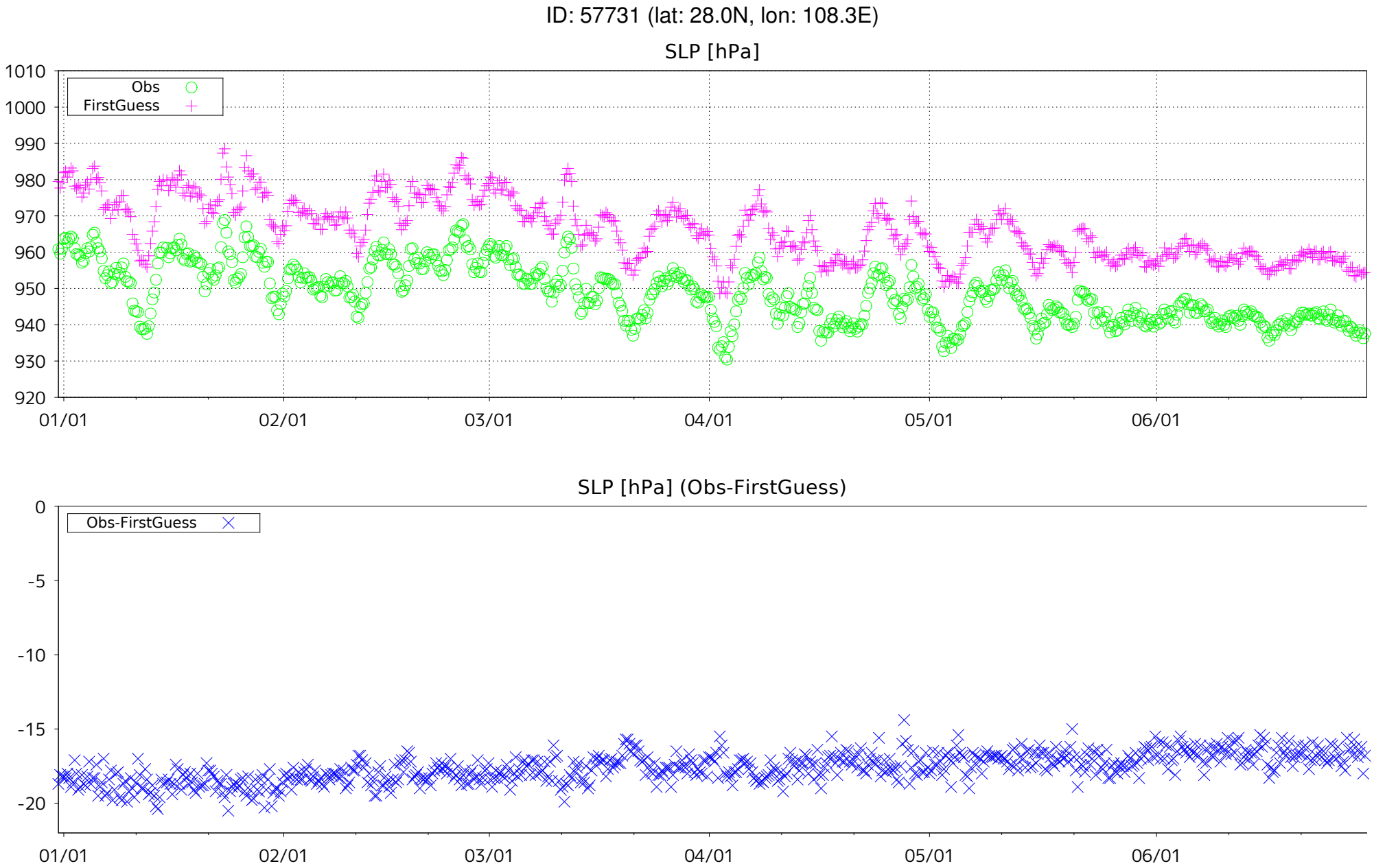

Figure 64 Time-series representation of SLP Obs minus FirstGuess for station 57731

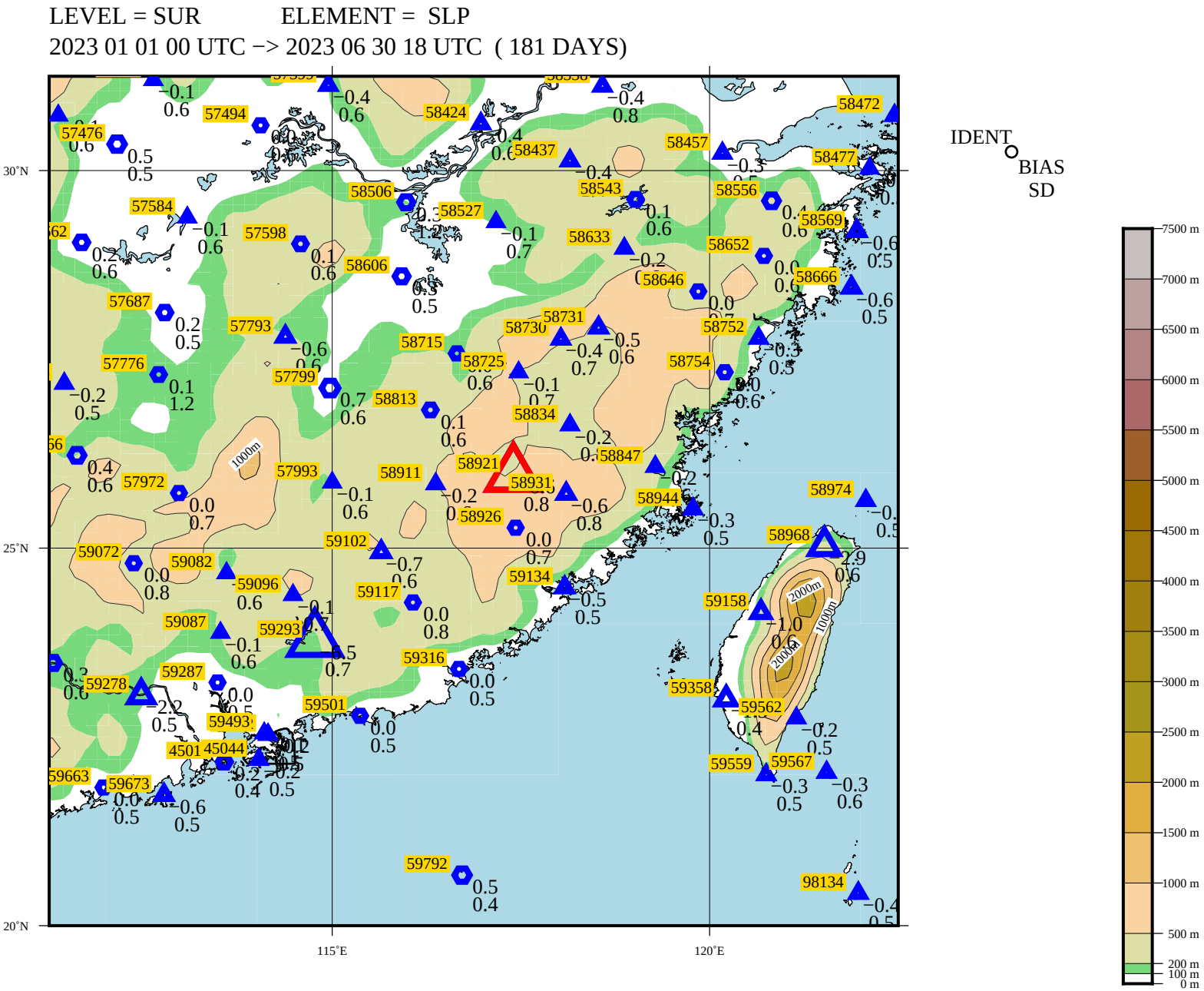

Figure 65 BIAS and SD of SLP for station 58921 (red) and surrounding stations (blue).
The number to the upper left of each symbol is the WMO IDENT, and those to the lower right are the values of BIAS and SD.
The size of each symbol is proportional to the value of BIAS, with hexagonal forms representing positive bias and triangular forms representing negative bias.

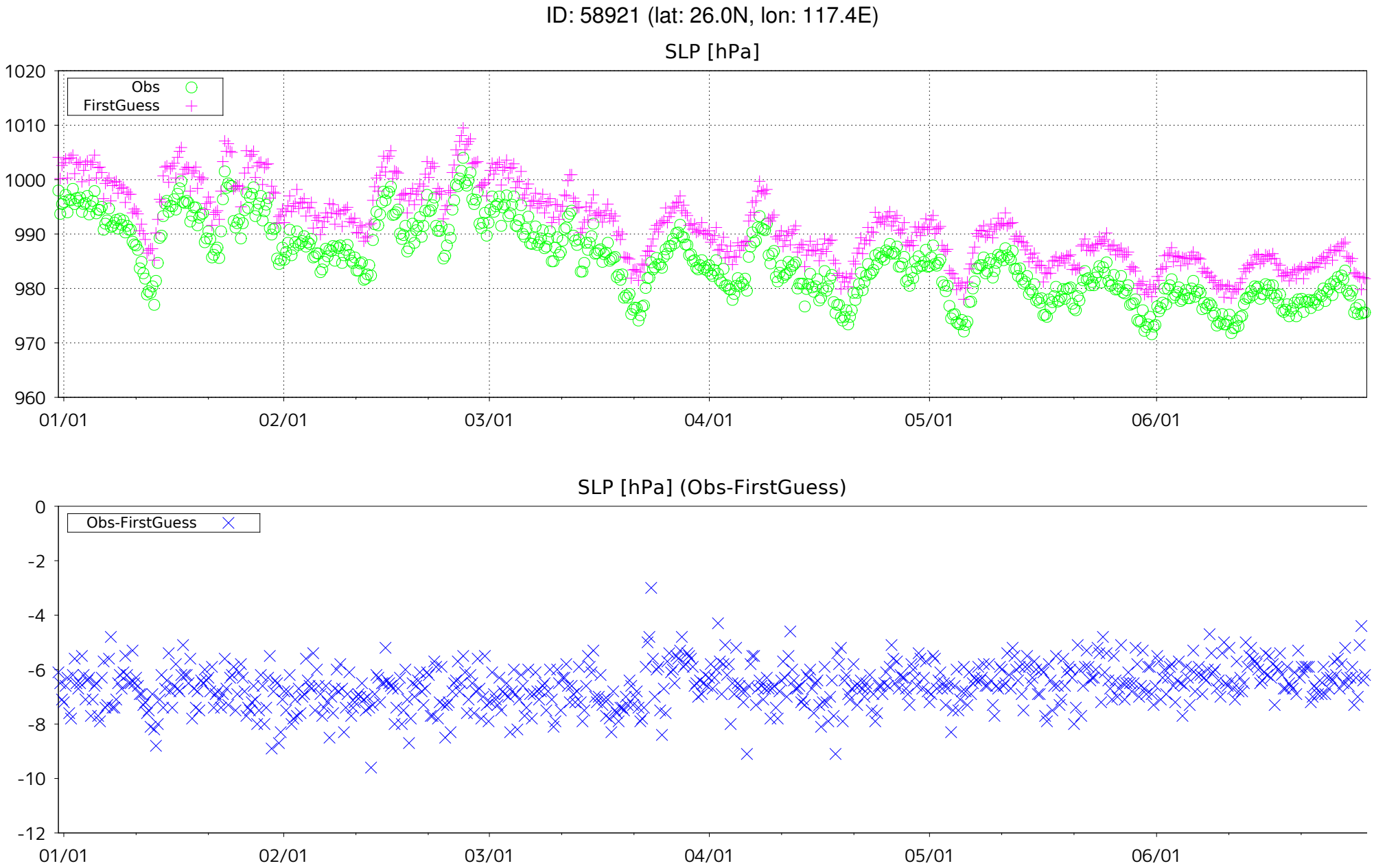

Figure 66 Time-series representation of SLP Obs minus FirstGuess for station 58921

LEVEL = SUR ELEMENT = SLP

2023 01 01 00 UTC -> 2023 06 30 18 UTC (181 DAYS)

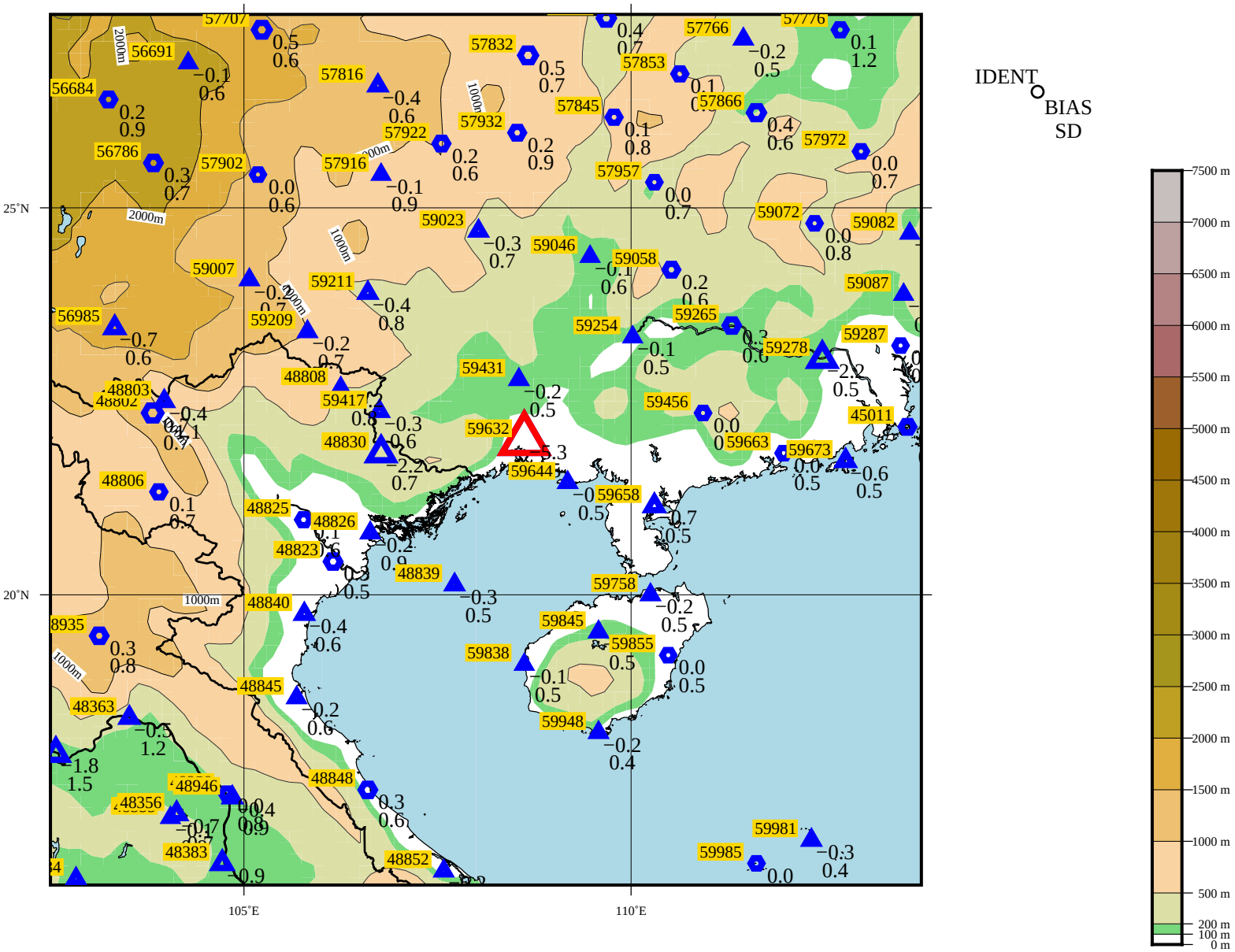

Figure 67 BIAS and SD of SLP for station 59632 (red) and surrounding stations (blue).
The number to the upper left of each symbol is the WMO IDENT, and those to the lower right are the values of BIAS and SD.
The size of each symbol is proportional to the value of BIAS, with hexagonal forms representing positive bias and triangular forms representing negative bias.

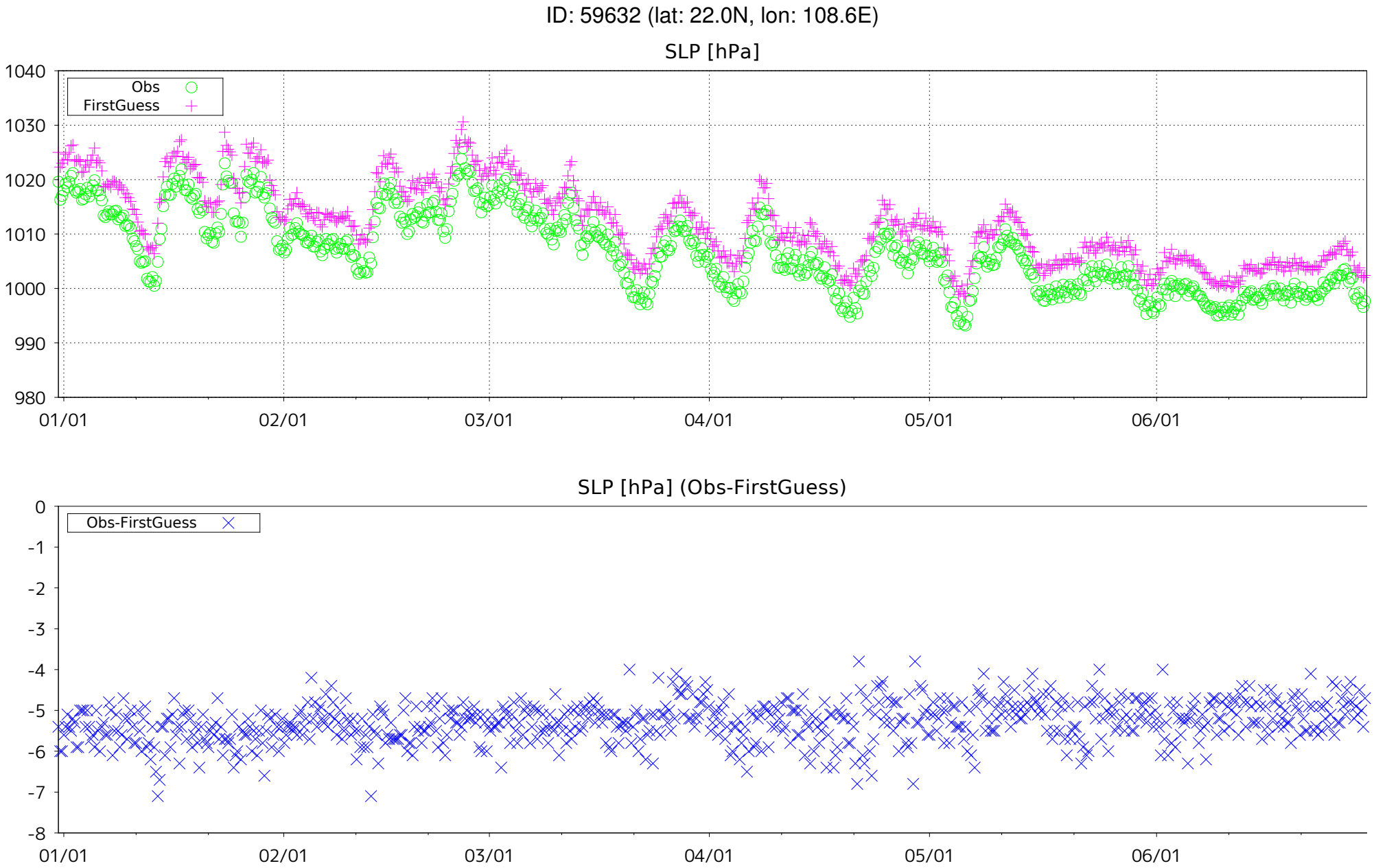

Figure 68 Time-series representation of SLP Obs minus FirstGuess for station 59632

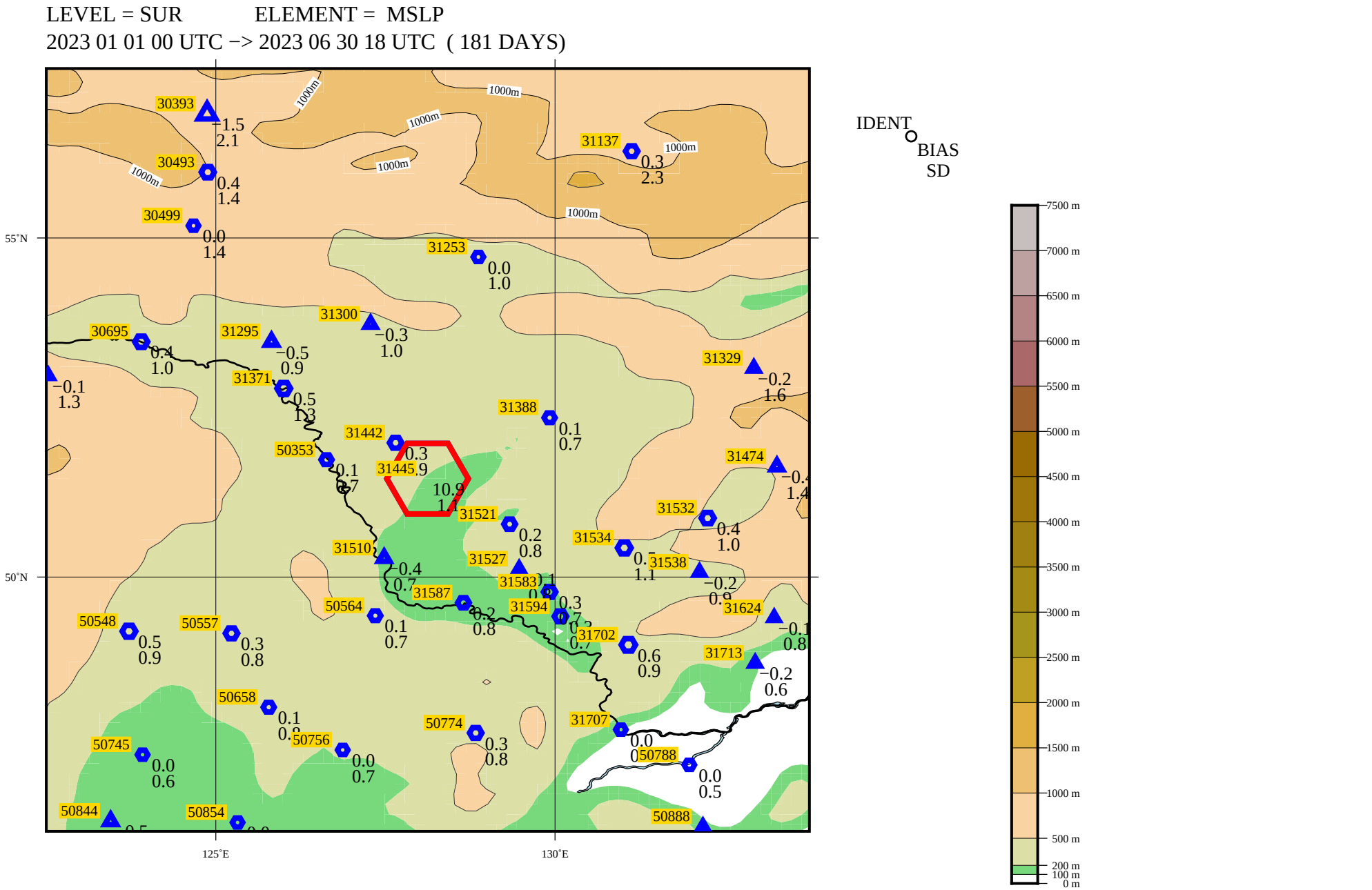

Figure 69 BIAS and SD of MSLP for station 31445 (red) and surrounding stations (blue).
The number to the upper left of each symbol is the WMO IDENT, and those to the lower right are the values of BIAS and SD.
The size of each symbol is proportional to the value of BIAS, with hexagonal forms representing positive bias and triangular forms representing negative bias.

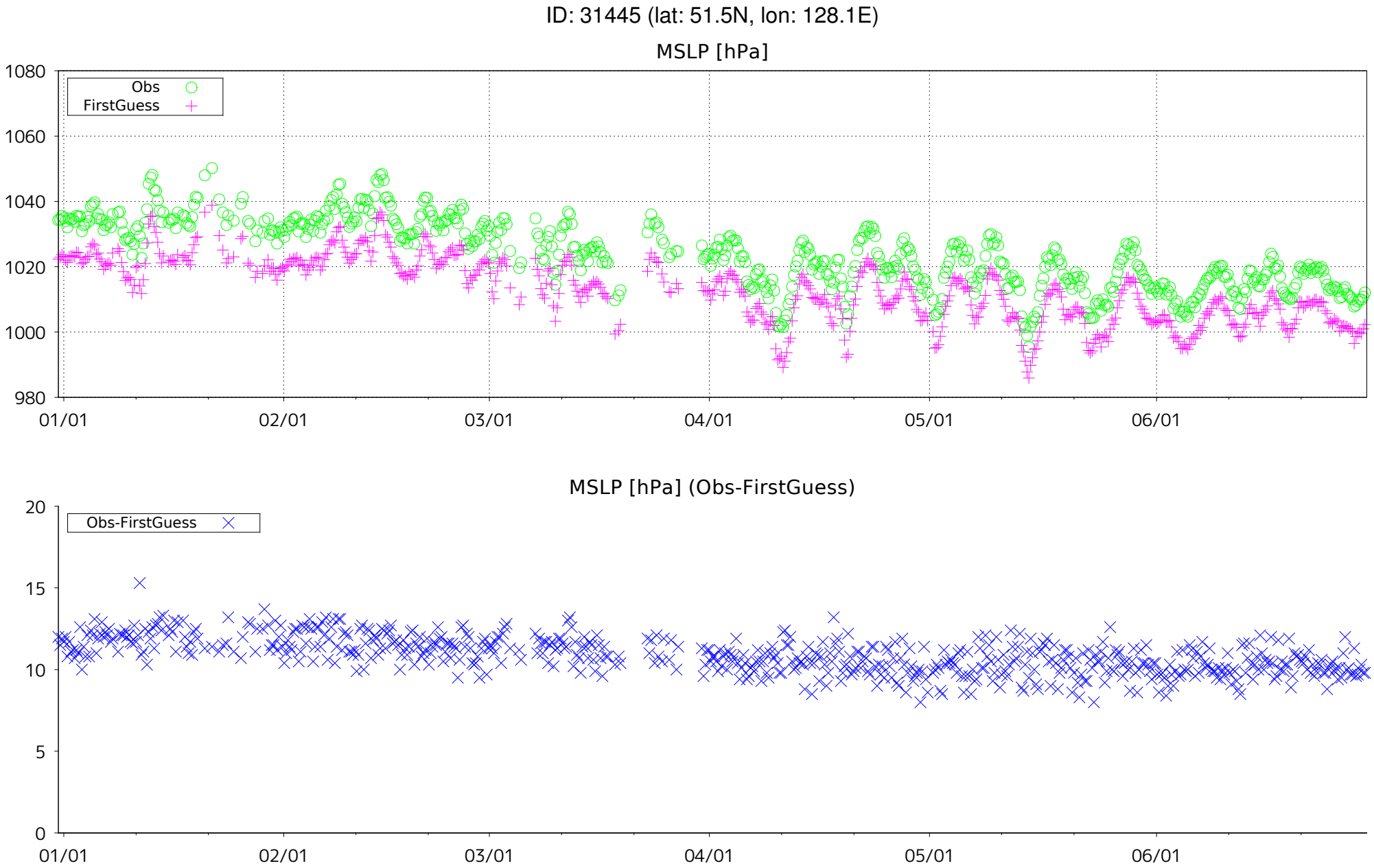

Figure 70 Time-series representation of MSLP Obs minus FirstGuess for station 31445

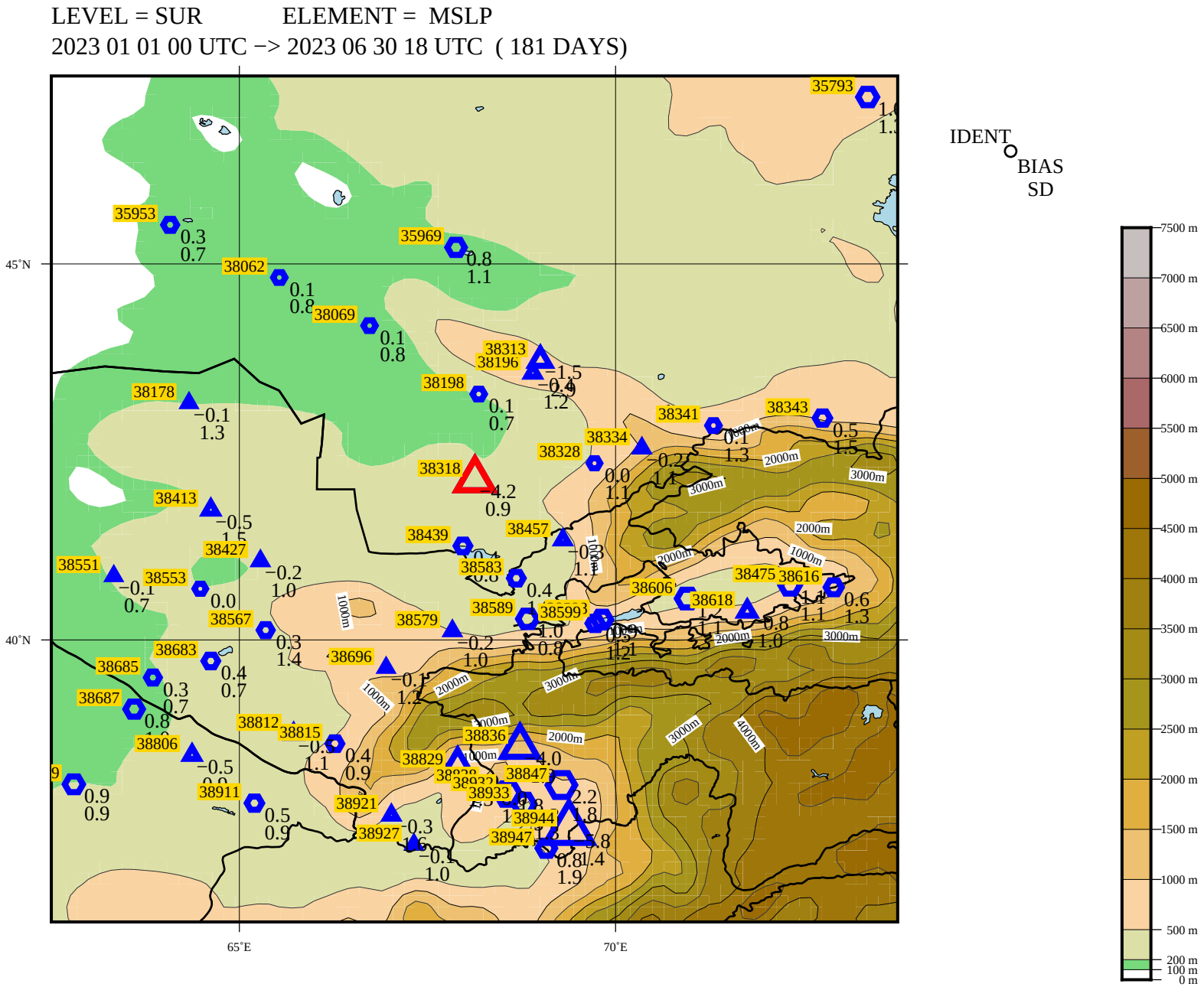

Figure 71 BIAS and SD of MSLP for station 38318 (red) and surrounding stations (blue).
The number to the upper left of each symbol is the WMO IDENT, and those to the lower right are the values of BIAS and SD.
The size of each symbol is proportional to the value of BIAS, with hexagonal forms representing positive bias and triangular forms representing negative bias.

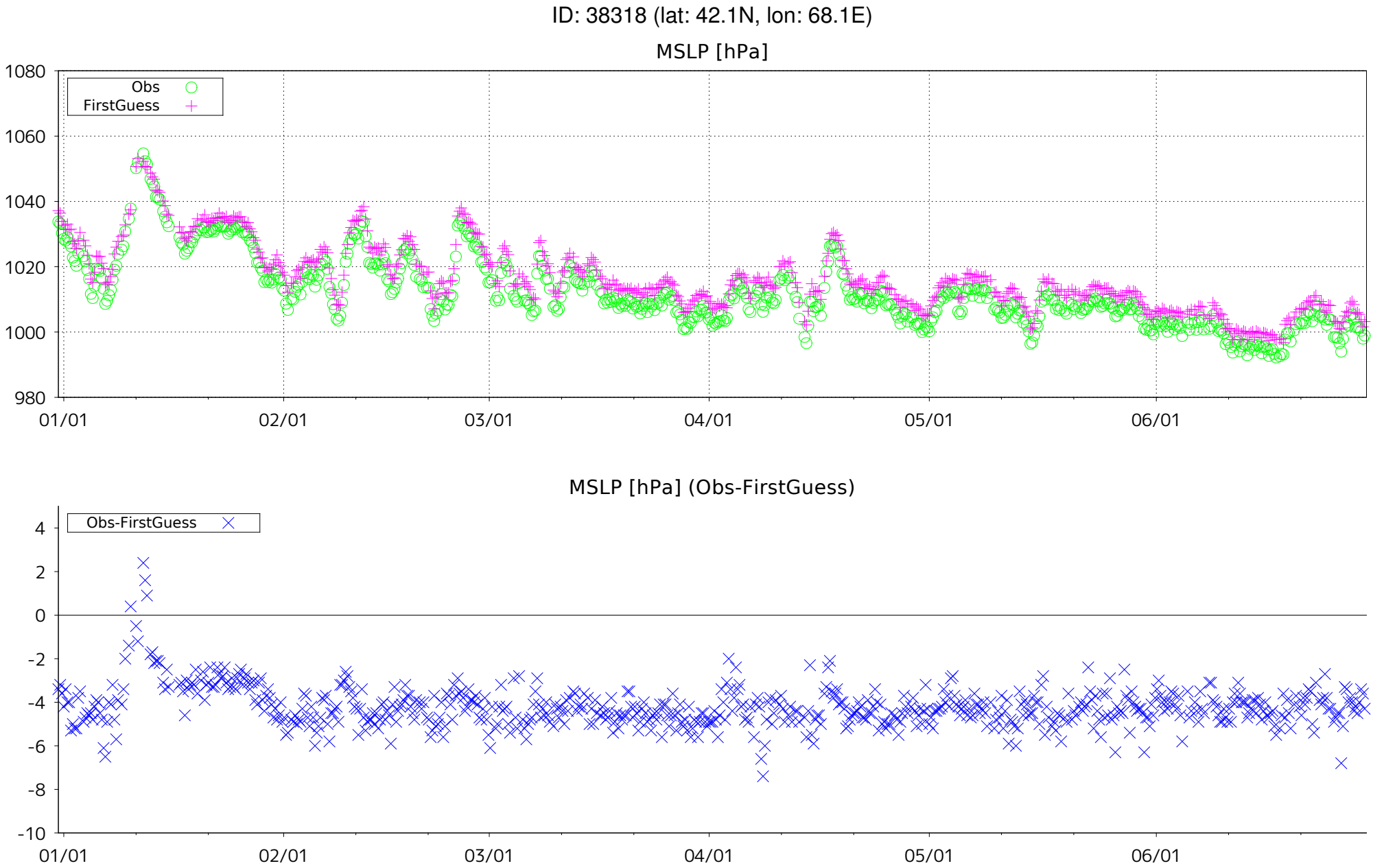

Figure 72 Time-series representation of MSLP Obs minus FirstGuess for station 38318

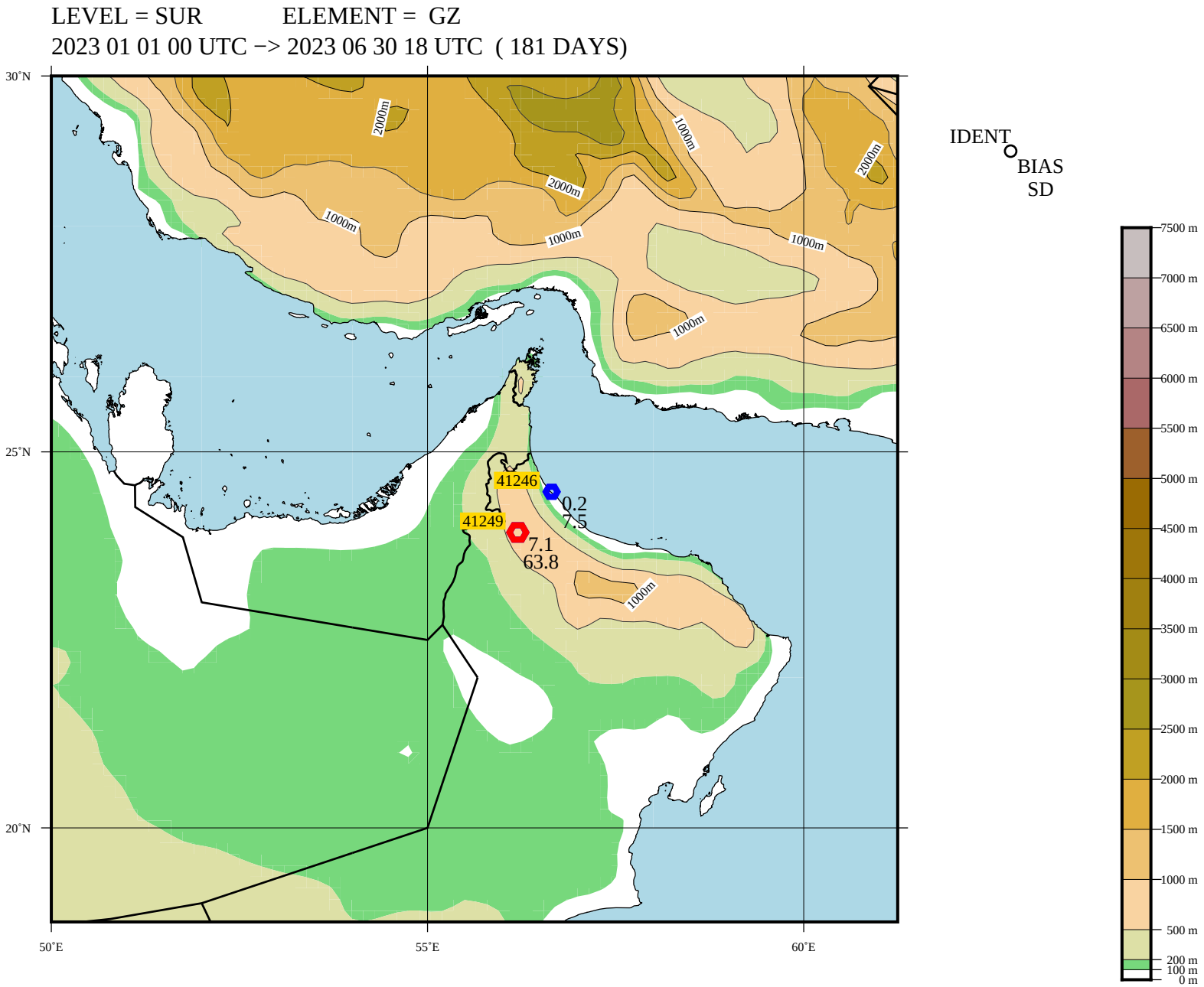

Figure 73 BIAS and SD of GZ for station 41249 (red) and surrounding stations (blue).
The number to the upper left of each symbol is the WMO IDENT, and those to the lower right are the values of BIAS and SD.
The size of each symbol is proportional to the value of BIAS, with hexagonal forms representing positive bias and triangular forms representing negative bias.

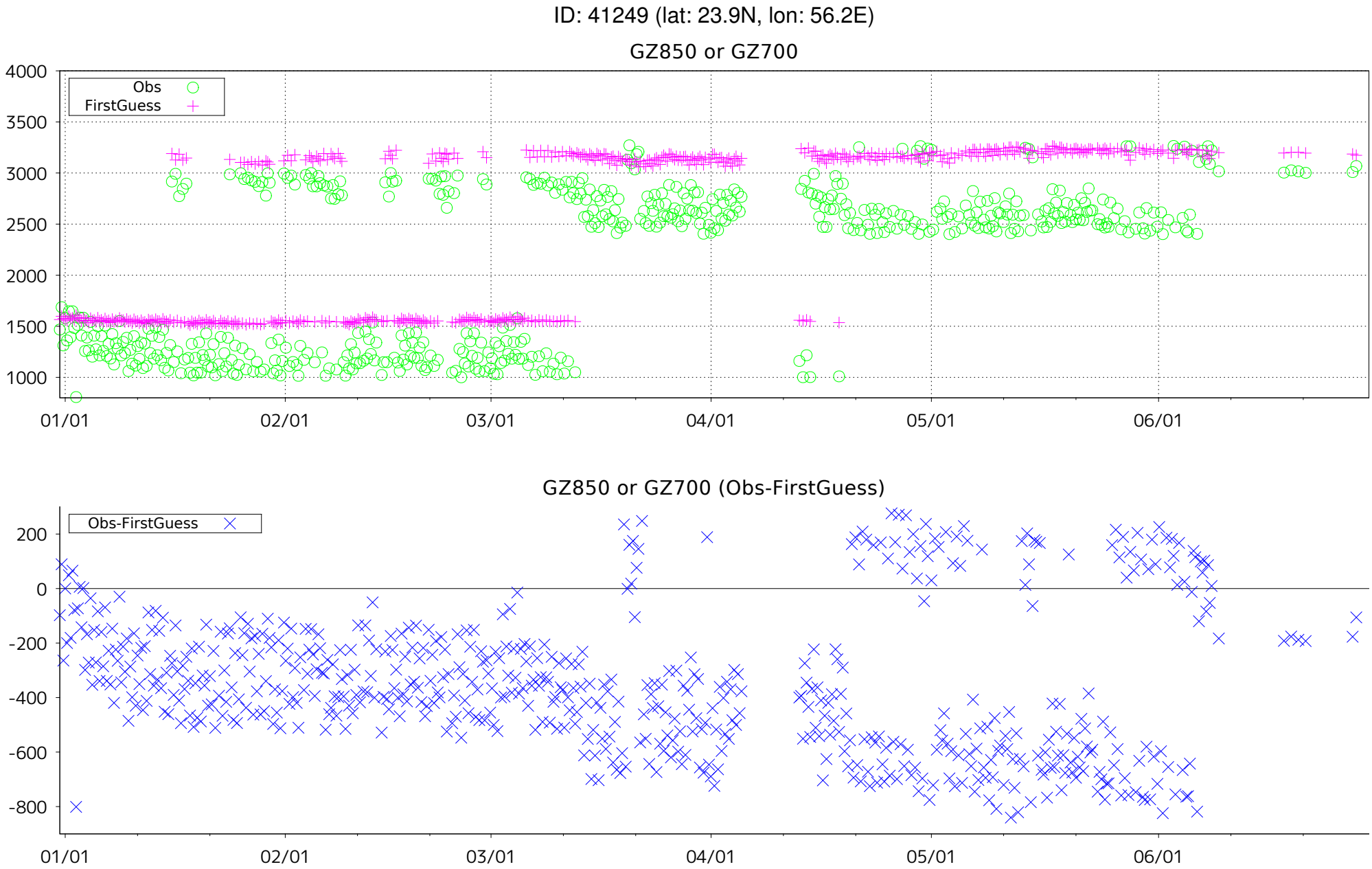

Figure 74 Time-series representation of GZ850 or GZ700 Obs minus FirstGuess for station 41249

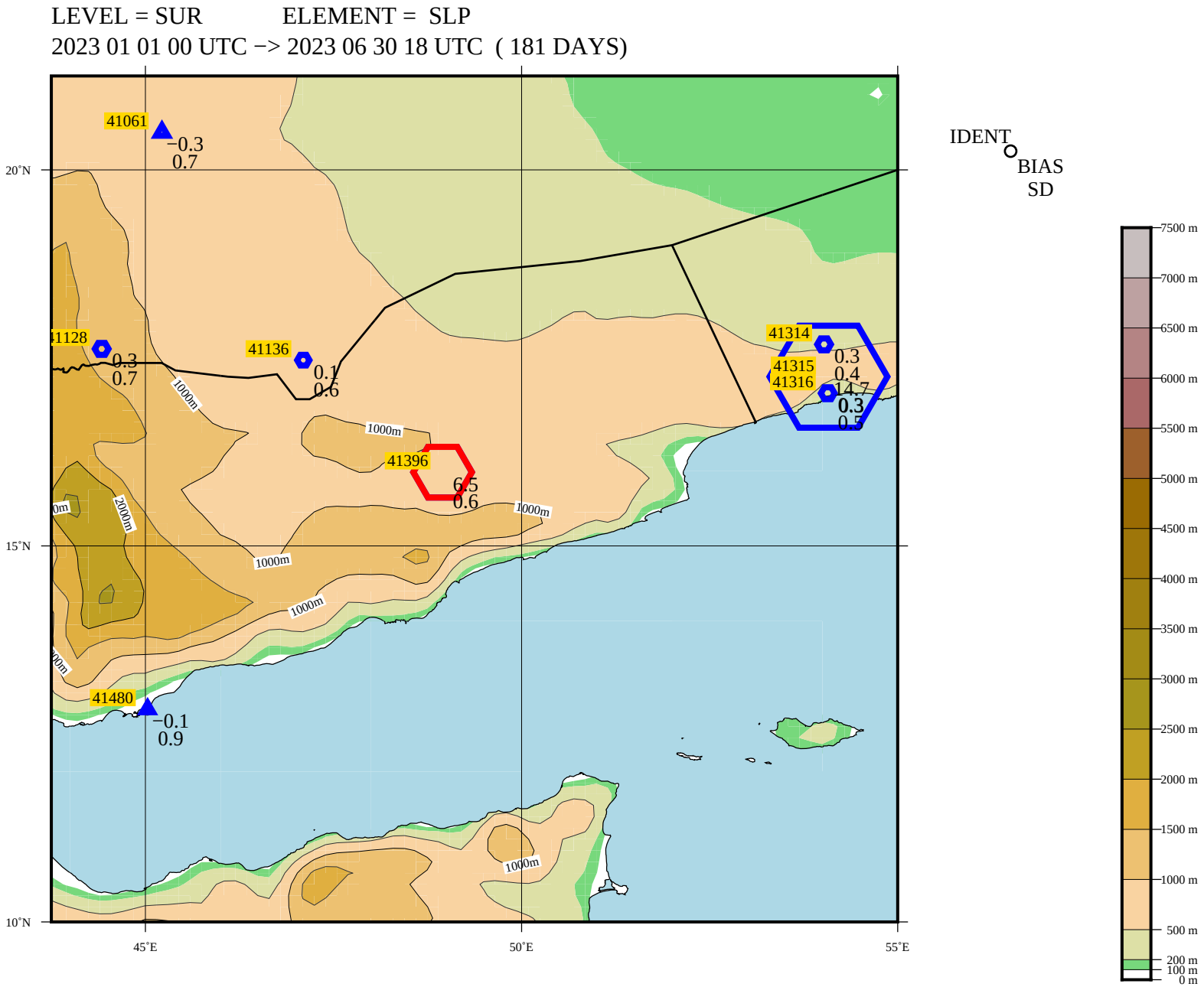

Figure 75 BIAS and SD of SLP for station 41396 (red) and surrounding stations (blue).
The number to the upper left of each symbol is the WMO IDENT, and those to the lower right are the values of BIAS and SD.
The size of each symbol is proportional to the value of BIAS, with hexagonal forms representing positive bias and triangular forms representing negative bias.

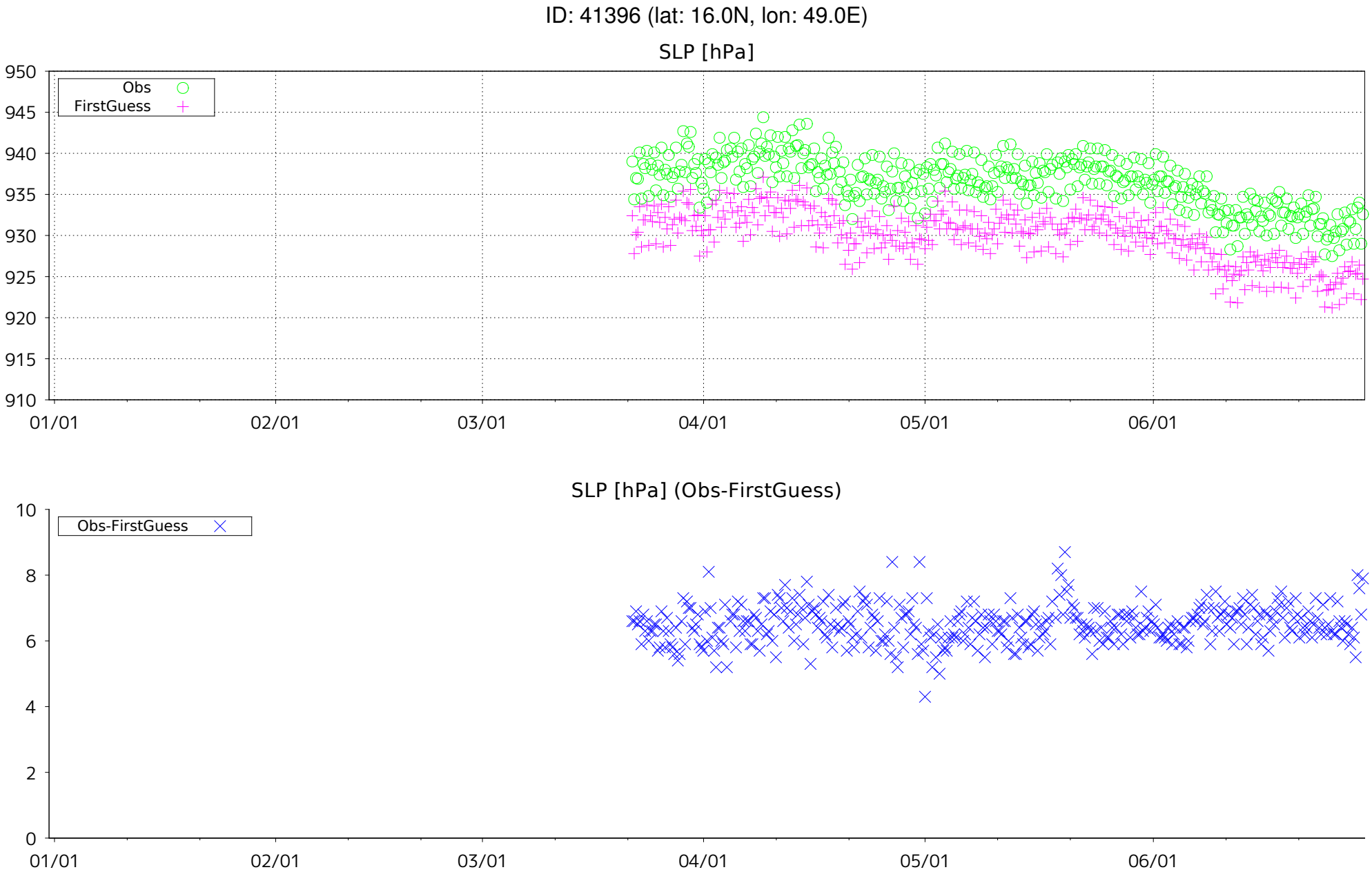

Figure 76 Time-series representation of SLP Obs minus FirstGuess for station 41396

Figure 77 Time-series representation of SLP Obs minus FirstGuess for station 44424

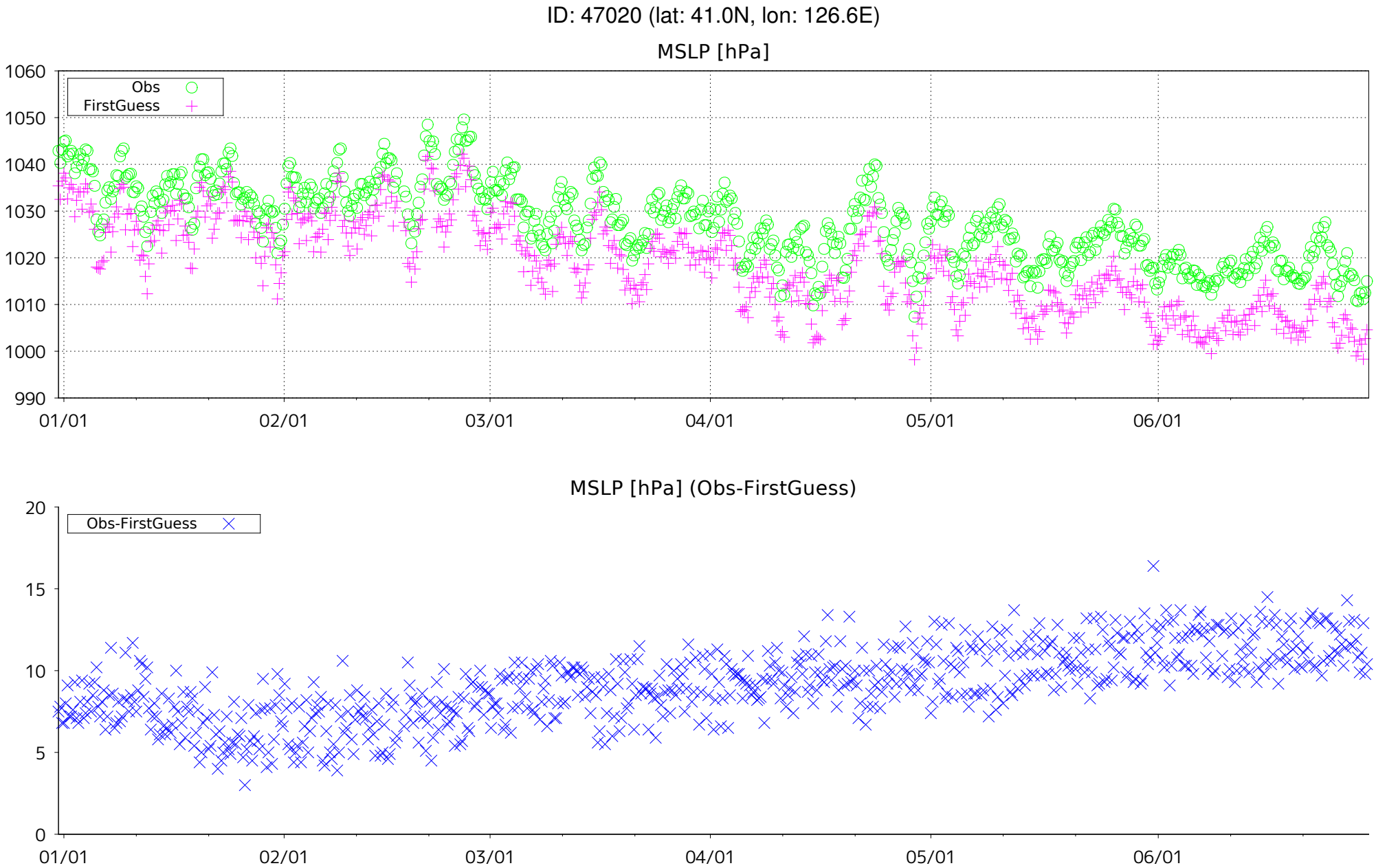

Figure 78 Time-series representation of MSLP Obs minus FirstGuess for station 47020

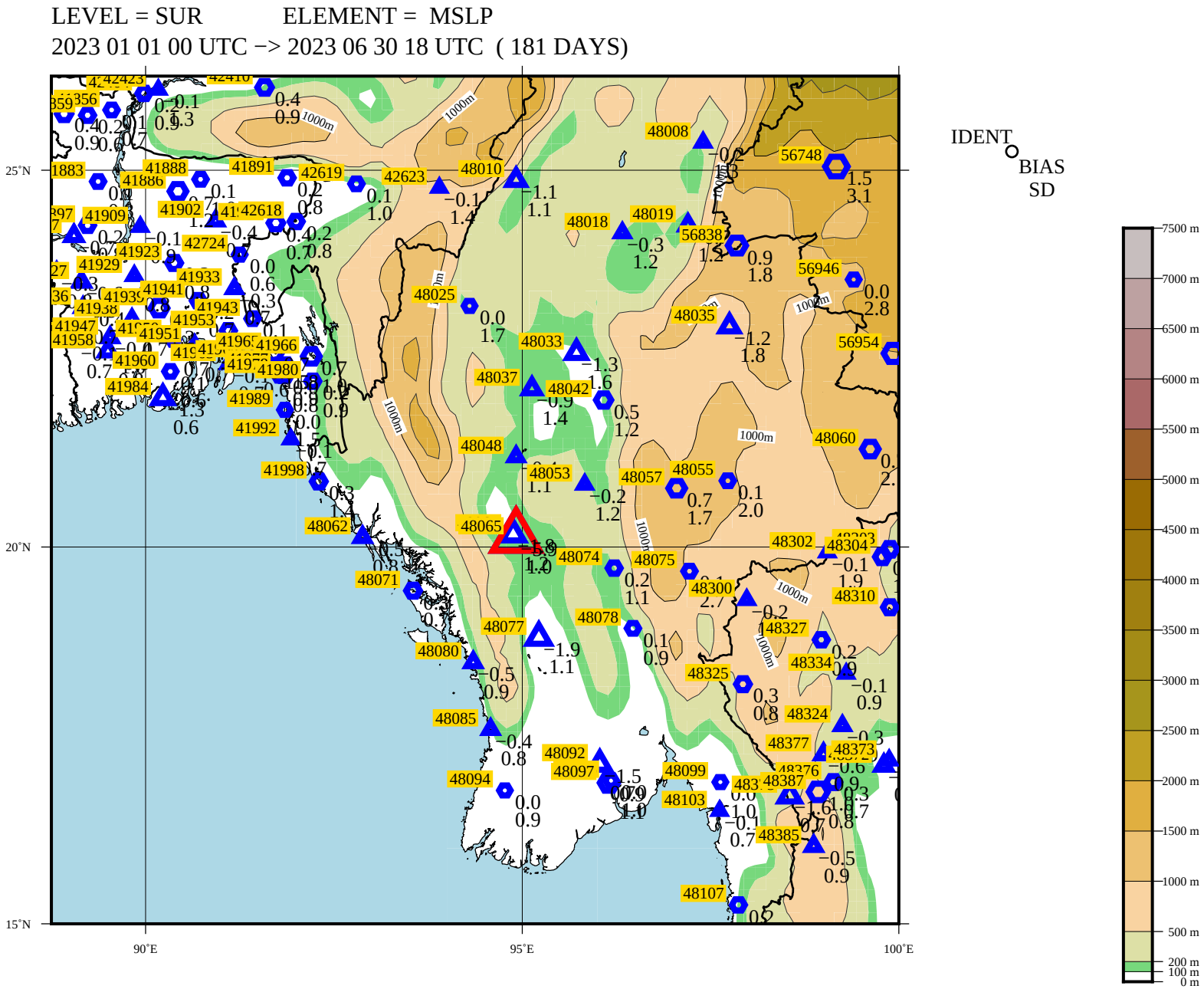

Figure 79 BIAS and SD of MSLP for station 48065 (red) and surrounding stations (blue).
The number to the upper left of each symbol is the WMO IDENT, and those to the lower right are the values of BIAS and SD.
The size of each symbol is proportional to the value of BIAS, with hexagonal forms representing positive bias and triangular forms representing negative bias.

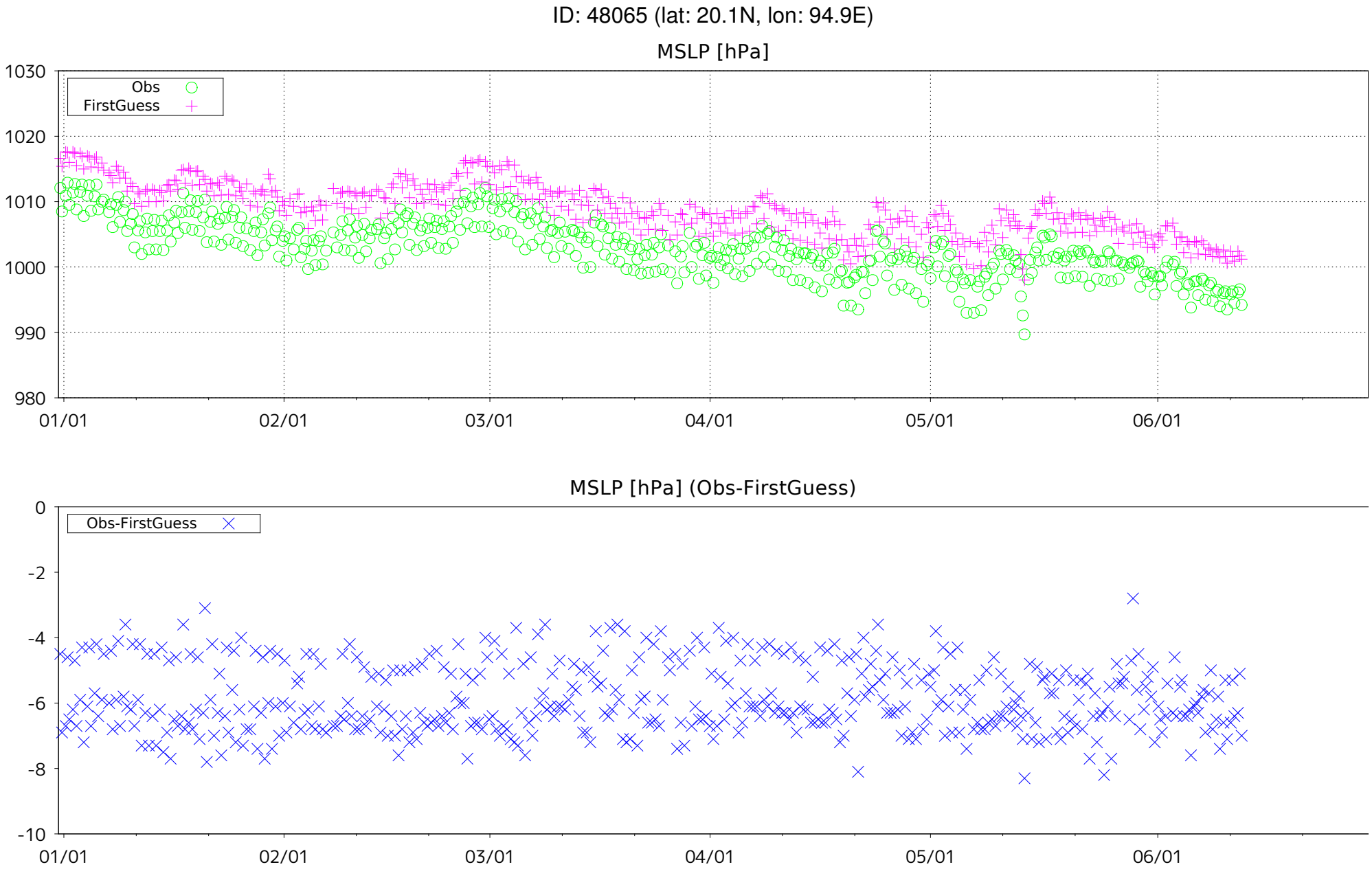

Figure 80 Time-series representation of MSLP Obs minus FirstGuess for station 48065

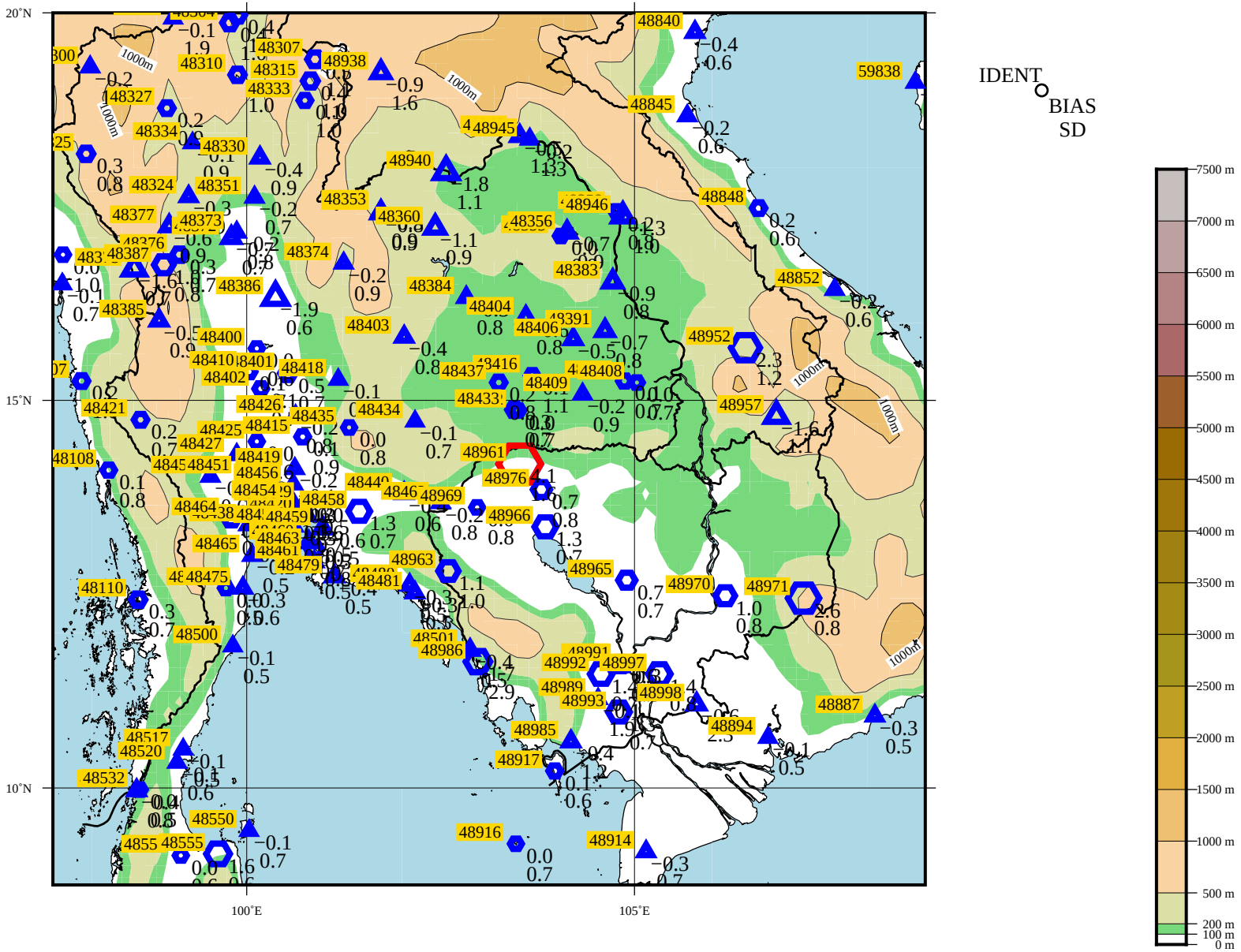

Figure 81 BIAS and SD of MSLP for station 48961 (red) and surrounding stations (blue).
The number to the upper left of each symbol is the WMO IDENT, and those to the lower right are the values of BIAS and SD.
The size of each symbol is proportional to the value of BIAS, with hexagonal forms representing positive bias and triangular forms representing negative bias.

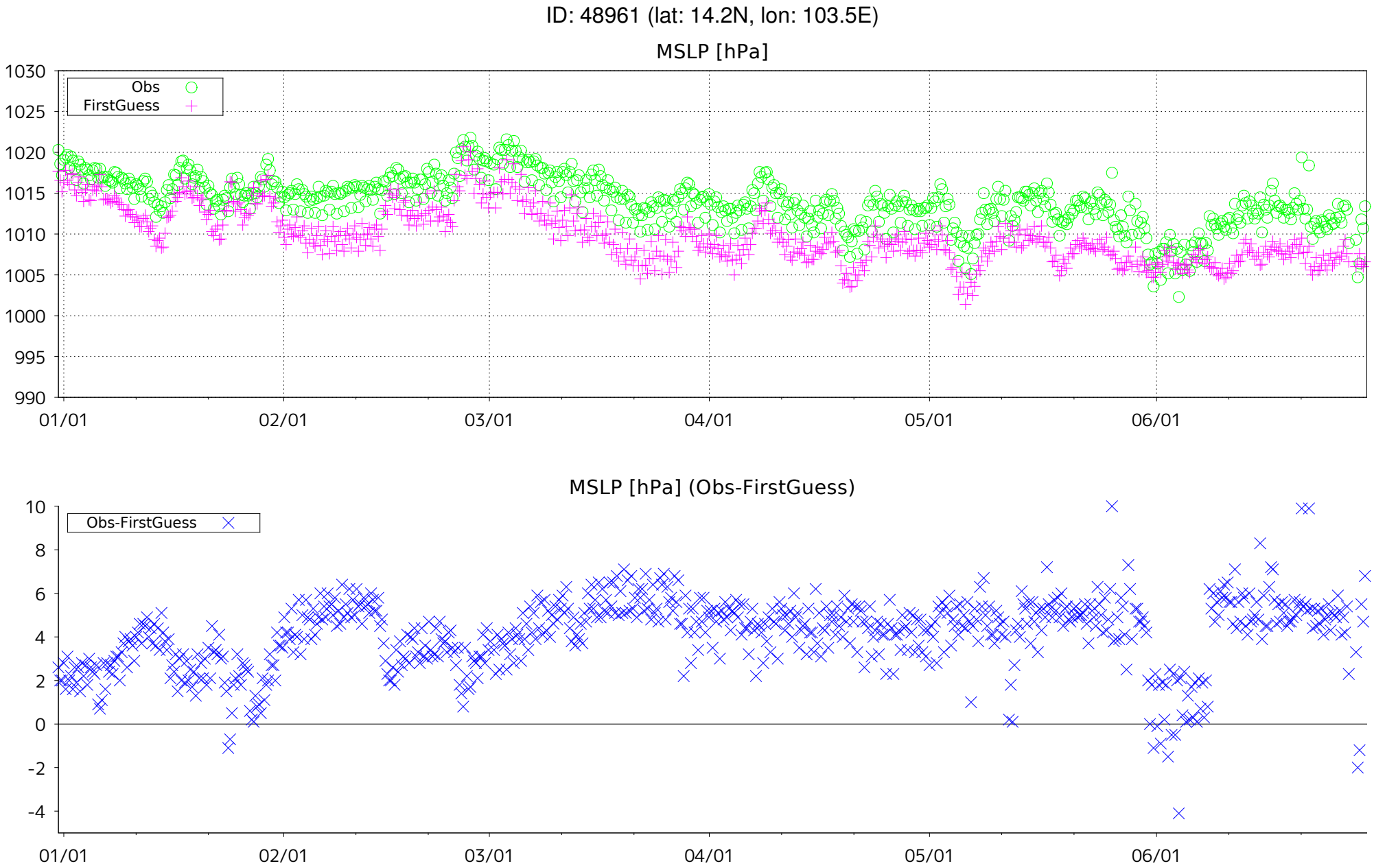

Figure 82 Time-series representation of MSLP Obs minus FirstGuess for station 48961

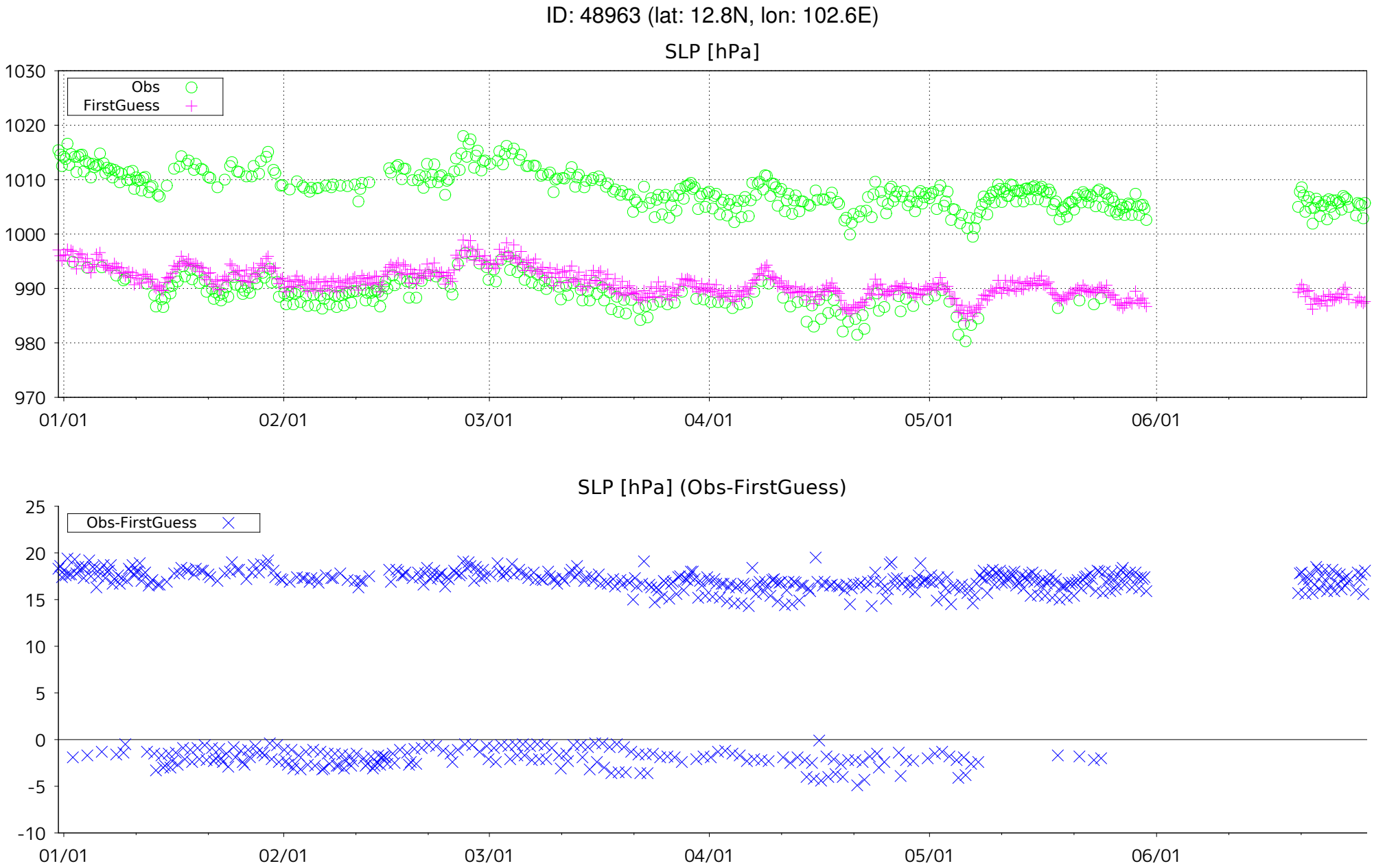

Figure 83(a) Time-series representation of SLP Obs minus FirstGuess for station 48963

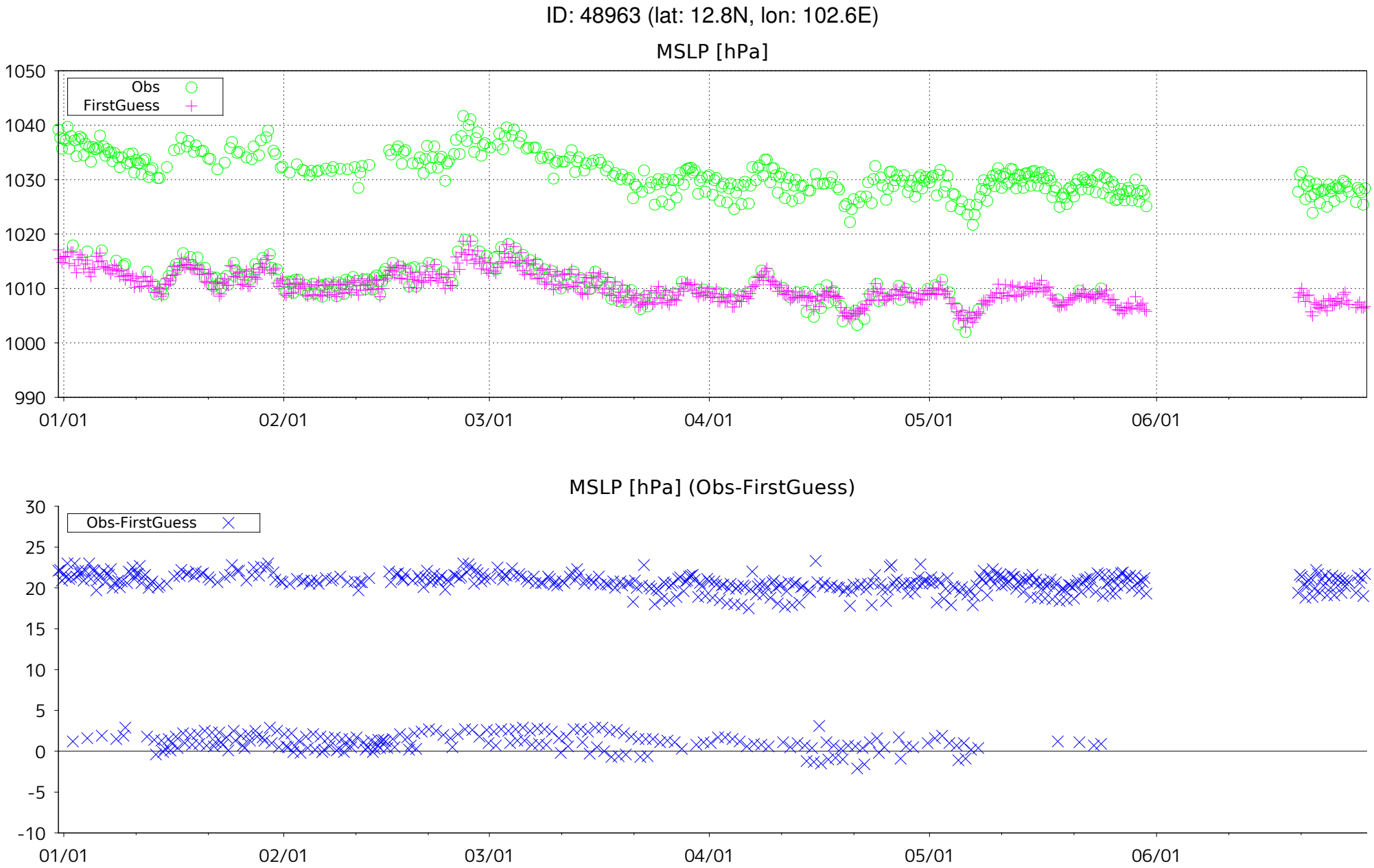

Figure 83(b) Time-series representation of MSLP Obs minus FirstGuess for station 48963

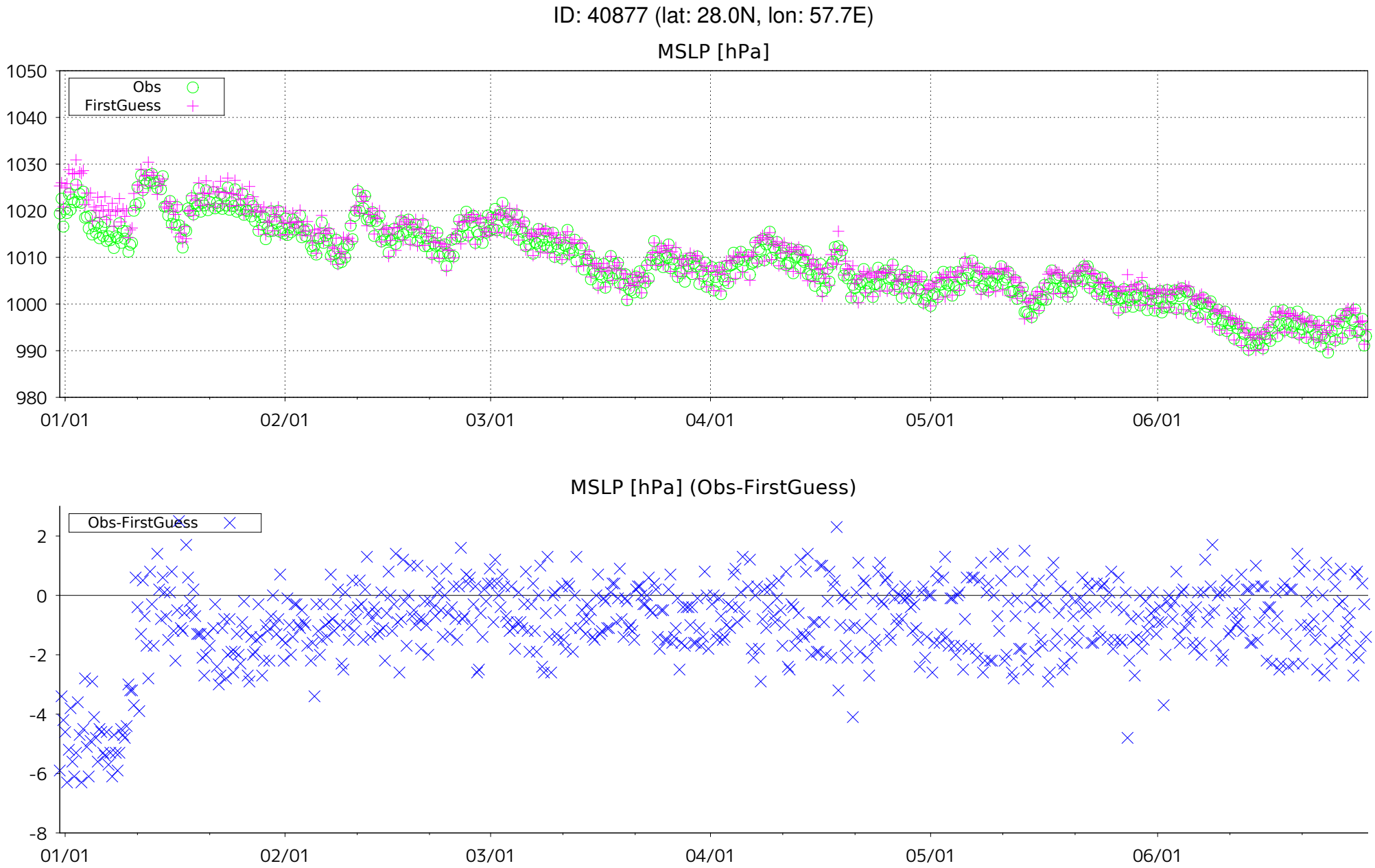

Figure 84 Time-series representation of MSLP Obs minus FirstGuess for station 40877